A TRANSGENIC MODEL FOR *IN VIVO* GENETIC ANALYSIS: CHARACTERIZING THE TRANSIENTLY-ACTING PROMOTER SWITCH THAT CONTROLS *DROSOPHILA* SEX DETERMINATION

A Dissertation

by

JAYASHRE RITHII RAJENDREN

Submitted to the Office of Graduate and Professional Studies of
Texas A&M University
in partial fulfillment of the requirements for the degree of

DOCTOR OF PHILOSOPHY

Chair of Committee,	James Erickson
Committee Members,	Arne Lekven
	Paul Hardin
	Sarah Bondos
Head of Department,	Thomas McKnight

December 2017

Major Subject: Biology

Copyright 2017 Jayashre Rithii Rajendren

ABSTRACT

To be male or female, that is the question. In *Drosophila melanogaster*, all aspects of somatic sex determination are under the control of the binary switch gene, *Sex lethal* (*Sxl*). The primary determinant of the activity state of *Sxl* is the number of X-chromosomes. XX embryos develop as females, while XY embryos develop as males. *Sxl* is stably expressed in females via autoregulatory mRNA splicing that occurs as a consequence of a brief pulse of transcription from establishment promoter *SxlPe*. Female-specific expression of *SxlPe* requires a two X chromosome dose of the X-signal elements *sisA*, *sc*, *upd* and *runt*. Males fail to express *SxlPe* as they carry a single dose of the X-signal elements (XSEs).

Understanding regulation of *SxlPe* demanded an advanced quantification tool to monitor *Sxl* activity *in vivo*. The *Sxl* transgene system thus developed enables the monitoring of endogenous *Sxl* activity, both as nascent transcripts and as mature mRNA. The key feature is that intron sequences are swapped between related species to allow allele-specific detection, by *in situ* hybridization, of expression from mutant and wild type transgenes side-by-side in every nucleus of the embryo. The transgene system is fully functional and helps exploit classical *Drosophila* genetics to monitor the biological effects of engineered *Sxl* mutations. Using this powerful system, I have characterized the cis interactions of the X-signal elements Sc/Da, repressor Dpn and also defined the regulatory regions of *SxlPe*, to discover the means by which this sensitive promoter switch operates.

In defining the different regulatory units our results validated the previous findings of Estes et al., using *SxlPe lacZ* fusions. The 3.0kb enhancer is indeed an equivalent of the full length endogenous *SxlPe* enhancer and drives a robust, wild type expression. In addition, studying the promoter deletions in context of full length *Sxl* transgenes confirmed that the minimal, 400bp enhancer that drove low *lacZ* expression in Estes et al., does activate *SxlPe* and is both necessary and sufficient for *SxlPe* activation.

In studying how binding site interactions impacted *SxlPe* regulation, my findings revealed that the loss of the single canonical E-box, Sc/Da 3 turned the *SxlPe* switch off, killing females. This not only led to the discovery of a prominent regulatory site critical for female-specific regulation but also challenged the previous notion that multiple Sc/Da are responsible for proper operation of *SxlPe* switch. Additionally, Sc/Da 3 proved that canonical E-box sites are important or even more so to *SxlPe* regulation, compared to the non-canonical sites.

Mutating repressor Dpn binding sites triggered ectopic *SxlPe* expression in males and subsequently male lethality. The non-canonical site 3 had the strongest effect on *SxlPe* regulation than the canonical Dpn sites 1 and 2. The surprising finding is that Dpn binding site mutation is not only capable of initiating *SxlPe* expression from the mutant bearing transgene, but also activating the wild-type *Sxl* from the control transgene *in trans*. This phenomenon suggests that transactivation might be a novel approach for the fly to amplify X dose signal and ensure female specificity.

DEDICATION

To my beloved grandparents, Amsi and Thatha,

who strive to make my dreams come true.

I am ever grateful to both of you.

ACKNOWLEDGEMENTS

I would like to express my sincere gratitude to my advisor, Dr. James Erickson for believing in me and shaping me into the graduate student I am today. I would also like to thank him for his encouragement, ever-ready enthusiasm to teach and guidance in finishing my graduate studies.

My sincere thank you also goes to my committee members, Dr. Arne Lekven, Dr. Paul Hardin and Dr. Sarah Bondos, for their guidance and support throughout the course of this research. I would like to extend my thank you to Dr. Stanislav Vitha, for helping me with confocal microscopy and most of all for developing the quantification program.

I would also like to thank the former and current members of the lab, Alejandra, Sharvani, Yi and Young for their valuable inputs, discussion and being great friends.

Finally, I would like to thank my family and friends for helping me through this journey. My parents for their devoted effort in supporting my dreams and standing by me, every step of the way. My sister whose courage, inspires me to face all challenges. My husband, Ram for his endless motivation, unconditional love and support which was monumental in crossing the finish line.

CONTRIBUTORS AND FUNDING SOURCES

This work was supervised by a dissertation committee consisting of Professors James Erickson (Advisor), Arne Lekven, and Paul Hardin of the Department of Biology and Professor Sarah Bondos of the Department of Molecular and Cellular Medicine. All the work for the dissertation was completed independently by the student.

This work was made possible in part by National Science Foundation under Grant Number 99-501761 and start up funds from Texas A&M University. Its contents are solely the responsibility of the authors and do not necessarily represent the official views of National Science Foundation or Texas A&M University.

TABLE OF CONTENTS

Page

ABSTRACT ii

DEDICATION iv

ACKNOWLEDGEMENTS v

CONTRIBUTORS AND FUNDING SOURCES vi

TABLE OF CONTENTS vii

LIST OF FIGURES x

LIST OF TABLES xii

CHAPTER I INTRODUCTION 1

The establishment and maintenance of *Sxl* 2
Sxl target genes and dosage compensation 4
Nature and regulation of the dose-sensitive promoter, *SxlPe* 6
XSEs and other *SxlPe* regulators 6
Sxl expression from the *SxlPe* promoter 12
SxlPe - structure and nature of signal sensing 12
Regulatory model of *SxlPe* 16

CHAPTER II SEX LETHAL TRANSGENE SYSTEM 19

Features of the *SxlTG* system 20
Design and development of the *Sxl* transgene system 21
galK recombineering 23
Functionality of the *Sxl* transgene system 24
Designing allele specific markers and its associated challenges 25
SxlPe activity of the *Sxl* transgene system followed by *in situ* hybridization 27
SxlPe activity of the *Sxl* transgene system followed by fluorescent *in situ* hybridization (FISH) 28
Automated quantification analysis of FISH images 30

CHAPTER III THE *SxlPe* PROMOTER – ENHANCER CONNECTION IN SEX DETERMINATION 32

Creating *SxlPe* promoter deletions in the *SxlTG* 34
Genetic tests of the effects of *SxlPe* deletions on promoter activity 36
A more stringent test: complementing Sxl^{f9}/Sxl^{f1} heterozygotes 38
In situ hybridization of *SxlPe* deletion constructs 40
SxlPe activity is absent in minimal enhancers, $SxlPe_{0.2kb}$ and $SxlPe_{0.4kb}$ 45
Adding spacer DNA to separate the $SxlPe_{0.4kb}$ enhancer from upstream sequences reinstates *SxlPe* activity 45
$SxlPe_{0.8kb}$ and $SxlPe_{0.4kgalK}$ enhancers are sensitive to reductions in the XSE dose 49

CHAPTER IV REGULATORY MODULE OF XSE BINDING SITES AT *SxlPe* 52

Characterizing the *cis* interactions of Sc/Da at *SxlPe* 55
Overview of Sc/Da binding at *SxlPe* 55
Creating *Sxl* transgenes carrying mutations in Sc/Da binding sites 56
Sc/Da site 3, an E-box, is a powerful *cis* regulatory element for *SxlPe* activation 57
Combinatorial Sc/Da mutants do not necessarily eliminate *SxlPe* expression 65
Characterizing repressor binding sites at *SxlPe* 69
Overview of Dpn binding at *SxlPe* 69
Creating *Sxl* transgenes carrying mutations in Dpn binding sites 70
Mutations in Dpn binding sites cause male lethality 71
Dpn binding sites mutation induced ectopic *SxlPe* expression in males and provided evidence of transvection between transgenic alleles 73
Evidence that a constitutive *SxlPe* promoter can activate a wild-type *SxlPe* promoter *in trans* 77

CHAPTER V CONCLUSIONS AND METHODS 79

Sxl transgene system in analyzing *SxlPe* activity 79
Structure and regulatory role of *SxlPe* enhancer in *Sxl* activation 83
Do upstream sequences normally influence *Sxl* transcription? 86
The roles of Sc/Da binding sites in regulating *SxlPe* 86
Analysis of Dpn binding site mutations: repressor function and a possible transvection mechanism for X-signal amplification 88
Methods 92
Fly stocks and genetic tests 92
Generation of *delPe-SxlTG* 92
Generation of binding site mutations 93
galK recombineering 93
Sxl transgenic flies 94
In situ hybridization 94
FISH (fluorescence *in situ* hybridization) 95
Confocal Imaging 96

REFERENCES 97

APPENDIX A 108

APPENDIX B 117

LIST OF FIGURES

Page

Fig. 1.1: Establishment of SXL autoregulatory loop 2

Fig. 1.2: Somatic sex determination hierarchy 5

Fig. 1.3: Positive and negative regulators of SxlPe 7

Fig. 1.4: *SxlPe* expression in females 12

Fig. 1.5: The *cis* regulatory binding sites at *SxlPe* 14

Fig. 1.6: Regulatory model of *SxlPe* 17

Fig. 2.1: *Sxl* transgene for quantitation of allele-specific expression 21

Fig. 2.2: Integration of *Sxl* transgene into the *Drosophila* genome 23

Fig. 2.3: Introducing changes in the *Sxl* sequence by *galK* recombineering 24

Fig. 2.4: *In situ* hybridization showed that the *Sxl* transgenic lines mimicked wildtype *SxlPe* expression 28

Fig. 2.5: FISH image depicting the *SxlPe* activity of the *Sxl* transgene system 29

Fig. 2.6: Example of an automated quantification analysis 31

Fig. 3.1: Schematic representation of $SxlPe_{0.8kb}$, $SxlPe_{1.1kb}$, $SxlPe_{1.4kb,}$ $SxlPe_{3.0kb}$ and $SxlPe_{3.7kb}$ promoter constructs in the *SxlTG* 36

Fig. 3.2: *In situ* hybridization of $SxlPe_{0.8kb}$ and $SxlPe_{1.1kb}$ transgenic lines 41

Fig. 3.3: *In situ* hybridization of $SxlPe_{1.4kb,}$ $SxlPe_{3.0kb}$ and $SxlPe_{3.7kb}$ transgenic lines 44

Fig. 3.4: $SxlPe_{0.4kbgalk}$ promoter construct reinstates *SxlPe* activity 47

Fig. 4.1: Sc/Da binding sites at *SxlPe* 56

Fig. 4.2: *In situ* hybridization of *Sc/Da 1⁻SxlPe* and *Sc/Da 2⁻SxlPe* transgenic lines 62

Fig. 4.3: *In situ* hybridization of *Sc/Da 3⁻SxlPe* transgenic lines 63

Fig. 4.4: *In situ* hybridization of *Sc/Da 1⁻2⁻SxlPe* and *Sc/Da 1⁻4⁻SxlPe* transgenic lines 67

Fig. 4.5: Dpn binding sites at SxlPe..... 69

Fig. 4.6: Ectopic *SxlPe* expression in $Dpn^{M}SxlPe$ transgene carrying Sxl^{7BO} male (XY) embryos..... 74

Fig. 4.7: FISH image depicting the ectopic *SxlPe* expression in $Dpn^{M}SxlPe$ transgene carrying Sxl^{7BO} male (XY) embryos 77

LIST OF TABLES

Page

Table 2.1: *Sxl*^{f1} and *Sxl*^{7bO} female viability data 25

Table 2.2: Analysis of the transgenic lines with the designed allele-specific changes in E1 to A2 region 26

Table 3.1: All *delPe-SxlTG* rescued female lethality in *Sxl*^{f9} mutant females 37

Table 3.2: Promoter deletion restores female viability in *Sxl*^{f9}/*Sxl*^{f1} mutant females 39

Table 3.3: *SxlPe*$_{0.2kb}$ and *SxlPe*$_{0.4kb}$ are not sex specific 45

Table 3.4: *SxlPe* activity of *SxlPe*$_{0.4kbgalK}$ and *SxlPe*$_{0.8kb}$ depend on XSE dose 50

Table 4.1: Mutated sequences of Sc/Da binding sites 57

Table 4.2: Mutations in Sc/Da binding site affected female sex specificity 59

Table 4.3: Phenotypic categories of *SxlPe* activity in Sc/Da binding site mutants 61

Table 4.4: Combinatorial Sc/Da binding site mutations retained some *SxlPe* activity ... 66

Table 4.5: Mutated sequences of Dpn binding sites 70

Table 4.6: Dpn binding site mutations reduced male viability 73

CHAPTER I

INTRODUCTION

Cell fates are established through an intricate cascade of regulatory pathways, often triggered by small quantitative differences in transcription factors or signaling molecules. How the quantitative difference is interpreted at a molecular level by enhancers or *cis* regulatory modules to give rise to complex and precise pattern of gene expression in a specific spatiotemporal manner has been an intensively investigated field for the past few decades. Some well-studied examples in *Drosophila* include how changes in levels of Bicoid and Dorsal, two maternally deposited transcription factors, establish distinct gene expression patterns and specify anterior-posterior and dorsal-ventral axes of the embryo [1-4].

Drosophila somatic sex determination is another classical model of how cell fate commitment relies on subtle differences of regulatory protein concentrations. The X chromosome dose is conveyed to the master regulatory gene, *Sxl-lethal* (*Sxl*) by four X-linked signaling elements (XSEs) [5-7]. The two-fold difference is sensed by the establishment promoter, *SxlPe* and the subsequent activity of *Sxl* controls the sexual development via a cascade of regulatory events [5, 7, 8]. In XX embryos, *Sxl* is activated by *SxlPe*, which results in female differentiation and development. In XY embryos, *Sxl* remains OFF as one dose of XSE proteins is not enough to activate *SxlPe*. Consequently, dosage compensation and male development take place [7]. *SxlPe* converts the X dose

signal to an all or none response, in order to establish the opposite sexual identities. Therefore, deciphering the nature of dose-sensitive *SxlPe* and its regulation mechanism is of great importance and can greatly enhance our understanding of transcriptional regulation, cell fate decisions and embryonic development.

The establishment and maintenance of *Sxl*

Somatic sex determination in *Drosophila melanogaster* occurs as a result of *Sxl* regulation by a dual phase process – establishment and maintenance. The phases are governed by two distinct promoters; an early acting, establishment promoter *SxlPe* and the late acting, maintenance promoter *SxlPm*.

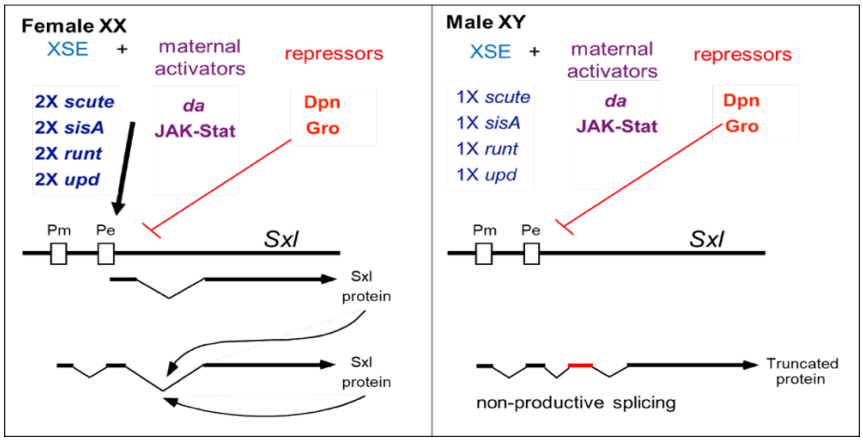

Fig. 1.1: Establishment of SXL autoregulatory loop
(Left Panel) In XX females, *SxlPe* is activated in response to the collective level of four XSEs. *SxlPe* activation provides the initial burst of SXL protein, which is then used to process the pre-mRNA from *SxlPm* to maintain the production of functional SXL. The autoregulatory splicing loop allows *Sxl* to be locked into the "ON" state in females. (Right Panel) In XY males, *SxlPe* remains inactive and the pre-mRNA from *SxlPm* is spliced into a male default form, which contains translation termination signal in the third exon. As a result, no functional SXL is produced in males.

SxlPe, one of the earliest developmental targets of *Drosophila* is activated during a small developmental window, the syncytial blastoderm stages by a transcriptional response to the X-chromosome dose [6, 8, 9]. The diplo-X dose of XSE turns *SxlPe* on in females while the haplo-X dose of XSE keeps *SxlPe* turned off in males. *SxlPe* produces a brief pulse of SXL before it shuts off and a subsequent activation of *SxlPm* takes place by the start of cellularization [10, 11]. The transient activation of *SxlPe* is the primary decision that helps establish the female sexual choice and reiterates this decision through maintenance and the rest of development by *SxlPm*.

SxlPm comes on in both sexes but earlier in females than males, briefly before *SxlPe* shuts off [11]. This overlapping event may be important to ensure a smooth transition, making the timing of *SxlPe* activation even more significant. In males, the *SxlPm* transcripts are spliced by default to include a premature stop codon within the third exon, the male specific exon and results in a truncated non-functional SXL (Fig. 1.1). On the contrary, in females, the initial burst of SXL protein from *SxlPe* directs female mode of splicing, of the *SxlPm* transcripts by skipping the male specific exon [12-14]. SXL being an RNA binding protein, recognizes the poly(U) rich sites that are located >200 nucleotides downstream and >200 nucleotides upstream of the third exon [14, 15]. The binding of SXL to these sites and its interaction with other general splicing factors like U1 snRFP and SNF, cause the third exon to be excluded from the final transcripts and lead to the production of functional SXL [16, 17]. The functional SXL continues to auto-regulate the splicing of its own transcripts, which helps maintain SXL expression from *SxlPm* in the

rest of the female's life (Fig. 1.1). Overall, the transient activation of *SxlPe* provides sufficient SXL to trigger an autoregulatory feedback loop, which enables the continuity of SXL generation from *SxlPm* [12, 13, 18]. Therefore, the establishment of autoregulation plays a pivotal role in converting the X-counting response of *SxlPe* to sexual dimorphism.

Sxl target genes and dosage compensation

SXL, as an RNA-binding protein, is capable of regulating the alternative splicing of not only its own transcript but also its immediate target gene, *transformer* (*tra*) [14, 19, 20]. A cascade of sex-specific splicing events starting from *Sxl* directed *tra* splicing is responsible for most of the sexual dimorphism. In females, SXL protein directly binds to *tra* pre-mRNA, directing female-specific splicing to produce active TRA protein. In males, default splicing takes place in the absence of SXL, producing truncated, non-functional TRA protein [19-21]. TRA also functions as an RNA-binding protein and the functional TRA in turns regulates the alternative splicing of its downstream target, *doublesex* (*dsx*) and *fruitless* (*fru*) [14, 22, 23]. The presence of TRA in females induced the production of female isoform, DSX^F and FRU^F, while the absence of TRA in males led to default splicing and production of male isoform, DSX^M and FRU^M (Fig. 1.2). DSX protein isoforms regulate the development of sexual characteristics both by activating genes that promote the same sex and repressing genes that are involved in the differentiation of the opposite sex [24, 25]. FRU^F is non-functional and FRU^M is known to be specifically expressed in the central nervous system (CNS) to control sexual orientation and male courtship behavior [26, 27].

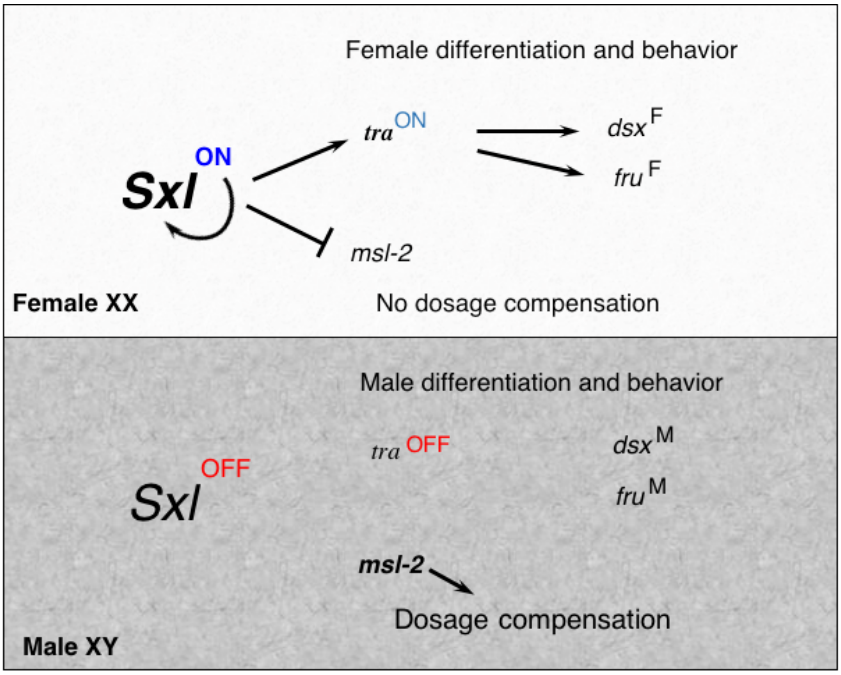

Fig. 1.2: Somatic sex determination hierarchy
(Top panel) In female flies, production of functional SXL is maintained by an autoregulatory feedback loop. In the presence of SXL, functional TRA protein is produced and it directs the female-specific splicing of transcripts from *dsx* and *fru*. SXL also ensures no dosage compensation in females by blocking *msl2* translation. (Lower panel) In male flies, SXL is absent. No functional TRA is produced and *dsx* and *fru* are spliced to default male mode. Translation of *msl2* also takes place, which results in dosage compensation.

SXL also controls dosage compensation through its immediate target, *male-specific-lethal 2* (*msl2*) [28]. Dosage compensation is an epigenetic mechanism to equalize gene expression between different sexes. In flies, this process is achieved by upregulating the transcription of the male X chromosome. In the absence of SXL, males are able to produce MSL2 protein, which works in conjunction with MSL1, MSL3, MLE, MOF and noncoding RNAs, roX1 and roX2 to assemble a ribonucleoprotein dosage compensation complex (DCC) [29-33]. DCC specifically associates with male X chromosome and

mediates the H4 acetylation at lysine 16 (H4K16ac), which facilitate the hyper transcription of the single X chromosome [34-36]. However, active SXL blocks *msl2* mRNA translation in females, ensuring that no dosage compensation takes place (Fig. 1.2) [37].

Nature and regulation of the dose-sensitive promoter, *SxlPe*

Sxl is at the top of sex determination cascade, modulating all aspects of somatic sex differentiation and dosage compensation [5, 6, 28, 38]. The on/off state of *Sxl* is determined by counting the number of X chromosomes [9]. Although the difference between haplo-X dose and diplo-X dose is subtle, *SxlPe* is able to discern the dose difference and elicit an all or none response. Failure to properly sense the X chromosome dose at *SxlPe* can disrupt *Sxl* expression and affect the downstream regulatory events to establish the correct cell fate. Given the key role of *SxlPe* in initiating sex determination, tremendous efforts have been made to interpret the dose-sensitivity nature and transcriptional regulation of *SxlPe*.

XSEs and other *SxlPe* regulators

The decision of whether or not to activate *SxlPe* depends on the X-chromosome dose. Current research indicates that *SxlPe* activity is primarily determined by the collective dose of four X-linked signal elements (XSEs), while several other activators and repressors also work in concert to mediate *SxlPe* activity (Fig. 1.3).

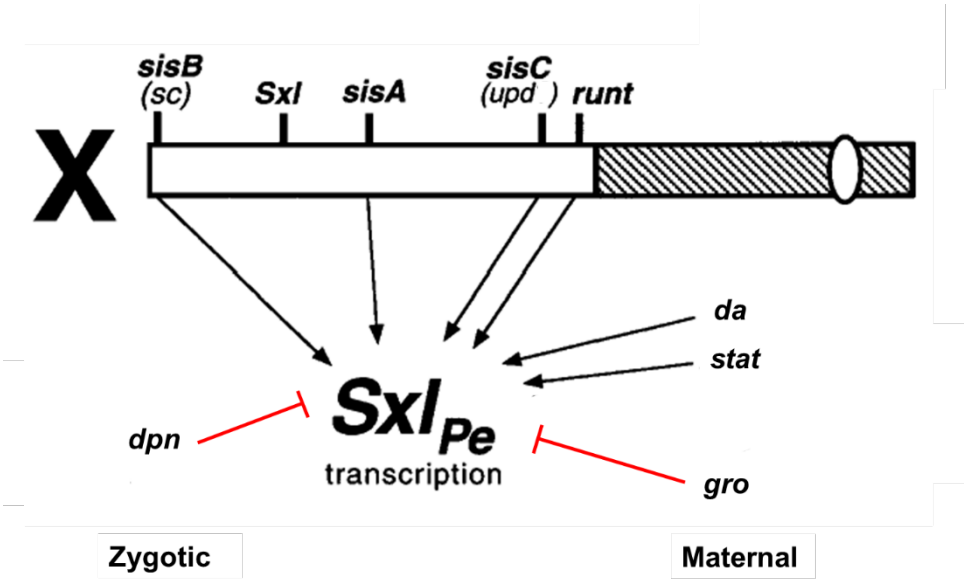

Fig. 1.3: Positive and negative regulators of SxlPe
XSEs, *sisA*, *sc*, *runt* and *upd* activate *SxlPe* along with the maternal factor, *da* and *stat*. Zygotically expressed *dpn* and maternally deposited *gro* function as *SxlPe* repressors.

The four XSEs, *sisterless A* (*sisA*), *scute* (*sc* or *sisB*), *runt* and *unpaired* (*upd* or *sisC*), function to activate *SxlPe* [39-44]. The XSEs are defined by the following characteristics; it exerts a zygotic effect on sex determination and acts early during embryogensis; decreasing the dose of the gene results in female-specific lethal effect; increasing the dose of the gene affects male viability [5, 41]. Among the four XSEs, SisA and Scute are the two strongest activators that are indispensable for *SxlPe* activation. Runt and Upd are weaker activators that show limited or spatial effects on *SxlPe* activity.

sisA was discovered as a key XSE due to its sex-specific lethal characteristics. *sisA* mutants show reduced female viability while duplication of *sisA* has a male-specific lethal effect [6, 41, 45]. *In situ* hybridization showed *sisA* expression was first detected at nuclear cycle 8 and peaked at cycle 12. In cycle 14, the expression began to disappear in somatic nuclei and was eventually restricted to only yolk nuclei [42, 45]. The peak of *sisA* expression overlaps with the onset of *SxlPe* transcription, which further support its crucial role in regulating *SxlPe* activity. The later expression of *sisA* in yolk is not sex-specific and is associated with midgut formation [45]. SisA is a basic leucine zipper (b-Zip) protein transcription factor and it is predicted to regulate *SxlPe* by forming heterodimer with a protein partner [42, 46]. However, the dimerization partner of SisA is still yet to be discovered.

Scute shares similar genetic characteristics as *sisA*. Loss-of-function mutation of *sc* is homozygous female lethal while *sc* duplication shows a strong male lethal effect in combination with *sisA* or *Sxl* duplication [41]. The temporal expression profiles of *sc* and *sisA* are also identical. *Sc* transcripts first appear at cycle 9, reach the peak at cycle 12 and decrease rapidly in early cycle 14 [9, 42]. The early expression of *Sc* before the first pulse of *SxlPe* activation is consistent with its role in initiation of *SxlPe* activity. At the molecular level, *Sc* is a better characterized XSE compared to *sisA*. *Sc* encodes a basic helix loop helix (bHLH) transcriptional factor, which heterodimerize with maternally deposited Daughterless (Da) and directly activate *SxlPe* via DNA binding [41, 47]. Sc/Da heterodimer is also known to activate other target genes during neurogenesis [48-50].

Runt was first identified as a pair rule gene known for its regulatory role in segmentation. Early *runt* expression is also found to be responsible for *SxlPe* activity as *SxlPe* expression was greatly reduced or completely eradicated in the central region of *runt* null mutants [40]. This matches the expression of *runt* in the central region of the embryo during cycle 13 [51]. The restricted expression pattern of *runt* and its relatively late onset suggest that *runt*'s role is to maintain and reinforce uniform *SxlPe* expression, presumably in the central region. While losing one copy of *scute* and one copy of *sisA* kills majority of the females, the female-specific lethal interaction between *runt* and *scute* or *sisA* is comparably less, making *runt* a weaker activator than *scute* and *sisA* [40, 52]. RUNT is a DNA binding protein that belongs to the RUNX family. Although RUNT is previously believed to regulate *SxlPe* by direct binding as a heterodimer [53], our recent work suggests that Runt functions to activate *SxlPe* by antagonizing the corepressor Groucho (Gro) via its WRPW domain (Erickson, unpublished).

Among all four XSEs, *upd* exhibits the weakest genetic interaction with the other XSEs and *Sxl* [44]. Instead of encoding a transcription factor like all the others, *upd* encodes a ligand of the Jak-Stat signaling pathway and modulate *SxlPe* expression via the activation of its downstream target, Stat [43, 44, 54]. The binding of Upd to receptor stimulates the Jak kinase, Hop, to activate the maternally supplied transcription Stat92E by phosophorylation [55]. *SxlPe* expression is compromised in Jak/Stat mutations, *upd*, *hop* and *stat*, but the effect is moderate and reduction of *SxlPe* only occurrs in cycle 14 in the central part of the embryo [43, 44, 54]. *In situ* hybridization reveals that *upd* expression

does not start until cycle 13, which is after the onset of *SxlPe* [54]. Therefore, *upd* is regarded as a reinforcement element that is involved in maintaining and fine-tuning *SxlPe* expression but is not required for the initiation of *SxlPe*.

diminutive (*dm*) encodes *Drosophila* bHLH transcription factor Myc and is claimed to be a newly found XSE [56]. However, our lab failed to observe the synergistic female lethal interaction between *dm* and other XSEs that has been published. Furthermore, the expression profile of *dm* indicates that *dm* is not zygotically expressed during *SxlPe* activation [57]. Hence, Myc probably regulates *SxlPe* unlike an XSE, but via maternal effects.

The maternally deposited zinc-finger protein Zelda is a transcription factor that functions as a global activator of early zygotic genome. Depletion of maternal Zelda down-regulates the activity of many genes involved in cellularization, sex determination and pattern formation, which lead to early development defects in embryos [58]. Zelda can specifically bind to TAGteam motif, which is abundant in the upstream region of many early expressed genes, including *Sxl* and *sc* [58-60]. Although Zelda is shown to regulate gene activation by promoting nucleosome depletion and increasing chromatin accessibility [61-63], the mechanism of *SxlPe* regulation by Zelda is still under investigation.

Negative regulators play important roles in adjusting *SxlPe* activation threshold in opposite sexes to ensure that the two dose differences can be accurately distinguished and *SxlPe* is activated in a female-specific manner. The two key negative regulators are maternally deposited Groucho (Gro) and zygotically expressed Deadpan (Dpn).

As a repressor, elimination of maternal Gro causes ectopic *SxlPe* expression in males and earlier shift of *SxlPe* onset in females [64]. Gro is a Gro/TLE family corepressor that lacks DNA binding domain. Its recruitment to DNA is through the interaction with several other DNA binding proteins [65-67]. Gro is proved to be able to interact with C-terminal "WRPW" motif [65, 68], which is present in both Runt and Dpn. It is proposed that Dpn recruits Gro to *SxlPe* to uplift the repression threshold in males [64] while Runt contributes to *SxlPe* activation in females by antagonizing Gro-mediated repression (Erickson, unpublished).

Dpn, which encodes a bHLH transcription factor from Hairy-Enhancer of Split (HES) family, is the only autosomal gene that is found to inhibit *Sxl* activity [10, 64, 69, 70]. *dpn* mutant males show inappropriate *SxlPe* expression, although the level of ectopic expression is relatively less compared to the males with no maternal Gro [10, 64, 69]. The initial transcription of *Dpn* is only detected around cycle 12 and it exhibits higher level of activity in the central region than the anterior and posterior during its peak in cycle 13 [10, 69]. The late onset of *Dpn* and its comparably weak effect on *SxlPe* indicate that other inhibitors exist to modulate early repression along with Gro.

***Sxl* expression from the *SxlPe* promoter**

In females, *SxlPe* expression begins at nuclear cycle 12. At this time, nascent transcripts are detected in some of the embryos as faint nuclear dots, by *in situ* hybridization. Also, *SxlPe* expression at the two X-chromosomes in the nucleus occurs independently, leading to a differential expression in the form of one/two nuclear dots at the early stages. By cycle 13 all the nuclei express two nuclear dots and the intensity of their expression steadily increases until early cycle 14. At mid cycle 14, *SxlPe* transcription ceases and the nuclear dots disappear [9, 42, 54].

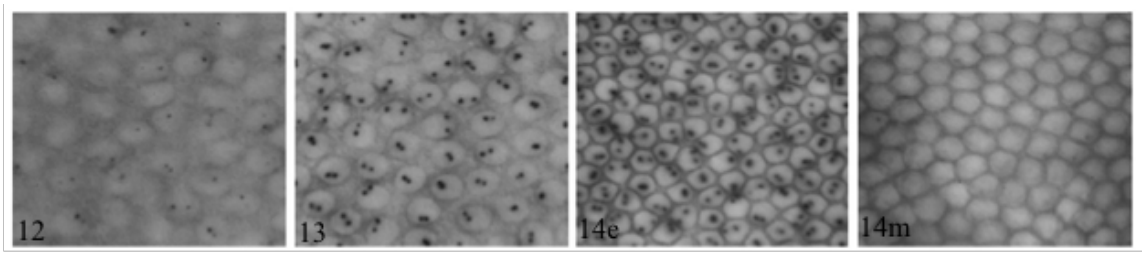

Fig. 1.4: *SxlPe* expression in females
Nuclear dots in the images represent nascent *SxlPe* transcripts. *SxlPe* expression starts at nuclear cycle 12 and ceases at mid cycle 14.

***SxlPe* - structure and nature of signal sensing**

The expanse of *SxlPe* enhancer region maps ~5kb upstream of the transcription start site in the early exon, E1 of *Sxl*. This regulatory region acts as a shared enhancer between the establishment promoter, *SxlPe* and the maintenance promoter, *SxlPm* [11]. *SxlPm* is housed upstream of *SxlPe*, at the end of the shared enhancer region. Although,

transcription factors respond to *cis*-sequences that span the breadth of the enhancer region, the 3kb region upstream of the transcription start site is essentially thought to be the regulatory region of *SxlPe*.

A shorter 1.4kb region when fused to *lacZ* drives expression comparable to the endogenous and has been popularly used to study *SxlPe* activity in the past [47, 71]. The *cis* regulatory sequences along the 1.4kb region comprises of two prominent clusters, a proximal 400bp region and a distal region between 0.8 and 1.0kb. Functionally, the 400bp region provides sex specificity but drives a low, non-uniform *lacZ* expression. The additional regulatory sequences comprised within the distal region supports and elevates *lacZ* expression to a more or less endogenous expression pattern [47, 71, 72]. The distal region thus functionally signifies an increase in promoter strength.

The *SxlPe* enhancer region contains reiterated *cis* acting sequences that are targets of both positive and negative regulators. The two key XSEs, *sisA* and *scute*'s interaction at *SxlPe* was demonstrated in Estes et al., using the sex-specific, *0.4kb-lacZ* construct. A decrease in *sisA* and *scute* gene dose caused reduction in levels of *lacZ* expression, validating that the two XSEs act through the 0.4kb region [71]. Although, genetic evidence supports *sisA* interaction at *SxlPe*, it remains unknown if this interaction is direct. Also, the binding sites of *sisA* along *SxlPe* are not detailed due to our lack of knowledge about its dimerization partner.

The *cis*-interactive sites of Scute are well characterized along the *SxlPe* promoter. Scute and its heterodimeric partner bind eleven sites within the 1.4kb region, upstream of the transcription start site [47]. Six of the binding sites are present in the 0.4kb region while the rest are distributed between the 0.8kb and 1.1kb region (Fig. 1.5). The binding sequences are a combination of canonical, E-box and non-canonical sequences, although they are predominantly non-canonical in nature. Functionally, both these sequences are pertinent to *cis*-regulation by Sc/Da [47].

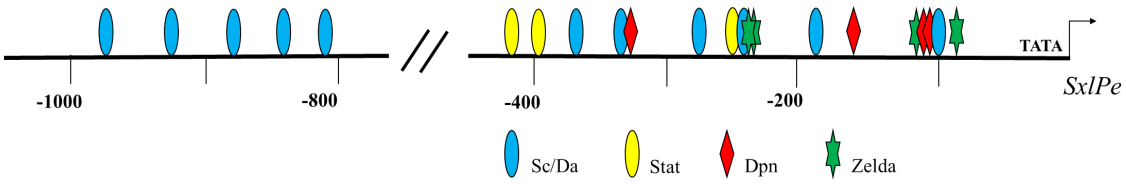

Fig. 1.5: The *cis* regulatory binding sites at *SxlPe*
Schematic representation of the regulatory binding sites along 1kb *SxlPe*. Sc/Da sites (blue), Stat sites (yellow), Dpn sites (red) and Zelda sites (green) are shown.

Activator, STAT has three sites mapped within the 1.4kb enhancer region, located at -253, -393 and -428bp respectively [54]. Only one of the STAT sites is present in the prominent 400bp region while the other two sites are the only one's present in between the proximal and distal binding site clusters (Fig. 1.5). The specific distribution of the STAT sites could indicate a regulatory significance as to why the STAT sites are dispensable for initial activation of *SxlPe*. Yet, all we know is that mutated STAT sites are

known to cause moderate reduction in *SxlPe* activity, mostly in the central region of the embryo [54].

XSE, RUNT has similar effects on *SxlPe* activity, much like STAT. It too is not needed for initial activation of *Sxl* and it appears to affect *Sxl* activity in the central broad region of the embryo [40]. However, no consensus RUNT binding sites have been characterized along the *SxlPe* enhancer.

Drosophila Myc, also known as Diminutive (Dm), is believed to be an activator of *SxlPe*. ChIP experiment showed that Myc is associated with the region that located around -96bp upstream of *SxlPe* start site. Although Myc binding sites at *SxlPe* are not identified, it is proposed that Dpn binding site 1 and 2 might be putative Myc binding sites [56].

The repressor Dpn binds *SxlPe* and all the four functional Dpn sites identified are located within the proximal 400bp enhancer region at -110, -121, -160 and -330bp (Fig. 1.5). Among these Dpn binding sites, sites 1 and 2 are canonical while sites 3 and 4 are non-canonical in nature [64].

TAGteam sites are bound by the transcriptional activator, Zelda and the *SxlPe* enhancer has a cluster of them present within 250bp of the transcription start site [59]. The cluster consists of a total of four sites, the CAGGTAG, tAGGTAG and a CAGGcAG doublet (Fig. 1.5). Mutations in TAGteam sites affected *SxlPe* activity when tested using the

1.4kbSxlPe-lacZ transgenes. Mutation in all of the TAGteam sites showed a compromised sex specific ratio as they were fewer stained embryos (females) with very low levels of *lacZ* expression. Mutated CAGGTAG and tAGGTAG proved to be less severe as it retained the sex specific ratio but had reduced levels of *lacZ* expression. The CAGGcAG doublet when mutated had the least effect with only a marginal reduction in *lacZ* levels [59]. The effect of the mutated doublet was harder to assess as it bordered the Sc/da, E-box site 3.

Regulatory model of *SxlPe*

The success of *SxlPe* regulation in females largely depends on the X-chromosome counting. This dose-sensitive activation of *SxlPe* is often quoted as a textbook example of how small, two-fold differences in XSE protein concentration controls developmentally significant cell fate decisions. However, the mechanism by which such small changes in protein concentration regulate and cause the all-or-none response still remains a mystery [6, 42, 53, 73, 74].

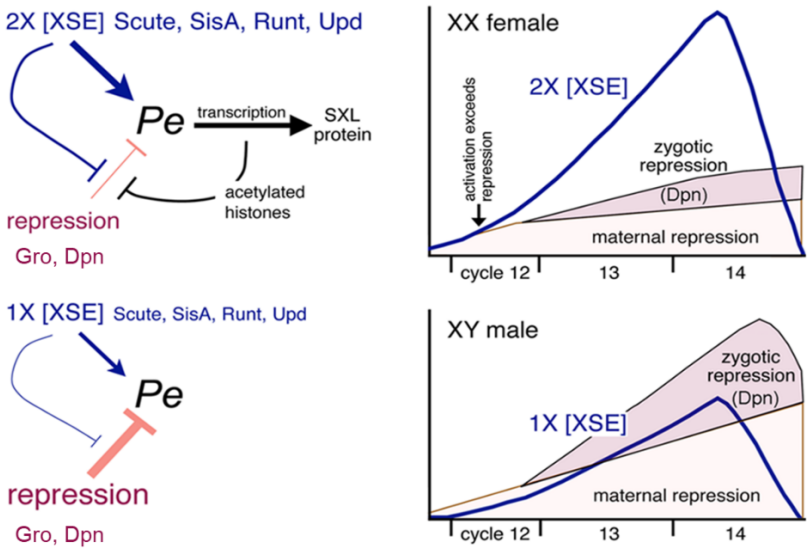

Fig. 1.6: Regulatory model of *SxlPe*
(Top Panel) The level of XSEs in females is sufficient to surpass the initial repression threshold set by the repressors like Gro and activate *SxlPe*. Activated *SxlPe* is likely to increase histone acetylation and further dampen Gro-medicated repression. (Lower Panel) The level of XSEs in males is not sufficient to overcome the initial repression. Maternal Gro, along with zygotically expressed Dpn further maintains the high repression threshold in cycle 13 and 14 to ensure that *SxlPe* remain inactive.

Our laboratory's theoretical model illustrates the possible mechanisms that help establish the sex specific regulation of *SxlPe*. The model is defined, based on the concept of signal amplification through the action of the maternal co-repressor Gro. Gro and the maternal supplied bHLH repressors establish the initial threshold for *SxlPe* activation. The increasing XSE concentration due to the double dose of X in females aids in surpassing the threshold and transcription is initiated. Once initiated, the transcriptional activation is maintained by the accumulation of continuously translated XSE proteins and the subsequent dampening of Gro mediated repression. Essentially, the dampening of

repression supplemented with the raising XSE's triggers a positive feedback loop that ensures elevated transcription - evidently a form of signal amplification [64]. The exact mechanism that supports the antagonizing of Gro mediated repression remains unknown. We believe that the transcriptionally active *SxlPe* in females potentially triggers histone acetylation and this chromatin modification could prevent Gro binding and ultimately dampen the repression.

In case of males, the single dose of X chromosome produces insufficient XSEs to overcome the initial repression. As nuclear cycles progress through cycles 13 and 14, the repression is further strengthened by Gro and the zygotic repressor Dpn. This ensures that the increase in XSEs is unable to compete with the higher repression levels and *SxlPe* remains inactivated [64].

CHAPTER II

SEX LETHAL TRANSGENE SYSTEM

Analyzing or quantifying the levels of *SxlPe* activity, as it dynamically changes during the nuclear cycles 12-14 is challenging. Past attempts to study the regulatory role of *SxlPe* relied largely on the use of *lacZ* promoter fusions. While, transgenic fusions provided several insights pertaining to the general spatial-temporal pattern and timing of *Sxl* expression in the developing embryo [47, 59, 64, 71], they suffered from several limitations.

Detecting nascent transcripts with *lacZ* is difficult yet the ability to do so is essential to understanding exactly how and when *SxlPe* is turned on and off. Analysis of the timing of *SxlPe* activity from the endogenous locus where nascent transcripts can be easily observed, has helped define the fundamental nature of the sex determination signal [9] and revealed important insight into the mechanism of X-signal amplification [64]. Quantification of *lacZ* expression is difficult as wild type and mutant lines need to be analyzed separately in different animals. With traditional P-element based transgenes the problem was compounded by the fact that each line inserted into a unique genomic locus, necessitating analysis of multiple insertions to compensate for a range of chromosomal position effects. Finally, promoter fusions cannot fully make use of the genetics - the fundamental strength of *Drosophila* as an experimental system. To give one illustration, it is impossible to rigorously define promoter sequences as both necessary and sufficient

using promoter-*lacZ* fusions as they allow no direct assessment of genetic function. Overcoming these concerns was our intent in creating a *Sxl* transgene system, that would allow advancements towards complete, functional validation of *SxlPe*.

Features of the *SxlTG* system

In developing an advanced system, the transgenic constructs were created with the entire *Sxl* locus including both upstream and downstream flanking regions. The transgenes should thus be fully functional allowing full application of the molecular and genetic tools available to study the native locus: the ability to detect nascent transcripts, measure mature mRNA levels and assess actual biological function. We incorporated the PhiC31 mediated recombination system to allow the integration of all transgenic constructs at the same locus, as both a means to facilitate direct comparisons between mutant and wild-type transgenes and to eliminate discrepancies arising from the influence of the surrounding chromatin on *SxlPe* activity.

In order to establish a direct standard for quantitation and comparison of *SxlPe* expression, the system was designed to detect mutant and wild type expression, side by side in every nucleus of the developing embryo. The differentiation between the two transgenes were made possible by exchanging the conserved region containing Exon E1 through A2 with corresponding sequences from related fly species. This served the dual purpose of retaining normal *Sxl* regulation and function while allowing allele specific detection of the transgenes using *in situ* hybridization (Fig. 2.1).

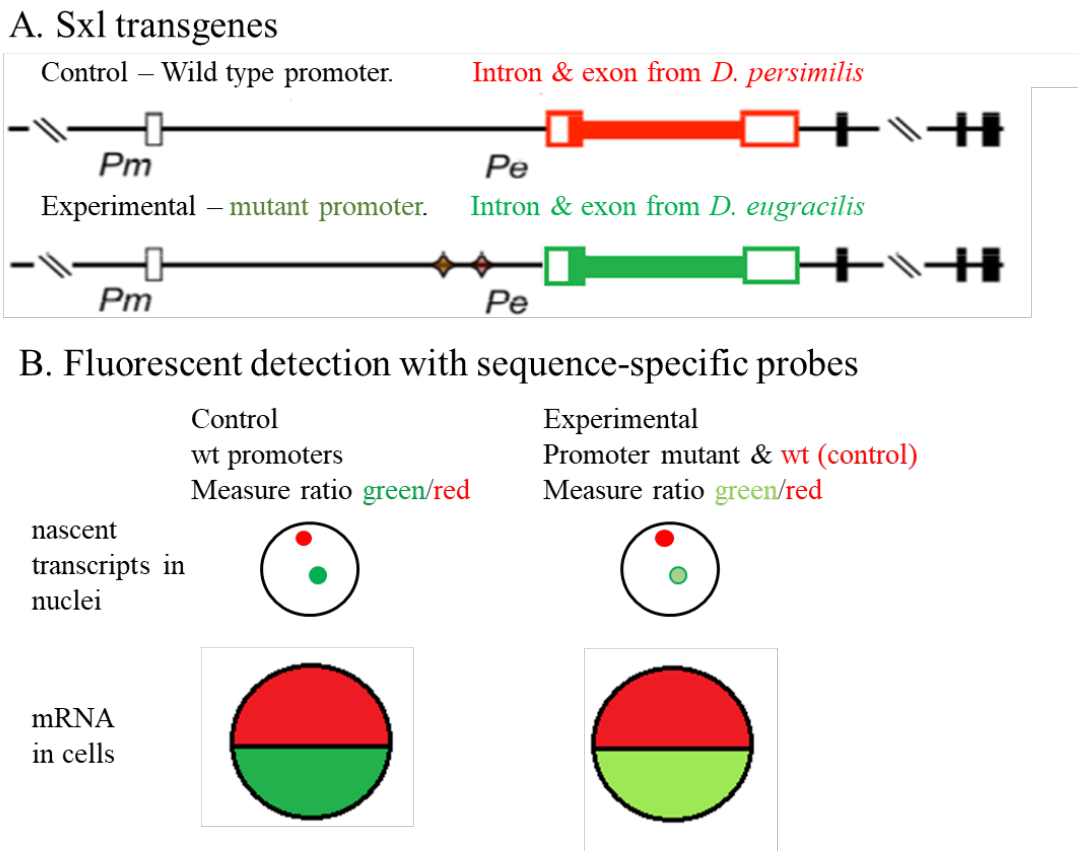

Fig. 2.1: *Sxl* transgene for quantitation of allele-specific expression
A) Control & experimental transgenes: 41.9kb construct, included the 23.5kb *Sxl* gene. 5 kb from *Pm* through *Pe* and exons E1 and exon A2 is detailed. *D. melanogaster* sequences from exon E1 through exon A2 were replaced by the same segments from *D. persimilis* (red) and *D. eugracilis* (green), allowing creation of allele-specific probes. B) Analysis of binding site mutations: Decreased (or delayed) nascent transcripts and lowered mRNA levels measured by allele-specific probes (green, red) using fluorescent in situ hybridization.

Design and development of the *Sxl* transgene system

The transgene system is equipped with two *Sxl* transgenes, one of which serves as the wild type (control transgene) and the other carries the engineered *Sxl* mutations (experimental transgene) to be analyzed. The transgenic constructs are created using *galK* recombineering in a P(acman) II vector [75, 76]. The Pacman vector was chosen because

it facilitated PhiC31-mediated integration of large genomic fragments [77] and its low copy number in *E. coli* allowed genetic manipulation via *galK* recombineering [75, 76]. My plan was that the transgenes carry the entire *Sxl* locus, ~ 20kb sufficient upstream and downstream flanking region so that *Sxl* would be both functional and insulated from any chromosomal effects due to the site of insertion. When I began, it was not known how much DNA upstream or downstream of *Sxl* would be needed to preserve full function. Accordingly, I adopted a trial and error method. I started out with a 92kb *SxlTG* construct, which included about 68.5kb of flanking region. The 92kb construct failed to yield transformants, owing to its large size and/or limitations of the commercial injection services we used. I decreased the construct size further to 79kb and 50kb, by deleting the flanking regions from both sides of the *Sxl* locus but these lines did not yield any transformants. Finally, a 41.9 kb *Sxl* construct yielded a viable transformant and this construct has since proven reliable for obtaining transformants from commercial injection services. All the transgenes detailed in my thesis have been integrated into the *attP40* site on chromosome 2 and is our desired site to maintain a comparison standard (Fig. 2.2).

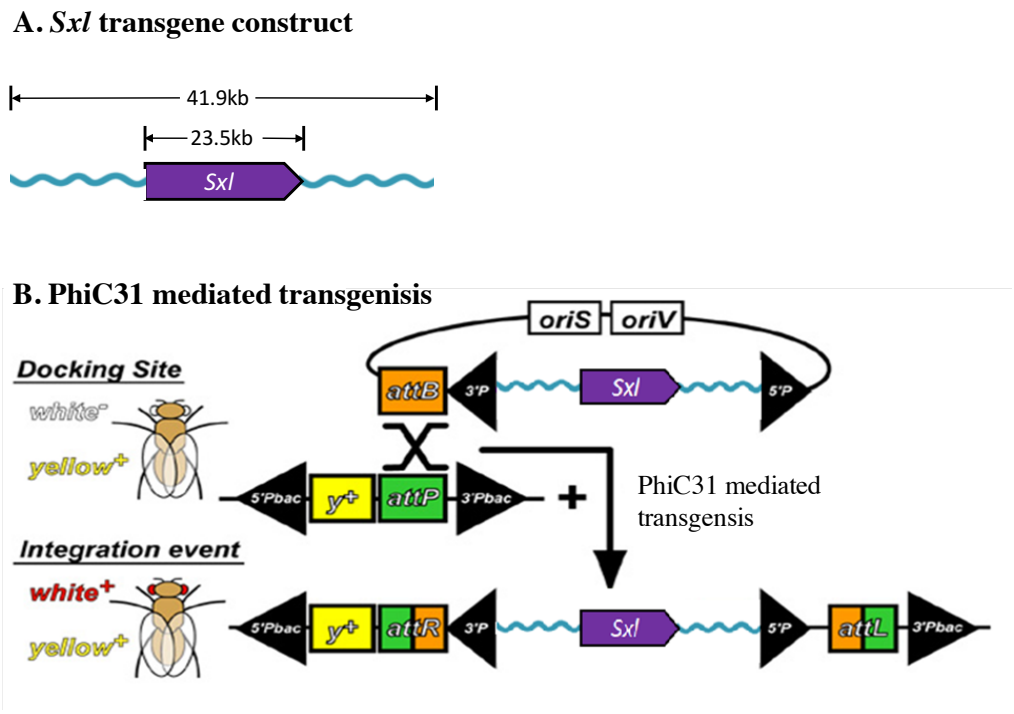

Fig. 2.2: Integration of *Sxl* transgene into the *Drosophila* genome
A) *Sxl* transgene construct, 41.9kb is detailed. It included the 23.5kb *Sxl* gene, flanked by 4.5kb upstream and 13.9kb downstream sequences. B) The attB-P[acman] is integrated at the *attP* docking site in flies expressing PhiC31 integrase. The *SxlTG* construct and the *white*$^{+}$ marker are introduced into the target location in the fly genome and the *white*$^{+}$ flies are selected.

***galK* recombineering**

galK recombineering provides a rapid method for creating small or large deletions, insertions as well as simple sequence changes to be introduced onto the transformation vector containing *Sxl*. It embodied a two-step process (Fig. 2.3). In the first step, the *E.coli galK* gene was inserted into the *Sxl*-P(acman) construct at the region where a desired mutation or a particular change is to be targeted. Recombinant bacteria were selected for the presence of *galK* by plating on minimal media containing galactose as the only carbon source. In the second step, *galK* was replaced by a repair fragment which was generated

by PCR and carried the corresponding engineered change. The recombinant bacteria here were selected by plating on minimal media containing 2-deoxy-galactose which is toxic to *galK*$^{+}$ cells. The colonies were further confirmed by PCR and sequencing [76].

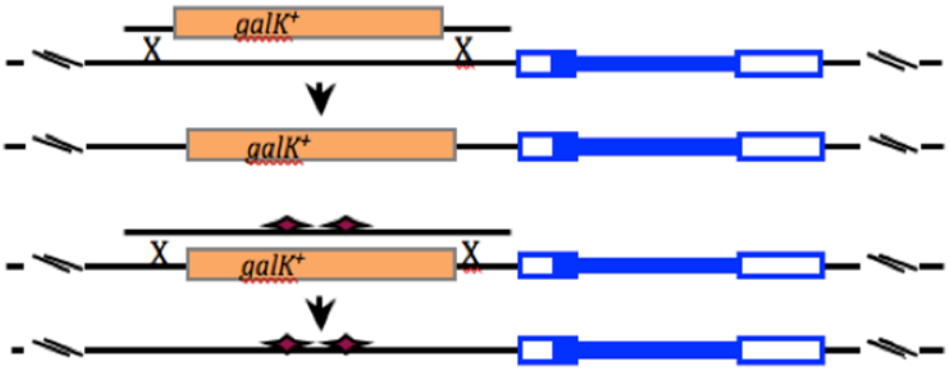

Fig. 2.3: Introducing changes in the *Sxl* sequence by *galK* recombineering
A) *galK*$^{+}$ fragment with 50bp homology to the flanking regions of the target site was introduced in the *Sxl* gene by homologous recombination. Selected for *galK*$^{+}$. B) *galK* replaced with the fragment containing the desired sequence changes via homologous replaced recombination. Selected for *galK*$^{-}$ (2-deoxy-galactose resistance).

Functionality of the *Sxl* transgene system

The transformants were tested for full function by performing genetic complementation tests in *Sxl* mutant backgrounds, Sxl^{f7bO} and Sxl^{f1}. Sxl^{f7bO} is a deletion mutation with the deletion of the entire *Sxl* transcription unit and an undefined amount of flanking DNA [78] while Sxl^{f1} is a null mutation that blocks the inclusion of exon 8 mRNA splicing of all *Sxl* transcripts. Both, Sxl^{f7bO} and Sxl^{f1} are female lethal. The transgene fully complemented the

two null *Sxl* mutations, as one copy of the *SxlTG* was able to fully rescue female lethality (Table 2.1) with the resulting fly lines appearing fully fertile.

Table 2.1: Sxl^{f1} and Sxl^{7bO} female viability data

Genotype	No of viable females	% female viability	Genotype	No of viable females	% female viability
$\frac{Sxl^{f1}}{+};\frac{+}{+}$	138	100 (reference)	$\frac{Sxl^{7bO}}{+};\frac{+}{+}$	127	100 (reference)
$\frac{Sxl^{f1}}{+};\frac{Sxl-TG}{+}$	161	116	$\frac{Sxl^{7bO}}{+};\frac{Sxl-TG}{+}$	118	92
$\frac{Sxl^{f1}}{Sxl^{f1}};\frac{+}{+}$	0	0	$\frac{Sxl^{7bO}}{Sxl^{7bO}};\frac{+}{+}$	0	0
$\frac{Sxl^{f1}}{Sxl^{f1}};\frac{Sxl-TG}{+}$	150	108 (experiment)	$\frac{Sxl^{7bO}}{Sxl^{7bO}};\frac{Sxl-TG}{+}$	117	92 (experiment)

Progeny from the cross ♀♀ *Sxl*$^{-}$/+; +/+ × ♂♂ *Sxl*$^{-}$/*Y*; TG/+ were counted. The *Sxl*$^{-}$ alleles tested were *y w cm* Sxl^{f1} *ct*/*Binsincy* and *y w cm* Sxl^{7bO}/*Binsincy*.

Designing allele specific markers and its associated challenges

The first exon and intron of *SxlPe* transcripts, and the second exon of *Pm*-RNA of the transgenes are known to be conserved [79] and this region was swapped in each of the transgenes for corresponding sequences from another fly species. A variety of species, phylogenetically far and near were used because the outcome of the change on *Sxl* function could not be predicted. The transgenic lines with changes from *D. ananassae, D. persimilis and D. virilis*, failed to complement Sxl^{f7bO} and Sxl^{f1} but those from *D. eugracilis* and *D. erecta* complemented Sxl^{f7bO} and Sxl^{f1}.

In theory, interchanging exons should not have affected *Sxl* function but some of them did. Further genetic tests were carried out to learn, if these transgenic lines complemented Sxl^{f9}. Sxl^{f9} is a loss of function allele that is defective for the early function of *Sxl* and thereby affects the establishment of female identity [20, 80]. It carries a nonsense mutation in exon E1 that truncates the early form of *Sxl* protein after amino acid 21. As expected, the transgenic lines with changes from *D. eugracilis and D. erecta* complemented Sxl^{f9} but so did *D. persimilis* (Table 2.2). This showed that the changes from *D. persimillis* did not affect the early function of *Sxl*, and so can be used to study *SxlPe* activity. Transgenic lines with changes from *D. ananassae, and D. virilis,* however, failed to complement Sxl^{f9} and could not be used.

Table 2.2: Analysis of the transgenic lines with the designed allele-specific changes in E1 to A2 region

Species source for the allele-specific changes	**Complemented** Sxl^{f9}	**Complemented** Sxl^{f7bO} & Sxl^{f1}	**Specific detection by *in situ* hybridization**
D. melanogaster	+	+	+
D. persimilis	+	-	+
D. ananassae	-	-	n/d
D. virilis	-	-	n/d
D. eugracilis	+	+	+
D. erecta	+	+	+
D. willistoni	-	-	n/d

+ denotes a positive outcome, - denotes a negative outcome and n/d denotes not done.

SxlPe activity of the *Sxl* transgene system followed by *in situ* hybridization

The genetic tests characterized the viability function of the transgenes in detail. To analyze the *SxlTG* further at the molecular level, *SxlPe* expression from the transgenes was observed by *in situ* hybridizations. *In situ* hybridization experiments were performed on the transgenic line with changes from *D. persimilis* (*Sxl-Persi-TG*), *D. erecta and D. eugracilis* (*Sxl-Eug-TG*) in a wild type background. The *SxlPe* activity of the *Sxl-Persi-TG* and the *Sxl-Eug-TG* lines mimicked the endogenous *Sxl* expression observed in wild type embryos (Fig. 2.4). In case of the transgenic line with changes from *D. erecta,* the probe used in the experiment, detected transcripts both from the *SxlTG* as well as the endogenous loci. The high sequence similarity between *D. melanogaster and D. erecta* was indeed a limitation and attempts to design a probe to overcome this problem was futile. From the collective information regarding the transgenic lines, the *Sxl-Persi-TG* and *Sxl-Eug-TG* lines were determined as the most suited to build the *SxlTG* system. *Sxl-Persi-TG* was the designated control and *Sxl-Eug-TG,* the experimental transgene. The experimental transgene being fully functional could be used to perform both, molecular and genetic analyses.

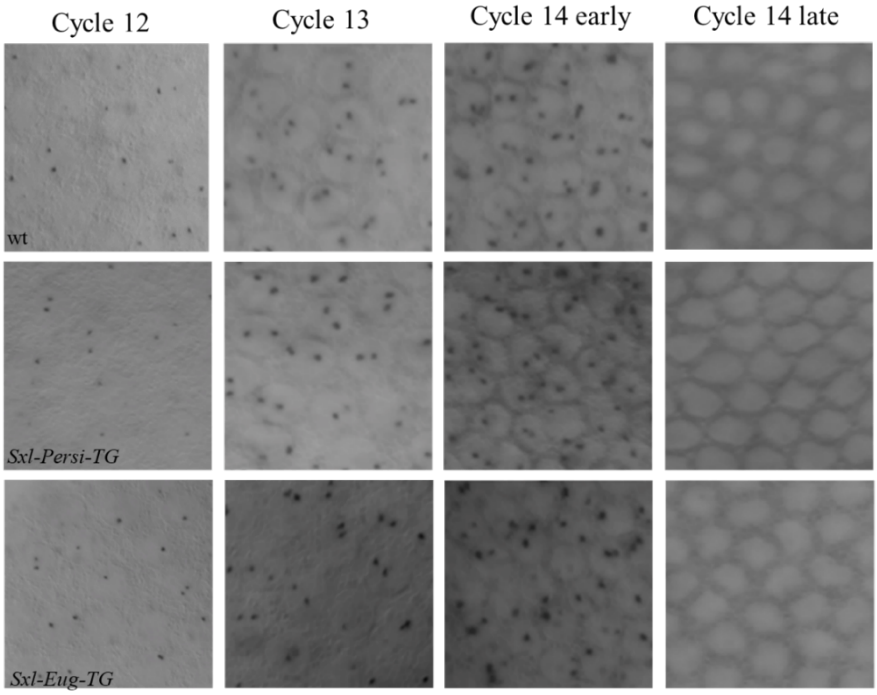

Fig. 2.4: *In situ* hybridization showed that the *Sxl* transgenic lines mimicked wildtype *SxlPe* expression

Nuclear dots represent nascent *SxlPe* transcripts. Top row: wildtype (wt) female embryos stained using *SxlPe* probe. Middle row: Female embryos carrying *Sxl-Persi-TG* (control transgene) stained using *D. persimilis SxlPe* intron-exon probe. Bottom row: Female embryos carrying *Sxl-Eug-TG* (experimental transgene) stained using *D. eugracilis SxlPe* intron-exon probe. Nuclear cycles (12, 13 and 14) are indicated; nuclear cycle 14 can be divided into early (≤ 5min) and late (≤ 30min) stages of cellularization cycles.

SxlPe activity of the *Sxl* transgene system followed by fluorescent *in situ* hybridization (FISH)

FISH was performed on Sxl^{7bO}/ Sxl^{7bO} embryos heterozygous for *Sxl-Persi-TG* (control) and *Sxl-Eug-TG* (experimental). The designed FISH probes, fluorescein-labeled *D. persimilis SxlPe* intron probe and dig-labeled *D. eugracilis SxlPe* intron probe specifically detected the control transgene and experimental transgenes respectively without

hybridizing to the endogenous *SxlPe* and therefore could be used in any genetic background including wild type. Each FISH probe was attached to a different fluorescent dye, which allowed us to visualize the *SxlPe* mRNA from control (false colored as red) and experimental (false colored as green) transgenes in separate laser channels (Fig. 2.5). As a result, the *SxlPe* activity of both the transgenes were followed independently in every nucleus of the embryo using high quality FISH signals.

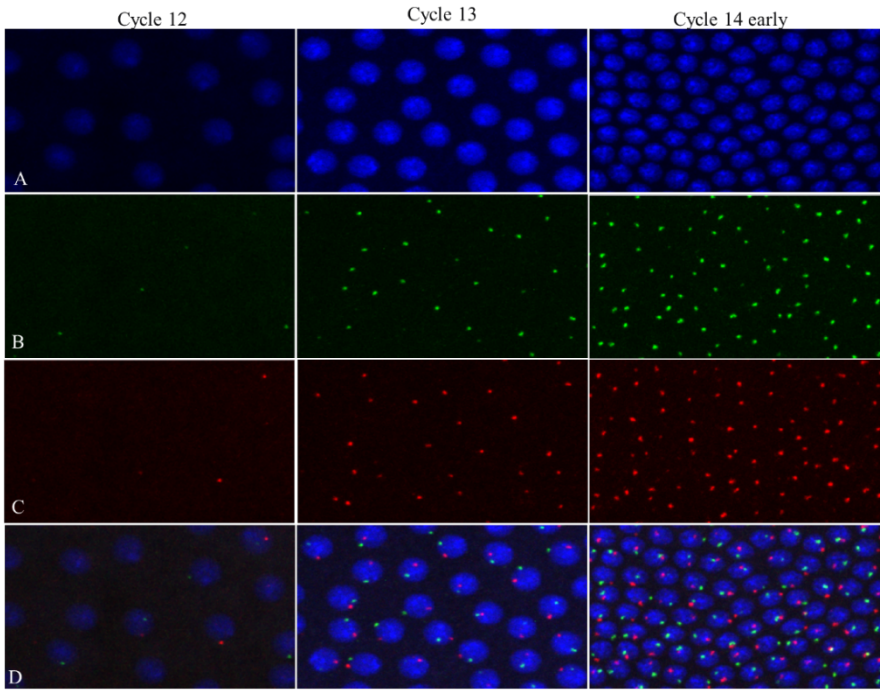

Fig. 2.5: FISH image depicting the *SxlPe* activity of the *Sxl* transgene system
Magnified confocal images of cycle 12, cycle 13 and early cycle 14 embryos carrying both *Sxl-Persi-TG* (control) and *Sxl-Eug-TG* (experimental). A) DAPI staining of nucleus. B) Nuclear dots (green) represent *SxlPe* transcripts from *Sxl-Eug-TG*. C) Nuclear dots (red) represent *SxlPe* transcripts from *Sxl-Persi-TG*. D) Merged images of A, B and C.

Automated quantification analysis of FISH images

The high-resolution confocal images of *Sxl* transgene system not only allowed qualitative analysis of *SxlPe* expression pattern but also provided the possibility of obtaining quantitative expression profiles for comparing our control and experimental transgenes. At present this aspect of my transgenic system remains incompletely developed. Our plan is to continue to work with Dr. Stan Vitha of the Texas A&M MIC center to better exploit the potential of the system. So far, quantification assessment of FISH images was achieved via ImageJ marco script developed by Dr. Vitha. To begin with, 2D image for each whole-mount embryo are generated by combining the maximum pixel intensity from every Z-stack. In the blue channel, boundaries of each nuclei were determined by DAPI signal to generate a nuclei mask image. Using this image, pixels from red (control) and green (experimental) channels could then be assigned to their corresponding nuclei (Fig. 2.6A). Each nucleus was selected as a region of interest (ROI) and the built-in ImageJ function "Anaylze Particles" was performed in green and red channels separately for each ROI. As a result, the count of particles (nuclear dots), their area and integrated density in each ROI (nucleus) are determined (Fig. 2.6B) and used to calculate the percentage of the total expressing nuclei.

A

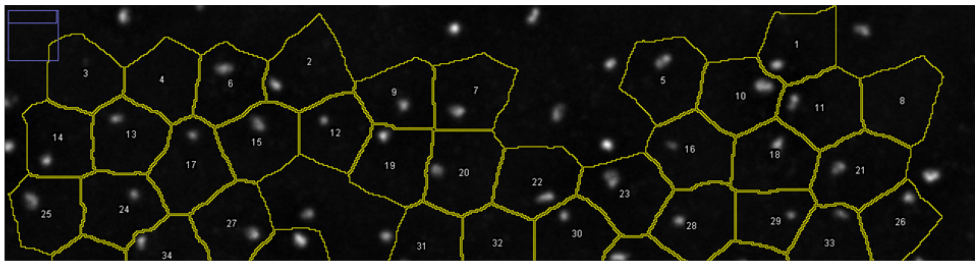

B

ROI #	Count	Total Area	Integrated Density
1	1	1.661	5946.403
2	1	1.661	5860.886
3	0	0	NaN
4	0	0	NaN
5	1	2.151	7033.714

Fig. 2.6: Example of an automated quantification analysis

A) Pixels from the red channel (control) were assigned to the corresponding nucleus. Each nucleus was selected as an ROI with boundaries determined. B) Results of "Analyze Particles" for Fig2.6A.

CHAPTER III

THE *SxlPe* PROMOTER – ENHANCER CONNECTION IN SEX DETERMINATION

The establishment promoter, *SxlPe* dictates the sexual fate decision, by sensing XSE dose [5, 8, 17]. The *cis* regulatory elements along the *SxlPe* enhancers are essential for XSE dose sensing and controlling the precise timing of *SxlPe*. However, our understanding of the roles of the specific *cis* regulatory elements and their contributions to regulation and the biochemical interactions of the XSEs is still rather primitive.

Previous attempts to learn about the *SxlPe* promoter have been insightful [71]. Estes et al. used an *in vivo*, promoter deletion analysis to functionally dissect the regions of *SxlPe* needed for sex-specific activation. They tested a series of *SxlPe* promoter fragments carrying DNA segments ranging from 0.2kb to 3.0kb upstream of the transcription start, by fusing them to *lacZ* and assaying for β-galactosidase expression in the corresponding transgenic animals.

The key findings of Estes et al. were, first, that a 1.4 kb *SxlPe*-lacZ construct behaved similarly to all larger *SxlPe-lacZ* fusions tested. The 1.4 kb *SxlPe-lacZ* line was sex specific and strongly and uniformly expressed. It produced levels of β-galactosidase that appeared to be slightly lower than the larger 3.0 ad 3.7 kb *SxlPe-lacZ* fusions but the differences, if real, were small. Deletions shorter than 1.4 kb showed declines in the levels

of *lacZ* expression and where characterized by, non-uniform expression levels along the anterior-posterior axis of the developing embryo. Surprisingly, the decrease in expression levels had little or no effect on sex specificity until promoter function was lost. Even a minimal *SxlPe* construct, 0.4 kb, maintains sex specificity, in spite of driving a low, non-uniform level of *lacZ* expression [71].

The second key finding of Estes et al. was that the minimal promoter segment required for sex-specific expression contained 0.4 kb upstream of the *SxlPe* start site. While the 0.4kb *SxlPe-lacZ* fusions maintained sex-specificity, their levels and patterns of expression were dramatically different from the 1.4, 3.0 and 3.7 kb fusions. The 0.4 kb expressed weakly and non-uniformly, with expression in some lines detectable only in the anterior regions of the embryos. An unexpected finding was that the 0.4kb lines showed higher levels of expression than the 0.8kb *SxlPe* fusions. This was attributed to the region from 0.4-0.8kb carrying negative regulatory sites proteins whose presence inhibited the function of positively acting XSE sites site in the 0.4kb promoter region. This, combined with a subsequent analysis of Sc/Da binding sites [47] led to the idea that *SxlPe* has a basal 0.4kb promoter unit, that functions as the primary determinant of female sex specificity and an augmentation region located between 0.8 and 1.4kb upstream, that drives the strong expression uniform expression needed for full *SxlPe* function [47, 71].

While these studies, provided valuable information about *SxlPe* structure, the use of *lacZ* fusions imposed limitations of what could be learned. Analysis of β-galactosidase activity

required that embryos be assayed well after the period when *SxlPe* is active. Subsequent analyses using *in situ* hybridization to *lacZ* mRNA [43, 54, 64] confirmed these general findings, however, because nascent transcripts cannot be easily detected with the intronless *LacZ* gene, key issues related to the precise timing of *SxlPe* expresion by the promoter constructs could not be assessed. Perhaps most important, the use of promoter fusions removed *SxlPe* from its normal chromosomal context and precluded any genetic assessment of whether the sequences were necessary or sufficient for *SxlPe* activity.

Defining the regulatory framework of the promoter and validating the promoter- enhancer interactions that contribute to regulation is of paramount importance to understanding *SxlPe* regulation. My approach was to use the *Sxl* transgenic system to reanalyze the previously tested promoter segments, to validate their corresponding findings.

Creating *SxlPe* promoter deletions in the *SxlTG*

A series of promoter deletions, spanning from a small 0.2 kb fragment to a large 3.7 kb segment, were tested using the *Sxl* transgene system. The *SxlPe* deletion transgene (*delPe-SxlTG*) constructs were engineered by deleting DNA upstream of the desired segment, including the distal *SxlPm* promoter. As a result, the gene upstream of *SxlPm,* CG4615 was fused directly with the desired *SxlPe* segment. This allowed the analysis of the desired promoter elements in a closer to normal genetic context and allowed them to be analyzed without interference from the upstream *SxlPm* [11].

All the promoter deletion constructs were created in the *SxlTG* and also in the experimental *TG*, *Sxl-Eug-TG* by *galK* recombineering. The idea was to use the *SxlTG* lines in the initial complementation analyses to eliminate any concerns that the related sequences from *D. eugracilis* in the region from exons E1 through L2 might influence promoter activity. Once the *D. eugracilis* and *D. melanogaster* deletion lines were confirmed to be genetically equivalent, either the *Sxl-Eug-TG* or *SxlTG* were used for *in situ* analysis according to experimental utility.

Initially, five promoter deletion constructs were created with 0.8 kb, 1.1 kb, 1.4 kb, 3.0 kb and 3.7 kb of DNA upstream of *SxlPe* (designated as $SxlPe_{0.8kb}$-*SxlTG* and so on) (Fig. 3.1). Our expectation, based on the findings of Estes et al. [71] and Yang et al. [47], was that this series would span the range from a fully functional to severely defective and allow us to define the minimal segment actually needed to provide *SxlPe* function. The number of base pairs of *SxlPe* included in the deletion constructs are the same as the ones described in Estes et al. Typically, for a $SxlPe_{0.8kb}$-*SxlTG* construct, 800 bp upstream from the first exon of the embryonic transcript was included and the termination site of the construct was also decided by the restriction site they used for every fragment respectively.

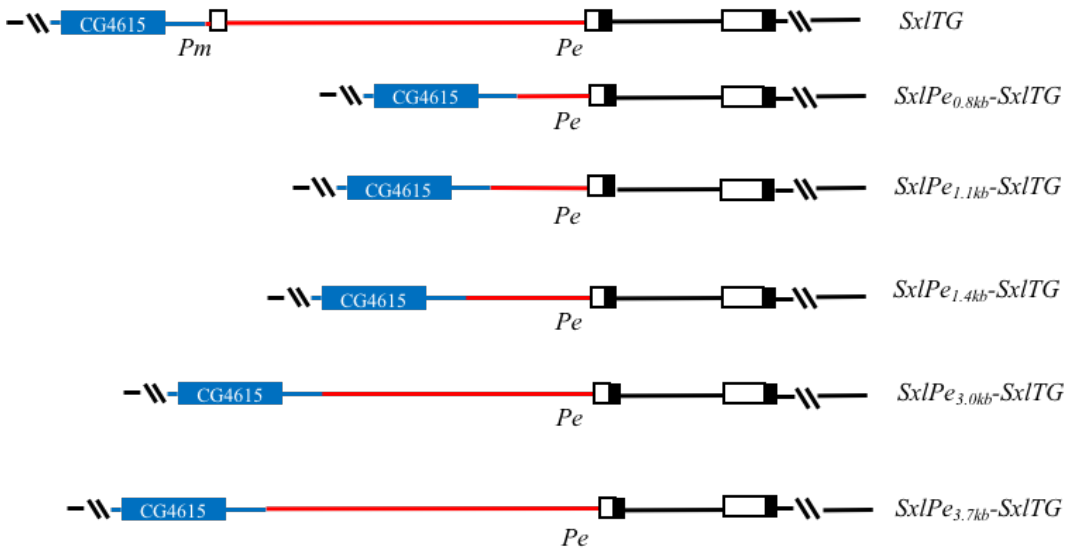

Fig. 3.1: **Schematic representation of *SxlPe*$_{0.8kb}$, *SxlPe*$_{1.1kb}$, *SxlPe*$_{1.4kb}$, *SxlPe*$_{3.0kb}$ and *SxlPe*$_{3.7kb}$ promoter constructs in the *SxlTG***
The red segment represents the *SxlPe* enhancer region included in the constructs. Sequences upstream from the first exon of *SxlPe* was included and the termination site of the construct was decided by the restriction site used for the corresponding fragments in Estes et al. The blue segment represents the region upstream of *SxlPm*.

Genetic tests of the effects of *SxlPe* deletions on promoter activity

Whether or not a *SxlPe* deletion transgene construct is truly sufficient to drive *Sxl* expression can be answered by its ability to complement *Sxl* mutations defective for the early (establishment) isoform of SXL. Therefore, the *delPe-SxlTG* constructs were subjected to a range of complementation tests to analyze their effects on female viability. Since, the *delPe-SxlTG* lack a functional *SxlPm* promoter, these constructs cannot complement *Sxl* null mutations such as, Sxl^{f1} or the deletion mutation, $Df(1)Sxl^{7B0}$. (Control experiments confirmed that deletion of *SxlPm* leaves the deletion constructs

unable to provide the *Sxl* maintenance function needed to complement Sxl^{f1} and Sxl^{7BO} (data shown in Appendix A)).

Instead I used Sxl^{f9}, an early defective allele carrying a nonsense mutation that truncates the *Sxl* exon E1 coding sequence at amino acid 21. Sxl^{f9} thus fails to provide the *SxlPe*-derived protein needed to initiate autoregulatory splicing but is capable of providing all other forms of *Sxl* protein. Complementation tests were carried with the Sxl^{f9} mutants with the results shown in Table 3.1. In each case a single copy of the respective *delPe-SxlTG* completely rescued female lethality as did the control *SxlTG* with all *Sxl* sequences intact. This proved that the *delPe-SxlTGs* were each capable of providing sufficient *Sxl* function to rescue the early-defective Sxl^{f9} allele, a result not anticipated based on the phenotypes observed for *SxlPe-lacZ* fusions [47, 71].

Table 3.1: All *delPe-SxlTG* rescued female lethality in Sxl^{f9} mutant females

Genotype	$SxlPe_{0.8kb}$ *SxlTG*	$SxlPe_{1.1kb}$ *SxlTG*	$SxlPe_{1.4kb}$ *SxlTG*	$SxlPe_{3.0kb}$ *SxlTG*	$SxlPe_{3.7kb}$ *SxlTG*	*SxlTG*
$\frac{Sxl^{f9}}{Sxl^{f9}}; \frac{TG}{+}$	92.4 (171)	111.2 (99)	98 (147)	92.3 (168)	140.3 (94)	110.9 (112)

Crosses ♀♀ *w Sxl*^{f9} *ct*/*Binsincy*; +/+ × ♂♂ *w Sxl*^{f9} *ct* /Y; TG/+
Numerical data represent percentage of female viability. Numerical data in parenthesis represent the number of viable females.
The siblings without transgenes were used as reference.

My finding that the 0.8 kb *SxlPe* TG rescued Sxl^{f9} was particularly surprising because the 0.8 kb construct used by Estes et al., expressed *lacZ* somewhat non-uniformly and at levels far below those produced by the larger promoter fragments. One possible explanation is that the Sxl^{f9} mutation may not be a complete null for early *Sxl* function [81] presumably due to read-through of the nonsense mutation, and thus can be rescued by lower than expected levels of *SxlPe* expression. A second possibility is that the 0.8 kb *SxlPe-lacZ* fusions may not have accurately reported promoter function given their artificial sequence context and chromosomal sites of insertion. Alternatively, it may be the case that only low-levels of *SxlPe* activity are all that is required to initiate the autoregulatory splicing loop in the embryo. To further test these ideas, I performed more stringent complementation tests and analyzed the expression from the *delPe* transgenes by *in situ* hybridization. As a first step, I tested the *delPe* constructs in the *Sxl-Eug-TGs*, for their ability to complement Sxl^{f9} and obtained results indistinguishable from those with the *SxlTG*s bearing only *D. melanogaster* DNA (Sxl^{f9} data for *delPe-Sxl-Eug-TGs* is shown in Appendix A). Accordingly, I used either *SxlTG* or *Sxl-Eug-TG* in subsequent experiments according to which was most appropriate experimentally.

A more stringent test: complementing Sxl^{f9}/Sxl^{f1} heterozygotes

In the genetic complementation tests with the Sxl^{f9} mutant, all the *SxlPe* deletion variants fully rescued female viability. As a more stringent test of *SxlPe* function I analyzed the ability of the *SxlPe* deletion TGs to complement Sxl^{f9}/Sxl^{f1} heterozygotes. Sxl^{f1} is a null mutation that blocks proper splicing of all *Sxl* mRNAs. Sxl^{f9}/Sxl^{f1} heterozygotes should

be less easily rescued by low level *SxlPe* expression than Sxl^{f9}/Sxl^{f9} females because there should be less residual early *Sxl* expression to initiate autoregulatory splicing and less late SXL protein to lock in and maintain stable RNA splicing [12, 18].

Table 3.2: Promoter deletion restores female viability in Sxl^{f9}/Sxl^{f1} mutant females

Genotype	$SxlPe_{0.8kb}$ *SxlTG*	$SxlPe_{1.1kb}$ *SxlTG*	$SxlPe_{1.4kb}$ *SxlTG*	$SxlPe_{3.0kb}$ *SxlTG*	$SxlPe_{3.7kb}$ *SxlTG*	*SxlTG*
$\frac{Sxl^{f9}}{Sxl^{f1}}; \frac{TG}{+}$	38.6 (39)	74.1 (83)	99.1 (106)	104.2 (99)	99.0 (99)	114.6 (55)

Crosses ♀♀ *y w cm* Sxl^{f1} *ct /Binsincy*; +/+ × ♂♂ *w* Sxl^{f9} *ct* /Y; TG/+
Numerical data represent percentage of female viability. Numerical data in parenthesis represent the number of viable females.
The siblings without transgenes were used as reference.
*Similar viability results were obtained when *delPe-Sxl-TGs* were tested (data shown in Appendix A).

I found that the five *delPe-SxlTG* lines all complemented Sxl^{f9}/Sxl^{f1} heterozygotes, however, the data revealed that the smaller $SxlPe_{0.8kb}$-*SxlTG* and $SxlPe_{1.1kb}$-*SxlTG* transgenes were less effective at rescue than were the $SxlPe_{1.4kb}$-*SxlTG*, $SxlPe_{3.0kb}$-*SxlTG* and $SxlPe_{3.7kb}$-*SxlTG* lines (Table 3.2). $SxlPe_{1.1kb}$-*SxlTG* showed some decrease in female viability and it could not rescue females as well as the larger *delPe-SxlTG*.

$SxlPe_{0.8kb}$-*SxlTG* on the other hand, showed a significant decrease in percentage female viability (38%), much lesser than what was observed with the homozygous Sxl^{f9}

complementation data (92%). This revealed that, although, the *SxlPe*$_{0.8kb}$ is sufficient for activation of *SxlPe*, it may not be a strong enhancer as the rest of the *delPe-SxlTG*.

In situ hybridization of *SxlPe* deletion constructs

The nature of *SxlPe* activation and *SxlPe* expression levels in embryos carrying two copies of the *delPe-SxlTGs* were analyzed by *in situ* hybridization using the *D. eugracilis SxlPe* intron probe. All the *SxlPe* deletion constructs initiated *SxlPe* expression at nuclear cycle 12, consistent with the onset of *SxlPe* activity in wild type. In the progression to cycle 13 and cycle 14, a myriad of expression levels was observed, ranging from a weak expression to a wild type *SxlPe* expression depending on the type of *SxlPe* deletion construct (Fig. 3.2 and 3.3). Each of the construct-specific *SxlPe* expression pattern is described below.

In embryos carrying the *SxlPe*$_{0.8kb}$*-SxlTG*, *SxlPe* expression was low, non-uniform and missing in a large fraction of nuclei in cycles 13 and 14. Among the expressing nuclei, a significant number of them only activated a single copy of *SxlPe*, represented as a single faint nuclear dot. The activity *SxlPe* expression differed greatly between the sibling embryos in cycles 13 and 14 (Fig. 3.2B). Approximately 50% of cycle 13 female embryos activated *SxlPe* in a very small fraction of nuclei while the rest of the embryos expressed *SxlPe* in about half of the nuclei. Similarly, cycle 14 were characterized by 70% of the female embryos with half or less, nuclei expressing with the rest expressing *Sxl* in a larger fraction of nuclei. Expression was predominantly evident as one nuclear dot. The 30% embryos with higher *SxlPe* activity are probably representative of those in the Sxl^{f9}/Sxl^{f1}

genetic background that produce enough SXL to successfully activate splicing of *SxlPm* transcripts and develop into adult females (Table 3.2).

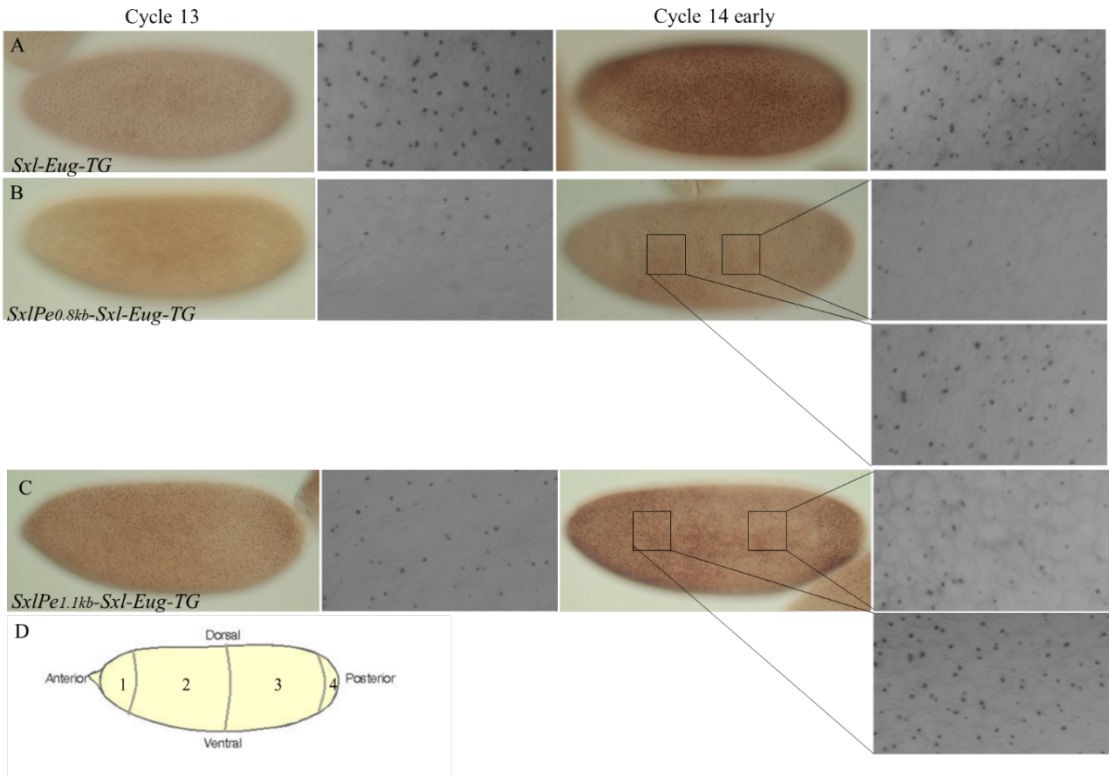

Fig. 3.2: *In situ* hybridization of $SxlPe_{0.8kb}$ and $SxlPe_{1.1kb}$ transgenic lines
Nuclear dots represent nascent *SxlPe* transcripts. Surface views of embryos were shown in both 20X and 100X. 100X pictures were taken at the center of the embryos unless indicated. A) *Sxl-Eug-TG* female embryos exhibited a uniform wild type expression, with two nuclear dots present in every nucleus. B) $SxlPe_{0.8kb}$ females failed to activate *SxlPe* in a large fraction of nuclei. None or one faint nuclear dot was detected in these nuclei. Squares indicated the regions where 100X pictures were taken. C) $SxlPe_{1.1kb}$ failed to activate *SxlPe* in some of the nuclei. Squares indicated the regions where 100X pictures were taken. D) A schematic representation of the lateral view of a whole-mount *Drosophila* embryo. The embryo is divided into regions 1-4 according to the spatial expression pattern observed in $SxlPe_{0.8kb}$-*Sxl-Eug-TG* and $SxlPe_{1.1kb}$-*Sxl-Eug-TG* embryos.

A striking feature of the *SxlPe*$_{0.8kb}$ construct, was that the majority of the embryos exhibited a strongly anterior-biased spatial expression pattern. Most of the expressing nuclei were concentrated in the anterior major (region 2) and the posterior end (region 4) compared to the anterior tip (region 1) and the posterior major (region 3) (Fig. 3.2B). The observed expression pattern here are consistent with the notion that *SxlPe*$_{0.8kb}$ enhancer may not include all the required *cis*-regulatory elements to achieve an embryo wide expression pattern [47, 71]. Overall, *SxlPe*$_{0.8kb}$ is able to activate *SxlPe* to a sufficient level to rescue females strongly deficient for early *Sxl* function, but the enhancer is challenged to do so.

SxlPe$_{1.1kb}$ is evidently a stronger enhancer than the *SxlPe*$_{0.8kb}$ as embryos carrying it show a substantial increase in the number of nuclei expressing, in the fraction of nuclei expressing two nuclear dots, and in nuclear dot staining intensity (Fig. 3.2C). Half of the female embryos carrying the *SxlPe*$_{1.1kb}$-*SxlTG*, in both cycle 13 and 14, displayed a uniform, almost wild type expression with a slightly lower staining intensity of the nuclear dots compared to wild type. However, the other half, failed to activate *SxlPe* in some nuclei and those that expressed showed an anterior-biased spatial expression pattern, reminiscent of the one observed in the *SxlPe*$_{0.8kb}$-*SxlTG* line. The expressing regions of the *SxlPe*$_{1.1kb}$-*SxlTG* was expanded compared to the 0.8 kb construct, where the active nuclei extended all the way to the anterior tip (region 1) and also further into posterior half (region 3) (Fig 3.2C). This indicates that the additional 300bp does enhance *SxlPe* expression, which is perhaps not surprising in that it carries two high-affinity E-box

binding sites for Sc/Da (see Chapter IV), but it is still apparently not enough to completely restore the wild type expression in all the female embryos. The non-uniform expression in some of the female embryos, may be the cause of the reduced female viability obtained in the Sxl^{f9}/Sxl^{f1} complementation test (Table 3.2).

Most female embryos carrying $SxlPe_{1.4kb}$-*SxlTG*, follow an expression pattern that is largely indistinguishable from wild type in both cycle 13 and 14 (Fig. 3.3B). Occasionally, there are embryos that have a small fraction of nuclei that are unable to activate *SxlPe*. Thus, it appears that while $SxlPe_{1.4kb}$ may not achieve fully wild-type expression, this has no impact on female viability. Comparison of the 1.1 kb and 1.4 kb constructs suggests that there are regulatory sequences located between -1.1 and -1.4 kb that are needed for uniform strong expression of *SxlPe*, and in this respect our findings are similar to those of Estes et al [71]. Curiously, however, the identified binding sites for the strong XSE activator Sc/Da map within 1.0 kb of the transcription start site and are thus included in both the 1.1 kb and 1.4 kb constructs [47]. It could be the case that binding sites for the XSE protein SisA, or for maternal activators map in the -1.4 to -1.1 kb interval. Alternatively, it could be the case that the lower activity of the 1.1kb fragment is a consequence of the upstream DNA fused to it. As discussed below, I have evidence that the upstream sequences can act to inhibit, or partially silence, the activity of the minimal 0.4 kb *SxlPe* promoter. If that is the case for the larger constructs, it may be the case that the sequences important for near full expression of *SxlPe* are actually located within the 1.1 kb segment but that they are not fully expressed in the context of the deletions. Arguing

against this interpretation is that the 1.1 kb and 1.4 kb *SxlPe-lacZ* fusions of Estes et al. [71], which had completely different DNA sequences fused upstream, showed similar comparative strengths to what I observed.

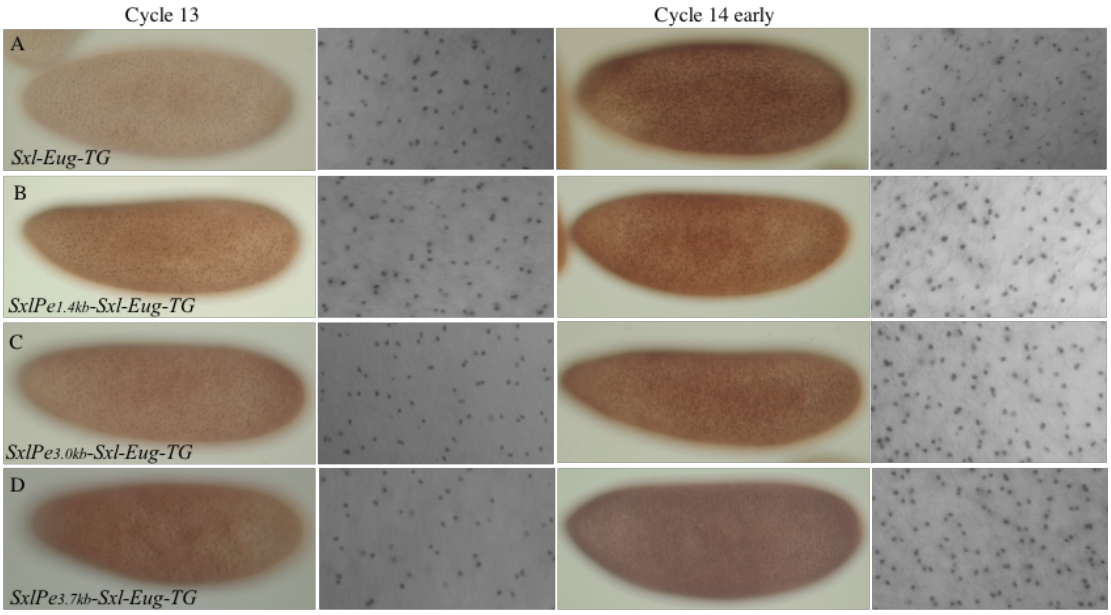

Fig. 3.3: *In situ* hybridization of $SxlPe_{1.4kb}$, $SxlPe_{3.0kb}$ and $SxlPe_{3.7kb}$ transgenic lines
Nuclear dots represent nascent *SxlPe* transcripts. Surface views of embryos were shown in both 20X and 100X. A) *Sxl-Eug-TG* female embryos exhibit a wild type expression. B) $SxlPe_{1.4kb}$ activated both *SxlPe* transcripts in most nuclei. C-D) *SxlPe* expression in $SxlPe_{3.0kb}$ and $SxlPe_{3.7kb}$ female embryos was indistinguishable from *Sxl-Eug-TG*.

The longer length $SxlPe_{3.0kb}$ and $SxlPe_{3.7kb}$ constructs function as strong, robust enhancers of *SxlPe*, as they drove a *SxlPe* expression that was indistinguishable from that of the *SxlTG* that contains all the sequences needed for *SxlPe* expression (Fig. 3.3C and 3.3D).

SxlPe activity is absent in minimal enhancers, $SxlPe_{0.2kb}$ and $SxlPe_{0.4kb}$

The surprising finding that $SxlPe_{0.8kb}$-*SxlTG* rescued the viability of Sxl^{f9} mutants, lead us to ask, if smaller promoter constructs could also activate *SxlPe*. In search for the smallest *SxlPe* deletion construct that retained sex specificity, two promoter deletion constructs, $SxlPe_{0.2kb}$ and $SxlPe_{0.4kb}$ were created in the *SxlTG*. The promoter activity of each was assayed by analyzing its ability to recue homozygous Sxl^{f9} females. Neither $SxlPe_{0.2kb}$ nor $SxlPe_{0.4kb}$ complement the Sxl^{f9} mutants when present in one or two copies (Table 3.3).

Table 3.3: $SxlPe_{0.2kb}$ and $SxlPe_{0.4kb}$ are not sex specific

Genotype	$SxlPe_{0.2kb}$ *SxlTG*	$SxlPe_{0.4kb}$ *SxlTG*
$\frac{Sxl^{f9}}{Sxl^{f9}}; \frac{TG}{+}$	0 (0)	0 (0)
$\frac{Sxl^{f9}}{Sxl^{f9}}; \frac{TG}{TG}$	0 (0)	0 (0)

Crosses ♀♀ *w* Sxl^{f9} *ct*/*Binsincy*; TG/+ × ♂♂ *w* Sxl^{f9} *ct* /Y; TG/+.
Numerical data represent percentage of female viability. Numerical data in parenthesis represent the number of viable females.
Numbers indicate the percentage of female viability.

Adding spacer DNA to separate the $SxlPe_{0.4kb}$ enhancer from upstream sequences reinstates *SxlPe* activity

Because the $SxlPe_{0.4kb}$ and the $SxlPe_{0.8kb}$ enhancer had opposite outcomes in functional tests, we scrutinized the sequences that differ between them. The $SxlPe_{0.4kb}$ contains all the known Sc/Da and Dpn binding in the region [47, 64] except two STAT binding sites,

STAT site 2 and site 3 that had minimal effect on *SxlPe-lacZ* activity [54]. In addition, the proximal 0.4 kb region is highly conserved between *Drosophila* species whereas the 0.8 kb segment is not [82] (Erickson unpublished). Additionally, Estes et al. [71] found that the 0.4 kb construct drove a stronger *lacZ* expression than the 0.8 kb version, suggesting that if anything, that the -0.8 to -0.4 kb segment might have negative regulatory sequences located within. We considered the possibility that the design of our promoter deletions could have juxtaposed upstream DNA that locally inhibited the expression of *SxlPe*.

I tested this idea by creating the $SxlPe_{0.4kbgalK}$ construct. $SxlPe_{0.4kbgalK}$ has 1.2 kb of bacterial *galK* sequences inserted between the - 0.4 kb breakpoint and the upstream DNA in the context of the *Sxl-Eug-TG* (Fig. 3.4A). Bacterial sequences were chosen for experimental convenience with the expectation that the *galK* segment would have no influence on the *SxlPe* promoter. I found that the $SxlPe_{0.4kbgalK}$-*SxlTG* fully rescued Sxl^{f9} and partially rescued the Sxl^{f9}/Sxl^{f1} heterozygotes, suggesting that the 0.4 kb proximal construct can activate *SxlPe* to levels comparable to those of the $SxlPe_{0.8kb}$-*SxlTG* (Fig. 3.4B and 3.4C).

A

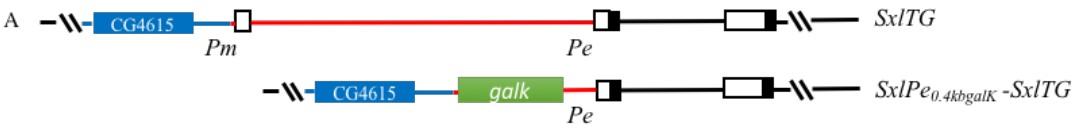

B

Genotype	*SxlPe0.4kb SxlTG*	*SxlPe0.4kbgalK SxlTG*	*SxlPe0.8kb SxlTG*	*SxlTG*
$\frac{Sxl^{f9}}{Sxl^{f9}}; \frac{TG}{+}$	0 (0)	92.6 (100)	102.9 (142)	89.7 (96)

C

Genotype	*SxlPe0.4kb SxlTG*	*SxlPe0.4kbgalK SxlTG*	*SxlPe0.8kb SxlTG*	*SxlTG*
$\frac{Sxl^{f9}}{Sxl^{f1}}; \frac{TG}{+}$	0 (0)	28.9 (28)	38.6 (39)	114.6 (55)

D

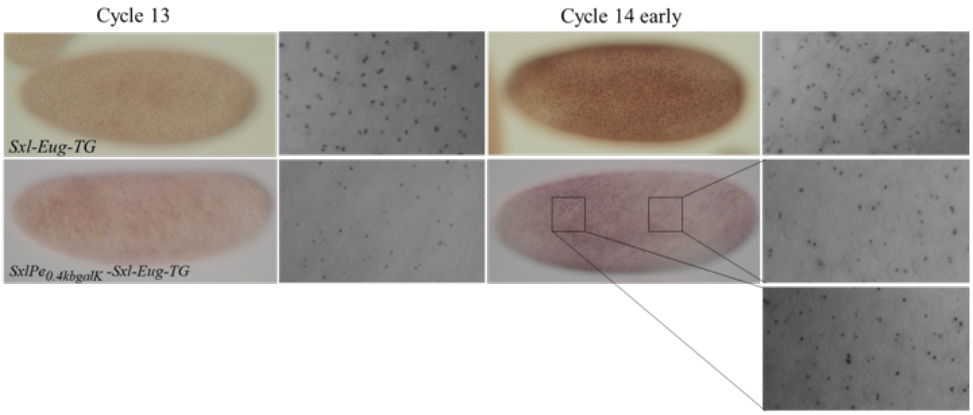

Fig. 3.4: *SxlPe*$_{0.4kbgalk}$ promoter construct reinstates *SxlPe* activity
A) Schematic representation of *SxlPe*$_{0.4kbgalk}$ promoter construct in the *SxlTG*. B) *Sxl*^{f9} complementation: crosses ♀♀ *w Sxl*^{f9} *ct*/*Binsincy*; +/+ × ♂♂ *w Sxl*^{f9} *ct* /Y; TG/+. Numbers indicate the percentage of female viability. The siblings without transgenes were used as reference. C) *Sxl*^{f9}/ *Sxl*^{f1} complementation: crosses ♀♀ *y w Sxl*^{f1} *ct*/*Binsincy*; +/+ × ♂♂ *w Sxl*^{f9} *ct* /Y; TG/+. Numbers indicate the percentage of female viability. The siblings without transgenes were used as reference. D) *In situ* hybridization of *SxlPe*$_{0.4kbgalK}$ transgenic lines. Nuclear dots represent nascent *SxlPe* transcripts. Surface views of syncytial nuclei were shown in both 20X and 100X.

In situ hybridization data from the *SxlPe*$_{0.4kbgalK}$-*SxlTG*, proved interesting. *SxlPe*$_{0.4kbgalK}$-*SxlTG* activated *SxlPe* as expected given the genetic tests and the *SxlPe* expression progressed from cycle 12-14. There were clear non-uniformities in expression during nuclear cycles 13 and 14 but the most distinguishing feature was that the *SxlPe*$_{0.4kbgalK}$-*SxlTG* derivative had stronger and more complete *SxlPe* expression, than did *SxlPe*$_{0.8kb}$-*SxlTG* (Fig. 3.4D). While, the expression pattern of the *SxlPe*$_{0.4kbgalK}$ line had several attributes in common with the *SxlPe*$_{0.8kb}$ line a minimal enhancer, such as a large number of the non-expressing nuclei and the presence of numerous nuclei with only single dots, the *SxlPe*$_{0.4kbgalK}$-*SxlTG* activated *SxlPe* in many more number of nuclei (~50% or higher) and appeared to drive stronger *SxlPe* expression than observed in most *SxlPe*$_{0.8kb}$-*SxlTG* embryos. As, the nuclear dot staining intensity of this line was slightly lower than *SxlPe*$_{1.1kb}$-*SxlTG* and the fact that none of the female embryos were able to reach a wild type expression, it was deemed a less effective enhancer than the *SxlPe*$_{1.1kb}$. The *SxlPe*$_{0.4kbgalK}$ construct still exhibited the anterior-biased, spatial expression pattern that is characteristic of the *SxlPe*$_{0.8kb}$-*SxlTG* construct.

The results obtained clearly demonstrate the minimal *SxlPe* promoter sufficient to complement the early defective *Sxl*^{f9} allele are contained within the *SxlPe*$_{0.4kbgalK}$-*SxlTG*. This finding also strongly suggests that DNA from CG4615, the gene upstream of and adjacent to *Sxl* had the effect of partially silencing *SxlPe* in at least some of our constructs. In particular, silencing may have influenced our comparisons between the 1.4 and 1.1 kb constructs (discussed above), and between the 0.8 kb, and 0.4 kb *galK* constructs. My

observation that *SxlPe*$_{0.4kbgalK}$-*SxlTG* expressed more strongly than did the *SxlPe*$_{0.8kb}$-*SxlTG* is consistent with the results of Estes et al. [71] who observed, using *SxlPe-lacZ* fusions with entirely different sequences abutting *SxlPe*, that their 0.4 kb lines expressed more strongly than the longer 0.8 kb versions. Estes et al [71] interpreted this as evidence that the -0.8 to -0.4 segment contained unidentified negative regulatory elements. That interpretation is also consistent with our findings; however, we cannot exclude the possibility that the -0.8 to -0.4 kb segment was simply less effective at suppressing the silencing DNA than was the longer *galK* segment. Regardless of the answer, the positive results obtained with the *SxlPe*$_{0.4kbgalK}$-*SxlTG* define the minimal upstream DNA needed to complement the early defective *Sxl*^{f9} allele.

SxlPe$_{0.8kb}$ and *SxlPe*$_{0.4kgalK}$ enhancers are sensitive to reductions in the XSE dose

The minimal *SxlPe*$_{0.8kb}$ and *SxlPe*$_{0.4kbgalK}$ *SxlPe* transgenes are able to fully rescue the early *Sxl* function missing in *Sxl*^{f9} mutants despite being expressed in fewer nuclei and at apparently lower levels than wild type. This weak expression suggested that the function of the shorter *SxlPe* transgenes might be extremely sensitive to alterations in XSE gene dose. Genetic complementation crosses were performed to scrutinize the viability of *Sxl*^{f9} females carrying a reduced XSE dose. I examined the alleles, *sc*^{M6} or *runt*^{3}. The larger *SxlPe*$_{1.1kb}$-*SxlTG*, *SxlPe*$_{1.4kb}$-*SxlTG*, *SxlPe*$_{3.0kb}$-*SxlTG* and the *SxlPe*$_{3.7kb}$-*SxlTG*, were unaffected by the loss of one dose of an XSE. Full female viability was seen in every case (Table 3.3).

Table 3.4: *SxlPe* activity of $SxlPe_{0.4kbgalK}$ and $SxlPe_{0.8kb}$ depend on XSE dose

A) Numbers of viable Sxl^{f9} mutant females with reduced *scute* dose

Genotype	$SxlPe_{0.4kbgalK}$ *SxlTG*	$SxlPe_{0.8kb}$ *SxlTG*	$SxlPe_{1.1kb}$ *SxlTG*	$SxlPe_{1.4kb}$ *SxlTG*	$SxlPe_{3.0kb}$ *SxlTG*	$SxlPe_{3.7kb}$ *SxlTG*
$\frac{Sxl^{f9}}{sc^{M6}\ Sxl^{f9}} ; \frac{TG}{+}$	19.2 (35)	0 (0)	102.6 (158)	100.9 (115)	103.4 (121)	97.8 (135)
$\frac{Sxl^{f9}}{Y} ; \frac{TG}{+}$	100 (182)	100 (72)	100 (154)	100 (114)	100 (117)	100 (138)

Crosses ♀♀ *w* Sxl^{f9} *ct* / *w* Sxl^{f9} *ct*; TG/TG × ♂♂ sc^{M6} *w* Sxl^{f9} *ct* /Y; +/+
Numerical data represent percentage of female viability. Numerical data in parenthesis represent the number of viable females.
The number of sibling brothers from the cross were used as reference.

B) Numbers of viable Sxl^{f9} mutant females with reduced *runt* dose

Genotype	$SxlPe_{0.4kbgalK}$ *SxlTG*	$SxlPe_{0.8kb}$ *SxlTG*	$SxlPe_{1.1kb}$ *SxlTG*	$SxlPe_{1.4kb}$ *SxlTG*	$SxlPe_{3.0kb}$ *SxlTG*	$SxlPe_{3.7kb}$ *SxlTG*
$\frac{Sxl^{f9}}{Sxl^{f9}\ runt^{3}} ; \frac{TG}{+}$	11.0 (16)	0 (0)	142.6 (134)	144.6 (120)	120.2 (149)	172.2 (155)
$\frac{Sxl^{f9}}{Y} ; \frac{TG}{+}$	100 (146)	100 (117)	100 (94)	100 (83)	100 (124)	100 (90)

Crosses ♀♀ *w* Sxl^{f9} *ct* / *w* Sxl^{f9} *ct*; TG/TG × ♂♂ *w* Sxl^{f9} *ct* $runt^{3}$ *f* /Y_{mal+}; +/+
Numerical data represent percentage of female viability. Numerical data in parenthesis represent the number of viable females.
The number of sibling brothers from the cross were used as reference.
*The >100% female viability in larger deletion constructs reflect the reduced viability of *w* Sxl^{f9} *ct* / Y*mal*+ males.

In contrast, $SxlPe_{0.8kb}$-*SxlTG* and $SxlPe_{0.4kbgalK}$-*SxlTG* were highly sensitive to reductions in XSE dose. Although, both were susceptible to reductions in XSE dose, $SxlPe_{0.8kb}$ was severely affected than the $SxlPe_{0.4kbgalK}$ construct. $SxlPe_{0.8kb}$ could not rescue female viability at all and the promoter activity was highly dependent on the dose of *sc* and *runt*. $SxlPe_{0.4kbgalK}$ construct rescued *sc* and *runt* mutants sparingly (Table 3.4), suggesting the

strength of the $SxlPe_{0.4kbgalK}$ promoter activity depends on the dose of *scute* and *runt* but still managed to be turned on in some embryos.

CHAPTER IV

REGULATORY MODULE OF XSE BINDING SITES AT *SxlPe*

The crucial decision of appropriate sexual choice is orchestrated by X signal sensing at *SxlPe*. XSE interactions at the *cis* regulatory elements present along *SxlPe* ensures proper activation of *Sxl* and sexual development. Functional validation of the known activator and repressor binding sites at *SxlPe* is key to understanding *SxlPe* regulation; from how the promoter senses XSE dose to how it responds by turning *SxlPe* on or leaving it off. Advancements in functional dissection of *SxlPe* promoter structure, however, have been held back by insufficient knowledge about the binding sites of the key regulator sisA, and also by the lack of a tool to accurately assay the effects of mutated *cis* regulatory elements *in vivo*.

Using the *Sxl* transgene system, individual or combinatorial *cis* regulatory site mutants can be easily engineered so that their effects on *SxlPe* activity and female fly viability can be studied. The system enables us to characterize each binding site mutation by detailing the onset of transcription, monitoring its timing, and comparing *SxlPe* expression levels with respect to the endogenous *Sxl*. The idea is to decipher the role of specific characteristics of the binding site, such as their location or binding affinities on promoter strength and *Sxl* activation.

Central to *Drosophila* sex determination is the X chromosome counting mechanism governed by the primary determinants, the X-signaling elements [5, 7]. Two of these XSEs, Scute and SisA are the key indicators of the X-chromosome dose [39, 41]. The XSE, Upd is the activating ligand for the JAK-STAT pathway and in turn activates the maternal Stat92E transcription factor that binds *SxlPe* to activate transcription [43, 44, 54]. Stat92E binds to three different sites at *SxlPe* but mutations in these sequences had relatively modest effects on *SxlPe.* Interestingly Stat92E function is dispensable for initial activation but is needed to maintain full expression through cycle 14 [54]. Although, *Runt*, encodes a transcription factor of the RUNX family, exerts its influence on *SxlPe* activation by antagonizing the repression of the maternally contributed co-repressor Groucho (Erickson, unpublished data).

Genetic, expression evidence and sequence evidence supports direct interaction of SisA and Scute at *SxlPe* [41, 71]. Unfortunately, nothing is known about how SisA binds *SxlPe* which leaves a significant gap in our understanding. The best understood XSE protein is Scute. Scute is a class A bHLH protein that binds DNA as a heterodimer with maternally supplied Daughterless (Da) protein. Eleven Sc/Da binding sites have been identified at *SxlPe* [47]. It seemed befitting to begin exploring Scute binding to establish the validity of our transgenic system as well as to better characterize the specific roles of the known Sc/Da binding sites in *SxlPe* regulation. While XSE activators are the central determinants of sex, they are only part of the story at *SxlPe*. Zygotically and maternally expressed negative regulators, including the bHLH repressor Dpn and its corepressor Gro are

required to maintain sex specific regulation [10, 65, 69, 83]. Our lab, previously researched the contribution of Dpn to the sex specific regulation and identified three specific binding sites at which, Dpn interacted with *SxlPe in vitro* using *SxlPe-lacZ* transgenes [64]. Mutations in each site lead to ectopic *lacZ* expression in males, consistent with their negative regulatory role, but their quantitative importance could not be assessed [64].

This chapter details the regulatory functions of Sc/Da binding sites at *SxlPe* as well as those of the repressor, Dpn. Preliminary work on other activators: including maternally supplied Stat and Zelda are described in the chapter appendix (Appendix B).

Characterizing the *cis* interactions of Sc/Da at *SxlPe*

Overview of Sc/Da binding at *SxlPe*

Scute is a class A, bHLH transcription factor that heterodimerizes with the maternal daughterless (Da) and binds to *SxlPe* to activate transcription [47, 73]. Our lab showed that Sc/Da binds to 11 sites located within the 1.4kb promoter and that binding occurred at both canonical, "E-box", and non-canonical sequences. The specific sequence information of the Sc/Da binding sites is listed in Fig.4.1A. The arrangement of these Sc/Da sites along *SxlPe* is concentrated in two clusters, sites 1-6 are located within the 400bp segment we now know to be necessary and sufficient for sex-specific expression of *SxlPe*. The others are located further upstream between 0.8kb and 1.1kb in the proposed promoter augmentation element as depicted in Fig. 4.1B. Sc/Da exhibited a range of binding affinities to the various sites, with most exhibiting relatively low affinity binding. Sites 2, 3 and 8 were bound with intermediate affinities whereas site 7, the only symmetrical canonical E-Box, was the only site bound with high affinity [47].

A mutational analysis using a variety of inactivating point mutations in the Sc/Da sites was carried out using *SxlPe-lacZ* fusions in embryos [47]. The binding sites mutants were characterized in the context of the 0.4kb, minimal *SxlPe* promoter in -390bp *SxlPe-lacZ* transgenes. Promoter activity exhibited differences between transgenic lines and also between different females within a mutant line. Despite this, a general consensus prevailed that no single site was critically important for *SxlPe* expression as each single site mutant analyzed retained sex-specific expression. Some binding site mutations caused modest

reductions in expression levels but dramatic reductions in *SxlPe-lacZ* expression were observed only when multiple Sc/Da sites were mutated. Most important for the work described here is that mutations in non-canonical Sc/Da sites 1, and 4, and in the E-box containing site 3, resulted in slightly reduced *lacZ* expression compared to unmutated transgenes. [47].

A

Type of Sequence	Consensus sequence	Sc/Da binding sites
Class A, E-box	CATCTG	3
	CAGCTG	7
	CACCTG	8
6bp, non E-box	CAGCCG	2
	CACCCG	9
7bp, non E-box	CACCTTG	1,4,11
	CAGCTTG	5,6
	CAATCTG	10

B

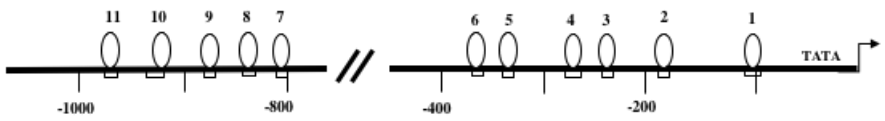

Fig. 4.1: Sc/Da binding sites at *SxlPe*
A) The nature and consensus sequences of Sc/Da binding sites. B) Schematic representation of the Sc/Da binding sites along 1.4kb, proximal *SxlPe*.

Creating *Sxl* transgenes carrying mutations in Sc/Da binding sites

I used my *Sxl* transgene system to analyze the roles of the known Sc/Da binding sites in the context of a fully functional *Sxl* locus. The experimental strategy was to create Sc/Da

site mutations in the *Sxl-Eug-TG* so that their genetic and molecular effects could be analyzed in detail. Specific sequence changes to disrupt the binding of Sc/Da for every targeted site were made using site directed mutagenesis [84, 85]. A PCR amplified fragment containing the sequence change was then incorporated into the *Sxl-Eug* transgene using *galK* recombineering. A variety of individual and combinatorial mutations in Sc/Da binding sites were successfully created. The sequence changes for each of the Sc/Da binding site analyzed are shown in Table 4.1.

Table 4.1: Mutated sequences of Sc/Da binding sites

Sc/Da site mutated	Original sequence	Mutated sequence
Sc/Da 1^-	CACCTTG	C**G**C**T**TTG
Sc/Da 2^-	CAGCCG	C**TAG**CG
Sc/Da 3^-	CATCTG	**GT**TCTG
Sc/Da 1^-2^-	CACCTTG	C**G**C**T**TTG
	CAGCCG	C**TAG**CG
Sc/Da 1^-4^-	CACCTTG	C**G**C**T**TTG
	CACCTTG	C**T**C**GA**TG

Sc/Da site 3, an E-box, is a powerful *cis* regulatory element for *SxlPe* activation

Single site changes in Sc/Da binding sites 1, 2, and 3 were analyzed. Sc/Da site 1 had the smallest effect on *SxlPe* activity. A single copy of *SxlTG* carrying a Sc/Da 1 site mutation (*Sc/Da 1*$^-$) effectively rescued both Sxl^{fl} and Sxl^{7B0} females to 77.9% and 73.1% respectively (Table 4.2). The *SxlPe* activity was scrutinized further by *in situ*

hybridization performed on embryos, homozygous for *Sc/Da 1*$^{-}$*SxlPe-Sxl-Eug-TG* using the *D. eugracilis* intron probe. I found that in spite of Sc/Da 1 being mutated, these embryos were able to turn on *SxlPe* in cycle 12 in all female embryos with defects first appearing in cycle 13. The majority of embryos examined in cycle 13 were indistinguishable from wild type, however, one-third exhibited a non-uniform pattern of *SxlPe* expression.

The range of non-uniform expression pattern observed in the Sc/Da binding site mutant embryos varied greatly and describing them was challenging. To better explain the different expression phenotypes observed, I classified them into five categories and used this as a comparison standard while describing the mutant phenotypes. (Each of the category is described in detail in Table 4.3 and the corresponding images for the categories are included in Appendix B). Classifying *SxlPe* expression into categories were primarily based on the estimated percentage of expressing nuclei. The staining intensity too contributed to the difference in expression but comparing intensity levels just by the naked eye was not reliable, making it unsuitable to be used as a main standard when categorizing. Simply using terms like high/medium/low *SxlPe* expression is misleading as it is more commonly referred to staining level rather than the expression pattern. Therefore, the term *SxlPe* activity was adopted to describe each category.

Table 4.2: Mutations in Sc/Da binding site affected female sex specificity

A) Viability of Sxl^{f1}/ Sxl^{f1} females with transgenes carrying Sc/Da binding site mutations

Genotype	*Sc/Da1⁻ SxlPe SxlTG*	*Sc/Da2⁻ SxlPe SxlTG*	*Sc/Da3⁻ SxlPe SxlTG*	*Sxl TG*
$\frac{Sxl^{f1}}{Sxl^{f1}}$; $\frac{TG}{+}$	77.9 (74)	32.2 (29)	1.3 (1)	109.9 (111)

Crosses ♀♀ *y w cm* Sxl^{f1} *ct*/*Binsincy*; +/+ × ♂♂ *y w cm* Sxl^{f1} *ct* /Y; TG/+
Numerical data represent percentage of female viability. Numerical data in parenthesis represent the number of viable females. The Sxl^{f1}/ Sxl^{f1} sibling females without transgenes were used as reference.

B) Viability of Sxl^{7BO}/Sxl^{7BO} females with transgenes carrying Sc/Da binding site mutations

Genotype	*Sc/Da1⁻ SxlPe SxlTG*	*Sc/Da2⁻ SxlPe SxlTG*	*Sc/Da3⁻ SxlPe SxlTG*	*Sxl TG*
$\frac{Sxl^{7BO}}{Sxl^{7BO}}$; $\frac{TG}{+}$	73.1 (68)	39.0 (39)	7.7 (6)	110.7 (93)

Crosses ♀♀ *y pn w* Sxl^{7BO}/*Binsincy*; +/+ × ♂♂ *y pn w* Sxl^{7BO}/Y; TG/+
Numerical data represent percentage of female viability. Numerical data in parenthesis represent the number of viable females. The Sxl^{7BO}/ Sxl^{7BO} sibling females without transgenes were used as reference.

The non-uniform expression observed in cycle 13 *Sc/Da 1⁻* females exhibited around 50% or more nuclei expressing *SxlPe* (categorized as moderately affected *SxlPe* activity or slightly affected activity), with still noticeable number of nuclei devoid of *SxlPe* expression. When advanced to cycle 14, all the embryos mimicked wild type expression (Fig. 4.2B). The wild type activity seen in cycle 14 likely explains why Sc/Da site 1 mutants exhibited such high female viability in genetic complementation tests. What is perhaps surprising is that we could not identify cycle 14 embryos with defects that might

explain why 1/4 of them failed to rescue *Sxl* mutants. One possibility is that the failure of some cycle 13 female embryos to fully activate *SxlPe* in all nuclei, caused the reductions in female viability. A second possibility, is that the two partially defective promoters interacted *in trans* to facilitate promoter activation. As discussed below in the context of Dpn binding site mutations, I have obtained evidence that active *SxlPe* promoters can exhibit transvection like effects that has been observed with transgenes in several systems.

In contrast to Sc/Da site 1, a mutation in Sc/Da site 2 (*Sc/Da 2*$^{-}$) had a significant effect on *SxlPe* activity. One copy of the *Sc/Da 2*$^{-}$ *SxlPe-Eug-TG* rescued some *Sxl*^{f1} and *Sxl*^{7bO} females but the percentage of female viability was only 32.2% and 39% (Table 4.2). To better understand why the *Sc/Da2*$^{-}$ mutants were unable to strongly rescue the *Sxl* null alleles, I analyzed expression using *in situ* hybridization. *SxlPe* activity in *Sc/Da 2*$^{-}$ mutants and wild type was indistinguishable in cycle 12. In cycles 13 and 14, however, there were obvious differences among the expressing embryos. Approximately 30% of cycle 13 female embryos (number of embryos observed in each cycle is listed in Appendix B) had a wild-type expression pattern shown with paired darkly stained nuclear dots in every nucleus. This wild-type pattern appeared to be retained through cycle 14 where I also observed that 30% of embryos appeared to be stained as the wild-type. The majority of embryos, however, had reduced *SxlPe* activity in both cycles 13 and 14. *SxlPe* activity were judged to range from strongly affected (less than 50% of the nuclei expressing with faint nuclear dots) to moderately or slightly affected activity during cycle 13 (Fig. 4.2C). In cycle 14, few expressers with strongly affected activity were observed, instead almost

all of the expressing embryos showed moderately or slightly affected *SxlPe* activity. The strong correspondence between the viability tests and expression pattern from the transgenes suggest that only those embryos which are able to achieve wild-type or near wild-type activity survive, whereas those with defects in cycles 13 and 14 fail to fully engage *Sxl* expression.

Table 4.3: Phenotypic categories of *SxlPe* activity in Sc/Da binding site mutants

Phenotypic categories	Percentage of nuclei expressing	Description
Severely affected activity	< 30%	*SxlPe* activity is observed in a small fraction (<30%) of nuclei. Majority of the expressing nuclei contain only one very faint nuclear dot.
Strongly affected activity	30%-50%	*SxlPe* activity is present in less than half of the nuclei. Expressing nuclei contain one or two faintly stained nuclear dots.
Moderately affected activity	~ 50%	*SxlPe* activity is observed in around 50% or slightly more than 50% of the nuclei. Expressing nuclei contain one or two nuclear dots that are stained slightly lighter than wildtype.
Slightly affected activity	>70%	*SxlPe* activity is detected in most (>70%) nuclei, although small patches of non-expressing nuclei still exist. Majority of the expressing nuclei contain two nuclear dots.
Wild-type activity*	100%	Embryos exhibit uniform expression pattern, with every nucleus expressing two nuclear dots.

* Wild type activity means the transgenes mimicked endogenous *SxlPe* expression with respect to all nuclei expressing two nuclear dots but does not necessarily reflect the staining intensity. The staining intensity of the nuclear dots (as seen in 100X) sometimes appeared slightly weaker than the ones observed in *Sxl-Eug-TG* (control) embryos. Staining differences however are more prominent with respect to the overall staining of embryos. A possible reason for lower staining intensity is that mutants might reach the uniform expression pattern slightly later than wild-type, leaving less time for transcripts to accumulate and subsequently resulting in lighter staining.

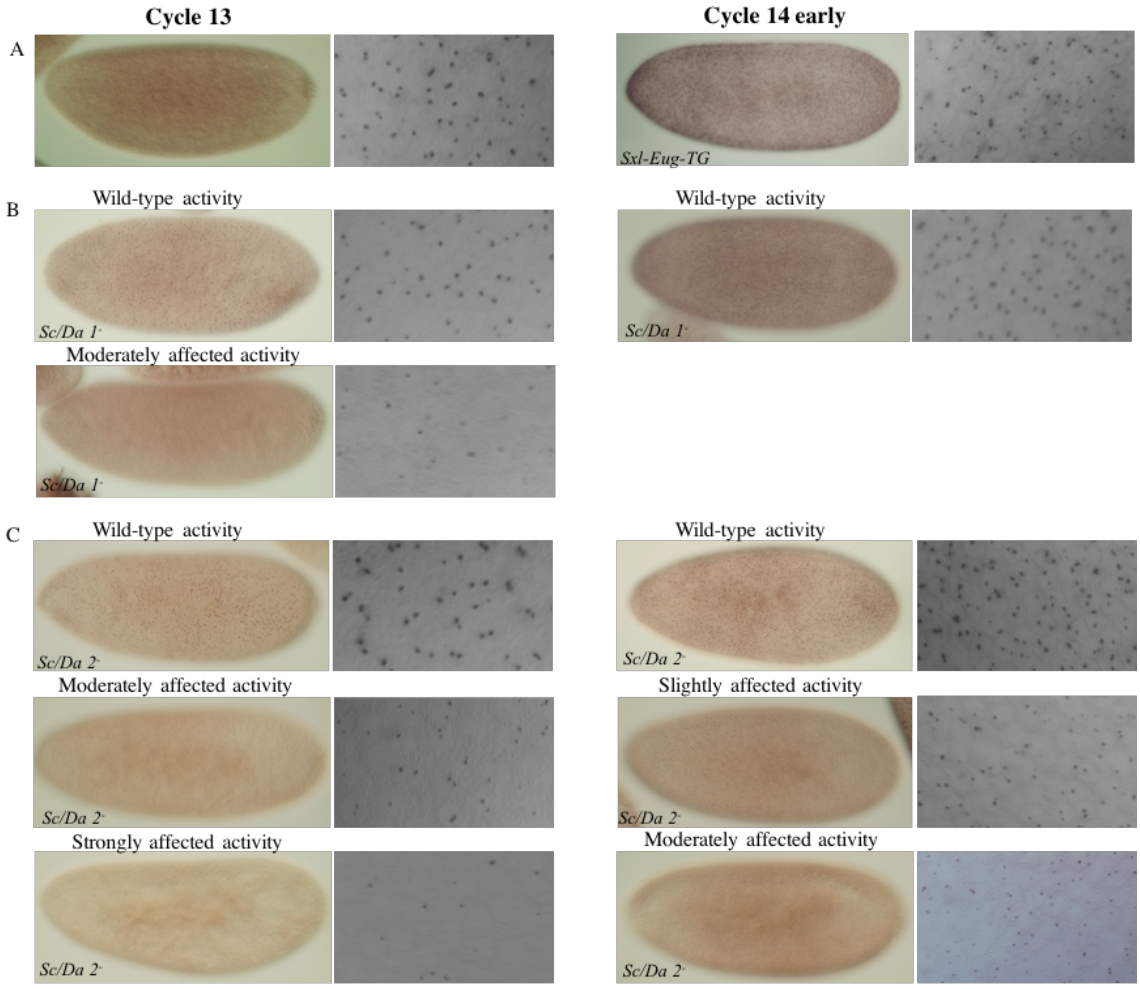

Fig. 4.2: *In situ* hybridization of *Sc/Da 1⁻SxlPe* and *Sc/Da 2⁻SxlPe* transgenic lines
Nuclear dots represent nascent *SxlPe* transcripts. Surface views of embryos were shown in both 20X and 100X. 100X pictures were taken at the center of the embryos. A) *Sxl-Eug-TG* female embryos exhibited a uniform wild type expression, with two nuclear dots present in every nucleus. B) One-third of *Sc/Da 1⁻SxlPe* females had reduced *SxlPe* expression during cycle 13. C) *SxlPe* expression in *Sc/Da 2⁻SxlPe* females varied between embryos in both cycle 13 and early cycle 14.

In contrast to what had been reported for *SxlPe-lacZ* transgenes, mutations in Sc/Da site 3 (*Sc/Da 3⁻*) had a severe effect on *SxlPe* function. A single copy of the transgene carrying *Sc/Da 3⁻* could barely rescue Sxl^{fl} or Sxl^{7bO} females as evidenced by 1.3% and 7.7%

viability respectively (Table 4.2). *In situ* hybridization of the *Sc/Da 3*$^{-}$ mutants provided several insights. *SxlPe* expression was detected in occasional nuclei at cycle 12, in 10% of the total embryos. In cycle 13, about half (44%) of the embryos showed some kind of *SxlPe* expression although, most of them had severely affected *SxlPe* activity with only a fraction of nuclei (10-30%) exhibiting faintly stained dots (Fig. 4.3B).

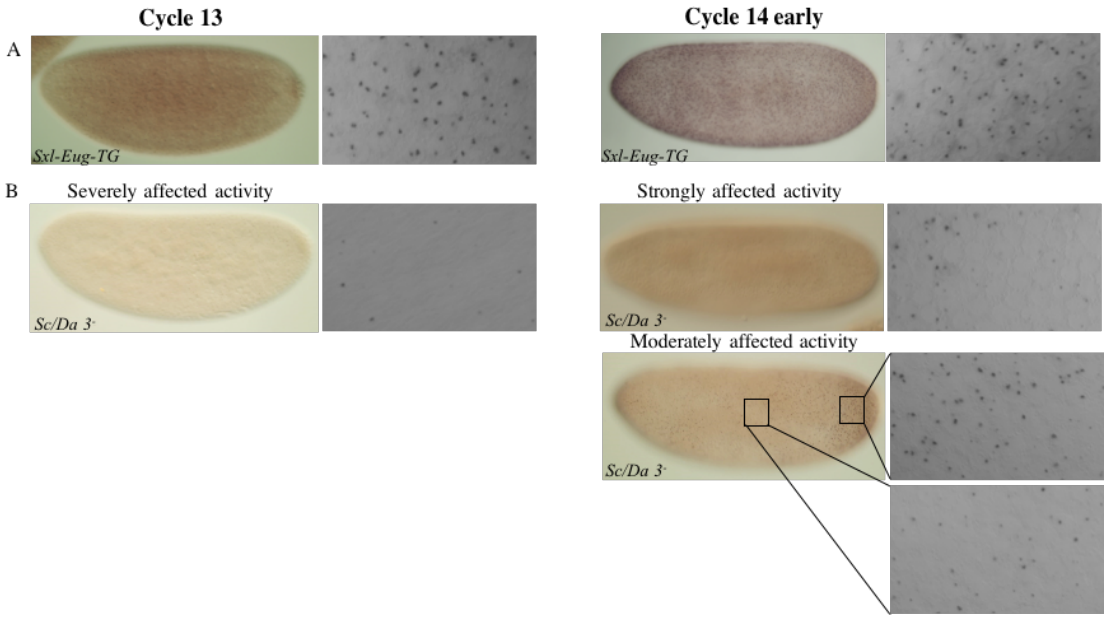

Fig. 4.3: *In situ* hybridization of *Sc/Da 3*$^{-}$*SxlPe* transgenic lines
Nuclear dots represent nascent *SxlPe* transcripts. Surface views of embryos were shown in both 20X and 100X. 100X pictures were taken at the center of the embryos unless indicated.
A) *Sxl-Eug-TG* female embryos exhibited a uniform wild type expression. B) *Sc/Da 3*$^{-}$*SxlPe* females had severely affected *SxlPe* activity. Squares indicated the regions where 100X pictures were taken.

The *SxlPe* activity increased in cycle 14 with half of the female embryos showing moderately affected activity. The other half remained to be severely or strongly affected. Notably none of the embryos showed a uniform wild-type expression pattern (Fig. 4.3B). The *in situ* hybridization experiments explain why *Sc/Da 3*$^{-}$ transgenes fail to rescue *Sxl* null mutations, but they offer no clear explanation of the occasional female that survived. It may be the case that the most strongly expressing females produced sufficient SXL protein to stably activate maintenance expression of *Sxl*. If so, it suggests that the diffusion of *Sxl* mRNA or protein in the syncytial embryos led to the activation of *Sxl* in more nuclei than actually activated *SxlPe*. Alternatively, we may not have sampled enough embryos to have identified those with near wild-type expression pattern.

A striking feature observed in the *Sc/Da 3*$^{-}$ line was related to the pattern of *SxlPe* expression. The *Sc/Da 3*$^{-}$ exhibited a strong regional bias in promoter activation. Staining appeared stronger in terms of nuclear dot intensity and in the proportion of expressing nuclei, in the posterior of the embryos. We have no obvious explanation for this regional variation, but it is clear that *Sc/Da 3*$^{-}$ mutation effectively eliminates *SxlPe* expression in the central region of the embryo. My results with Sc/Da site 3 are in direct conflict with those reported earlier from our lab and Paul Schedl's lab, using *SxlPe-lacZ* transgenes. We have no clear explanation for why *Sc/Da 3*$^{-}$ mutations had only a minimal effect in the context of 0.4 kb *SxlPe-lacZ* while nearly eliminating promoter activity in full length transgenes. Regardless, these findings offer a cautionary tale about relying on results obtained only with minimal promoter/enhancer *lacZ* fusions.

Combinatorial Sc/Da mutants do not necessarily eliminate *SxlPe* expression

In experiments with *SxlPe-lacZ* fusions, mutations of two or more Sc/Da sites typically eliminated *SxlPe* expression. I tested two Sc/Da binding site double mutants, *Sc/Da 1⁻2⁻* and *Sc/Da 1⁻4⁻* and found that neither combination had as strong an effect as *Sc/Da 3⁻*, the E-box mutation alone. Each combination, however, had a profound effect on *SxlPe* activity that seemed to reflect additive, rather than synergistic effects of the mutated Sc/Da sites.

Sc/Da 1⁻2⁻ for example, poorly complemented homozygous Sxl^{7BO}, and Sxl^{f1} (9% and 25% female viability respectively) (Table 4.4), but that represents only a slight worsening of the effects of *Sc/Da 2⁻* mutation alone (Table 4.2). (Exact results of complementation tests with Sxl^{7BO} and Sxl^{f1} differed in every case with rescue of Sxl^{f1} always being less effective. We do not know the reason although sex determination is known to be highly sensitive to genetic background effects. One speculative possibility is that Sxl^{f1} might have a small dominant negative effect if its aberrantly spliced pre-mRNAs interfered somehow with a functional *Sxl* allele in the same cell. A problem the deletion mutant $Df(1)Sxl^{f7bO}$ would not share.)

Table 4.4: Combinatorial Sc/Da binding site mutations retained some *SxlPe* activity

A) Viability of Sxl^{f1}/ Sxl^{f1} females with transgenes carrying Sc/Da binding site mutations

Genotype	*Sc/Da1-2 SxlPe SxlTG*	*Sc/Da1-4- SxlPe SxlTG*	*Sxl TG*
$\frac{Sxl^{f1}}{Sxl^{f1}}$; $\frac{TG}{+}$	8.6 (9)	34.2 (40)	109.9 (111)

Crosses ♀♀ *y w cm* Sxl^{f1} *ct*/*Binsincy*; +/+ × ♂♂ *y w cm* Sxl^{f1} *ct* /Y; TG/+
Numerical data represent percentage of female viability. Numerical data in parenthesis represent the number of viable females. The Sxl^{f1}/ Sxl^{f1} sibling females without transgenes were used as reference.

B) Viability of Sxl^{7BO}/Sxl^{7BO} females with transgenes carrying Sc/Da binding site mutations

Genotype	*Sc/Da1-2 SxlPe SxlTG*	*Sc/Da1-4- SxlPe SxlTG*	*Sxl TG*
$\frac{Sxl^{7BO}}{Sxl^{7BO}}$; $\frac{TG}{+}$	25.0 (29)	62.1 (59)	110.7 (93)

Crosses ♀♀ *y pn w* Sxl^{7BO}/*Binsincy*; +/+ × ♂♂ *y pn w* Sxl^{7BO}/Y; TG/+
Numerical data represent percentage of female viability. Numerical data in parenthesis represent the number of viable females. The Sxl^{7BO}/ Sxl^{7BO} sibling females without transgenes were used as reference.

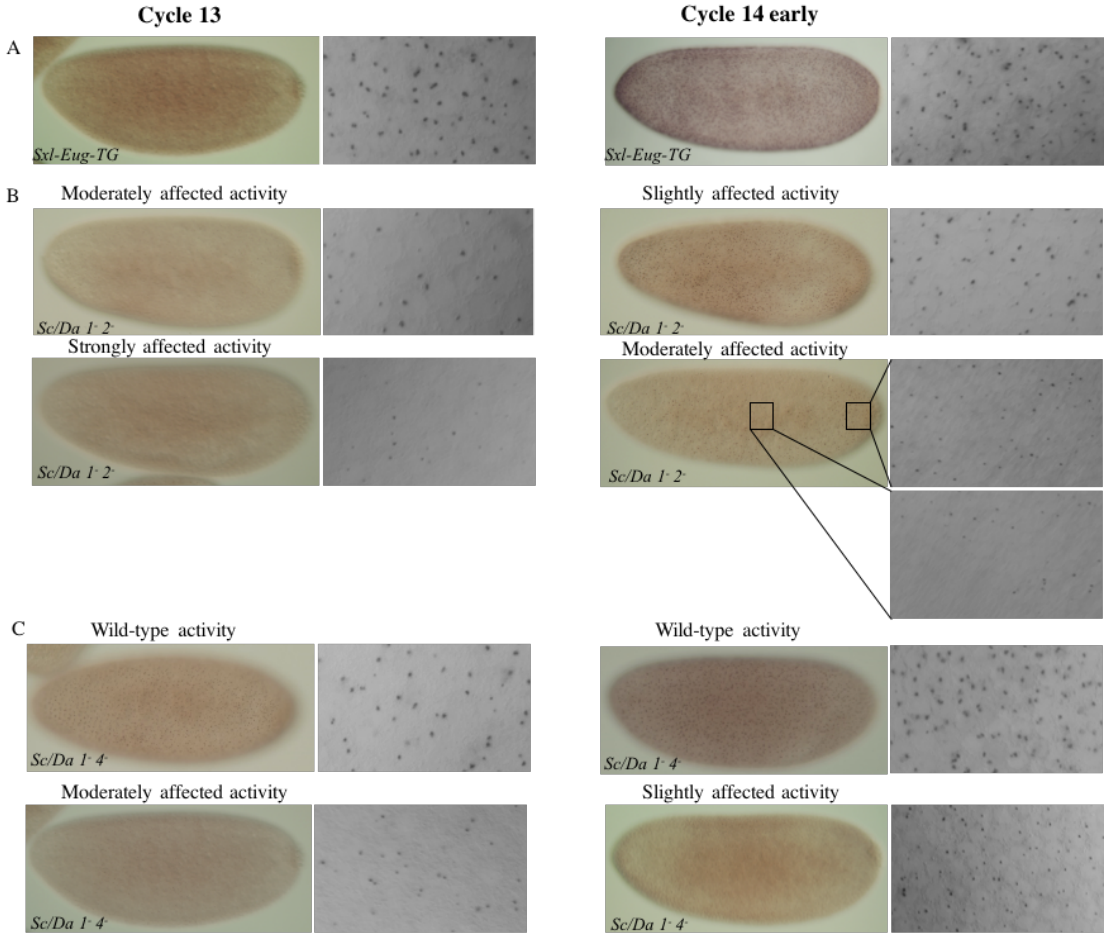

Fig. 4.4: *In situ* hybridization of *Sc/Da 1⁻2⁻SxlPe* and *Sc/Da 1⁻4⁻SxlPe* transgenic lines

Nuclear dots represent nascent *SxlPe* transcripts. Surface views of embryos were shown in both 20X and 100X. 100X pictures were taken at the center of the embryos unless indicated. A) *Sxl-Eug-TG* female embryos exhibited a uniform wild type expression. B) All *Sc/Da 1⁻2⁻SxlPe* females had reduced *SxlPe* expression. Squares indicated the regions where 100X pictures were taken. C) 50% and 88% *Sc/Da 1⁻4⁻SxlPe* females reached wildtype expression at cycle 13 and early cycle 14, respectively.

I tested the effects of Sc/Da site 4 in combination with Sc/Da site 1 because the *Sc/Da 4⁻* mutations in the context of 0.4kb *SxlPe-lacZ* transgenes appeared to have similar but stronger effects than observed with *Sc/Da 2⁻* mutants [47]. Despite, *Sc/Da 1⁻4⁻* having two

Sc/Da sites mutated, its effects were only slightly more severe than *Sc/Da 1*$^{-}$ alone. It had a moderate effect on *SxlPe* as percentage of female viability ranged from a 62.1% seen with Sxl^{7BO} complementation test to a 34.2% seen with Sxl^{f1} (Table 4.4). The effect did not seem as severe as *Sc/Da 1*$^{-}$*2*$^{-}$ naturally because it was essentially better than *Sc/Da 2*$^{-}$ alone. The *in situ* hybridization results too verified that the *SxlPe* expression was far better than the *Sc/Da 2*$^{-}$. Half of the cycle 13, *Sc/Da 1*$^{-}$*4*$^{-}$ female embryos reached wild-type activity and most of cycle 14 embryos (88%) showed wild-type *SxlPe* activity with only a few exhibiting mutant expression patterns (Fig. 4.4C). Certainly, the *SxlPe* activity or the viability data observed here were lesser compared to the individual *Sc/Da 1*$^{-}$ mutants but *Sc/Da 1*$^{-}$*4*$^{-}$ being only a slightly stronger mutant than *Sc/Da 1*$^{-}$ revealed that Sc/Da site 4 is the weakest *SxlPe cis*-regulator characterized thus far.

Characterizing repressor binding sites at *SxlPe*

Overview of Dpn binding at *SxlPe*

Dpn, as a member of the Hairy-Enhancer of split, HES family of bHLH repressors, binds to the E-box sequence CACGTG and a related sequence CACGCG [64, 65, 86-89]. The latter appears to represent the optimal binding sequence for Dpn and its relatives. The three known Dpn binding sites at *SxlPe* promoter are clustered within 200bp of the transcription start site and the exact location of the sites are specified in the Fig. 4.5. Dpn binding sites 1, 2 are canonical high-affinity CACGCG sequences whereas site 3 is non-canonical and of lower affinity [64, 70, 90].

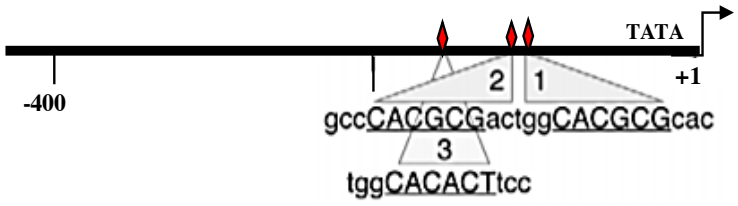

Fig. 4.5: Dpn binding sites at SxlPe
Schematic representation of the Dpn binding sites along the 400bp, proximal *SxlPe.* The corresponding binding site sequences are capitalized.

Experiments carried out in our lab using 1.4 kb *SxlPe-lacZ* transgenes to study the various Dpn site mutants showed that mutated Dpn sites 1,2, or 3 led to ectopic *SxlPe-lacZ* expression in male embryos but appeared to have little effect on expression in females [64]. I note that the Schedl lab reported different results in the context of 0.4kb *SxlPe-*

lacZ lines. There they found that double mutations affecting canonical Dpn sites 1 and 2 did not lead to ectopic expression in males and actually reduced *lacZ* activity in females. They attributed this to the binding sites being recognized both by Dpn and the postively-acting Myc transcription factor [56].

Creating *Sxl* transgenes carrying mutations in Dpn binding sites

To use the *Sxl* transgene system to perform the mutational analysis of Dpn binding sites, the experimental transgene, *Sxl-Eug-TG* was modified to carry the desired binding site mutation. The experimental procedure followed was the same as used to create *Sxl* transgenes carrying mutations in Sc/Da binding sites (described earlier in this chapter). The Dpn binding site mutations used are shown in (Table 4.5).

Table 4.5: Mutated sequences of Dpn binding sites

Dpn sites mutated	Original sequence	Mutated sequence
Dpn 1^-	CACGCG	CAC**TG**G
Dpn 2^-	CACGCG	C**T**CG**A**G
Dpn 3^-	CACACT	CAC**C**CT
Dpn 1^-2^-	CACGCG	CAC**TG**G
	CACGCG	C**T**CG**A**G
Dpn 1^-3^-	CACGCG	CAC**TG**G
	CACACT	CAC**C**CT
Dpn $1^-2^-3^-$	CACGCG	CAC**TG**G
	CACGCG	C**T**CG**A**G
	CACACT	CAC**C**CT

Mutations in Dpn binding sites cause male lethality

Several genetic tests were carried out with the *SxlTG* carrying the Dpn sites. The first were genetic complementation tests. Complementation tests with Sxl^{f9}, Sxl^{f1} and Sxl^{7bO} showed, as expected that mutating the Dpn repressor binding sites did not adversely affect *SxlPe* expression in females as a single copy of each fully complemented the *Sxl* mutations. Reciprocally, mutations in the Dpn sites were expected to exhibit male-lethal effects due to constitutive expression of *SxlPe* in XY animals. I found that was indeed the case; however, there were dramatic difference in the strengths of the lethal effects observed.

Genetic analysis of the effects of transgenic Dpn site mutations in males is complicated by *Sxl* autoregulation. A wild-type male carrying a single Dpn mutant transgene for example, should express the early form of *Sxl* protein exclusively from the transgene; however, the early *Sxl* protein will facilitate the splicing of *SxlPm*-derived maintenance transcripts from both the transgenic and endogenous *Sxl* loci. Normal males thus represent a sensitized system that should amplify the effects of Dpn site mutant transgenes. To simply compare between mutants, I asked whether the Dpn site mutant transgenes in either one or two copies exhibited lethal effects in Sxl^{f7bO} males, who are deleted for the endogenous *Sxl* locus. The results indicated that each mutant transgene expressed *SxlPe* and killed males but that the efficiency of killing varied. In single copy, none of the Dpn site mutants, including the $Dpn\ 1^{-}2^{-}3^{-}$, was fully lethal to males (Table 4.6B), indicating that the level of expression was too low to reliably engage the autoregulatory loop. However, when two copies were present strong lethal effects were observed for all Dpn

site mutants except *Dpn 1*$^{-}$. In agreement with the analysis of Lu et al. [64] the non-canonical Dpn site 3^{-} mutations had the strongest effects on viability with males being barely able to tolerate two copies of *Dpn 3*$^{-}$ mutant or *Dpn 1*$^{-}$*2*$^{-}$*3*$^{-}$ combination (Table 4.6B). The *Dpn 1*$^{-}$ mutants exhibited the weakest effect on its own, 57% male viability with two copies (Table 4.6B), but curiously the Dpn site 1^{-} change tended to ameliorate the lethal effects of *Dpn 2*$^{-}$ and *Dpn 3*$^{-}$ mutations. This may reflect the hypothesized dual nature [56] of the canonical sites as binding both activators and repressors. I also examined the effects of the Dpn site mutant transgenes in males carrying an intact copy of the endogenous *Sxl* locus (Table 4.6A) and or the early defective, but late effective, allele *Sxl*^{f9} (Appendix B). While the exact numbers differed, the same general trends were observed. Of note was the finding that the *Dpn 1*$^{-}$*2*$^{-}$*3*$^{-}$ transgene could never be recovered in males carrying two copies of *Sxl*, indicating that this combination leads to the greatest level of ectopic *SxlPe* expression.

Table 4.6: Dpn binding site mutations reduced male viability

A) Lethality test in wildtype males carrying *Dpn^{M}SxlPe-SxlTG*

Genotype	*Dpn1- SxlPe SxlTG*	*Dpn2- SxlPe SxlTG*	*Dpn3- SxlPe SxlTG*	*Dpn1-2- SxlPe SxlTG*	*Dpn1-3- SxlPe SxlTG*	*Dpn1-2-3- SxlPe SxlTG*	*Sxl TG*
$\frac{+}{Y};\frac{TG}{+}$	75.0 (84)	62.5 (65)	55.3 (84)	72.5 (116)	46.5 (40)	0 (0)	102.7 (113)
$\frac{+}{Y};\frac{TG}{TG}$	21.4 (12)	11.5 (6)	0 (0)	12.5 (10)	0 (0)	NA	74.5 (41)

Crosses ♀♀ +/+; TG/+ × ♂♂ +/Y; TG/+
Numerical data represent percentage of male viability. Numerical data in parenthesis represent the number of viable males. The +/Y sibling males without transgenes were used as reference.

B) Lethality test in *Sxl^{7BO}* males carrying *Dpn^{M}SxlPe-SxlTG*

Genotype	*Dpn1- SxlPe SxlTG*	*Dpn2- SxlPe SxlTG*	*Dpn3- SxlPe SxlTG*	*Dpn1-2- SxlPe SxlTG*	*Dpn1-3- SxlPe SxlTG*	*Dpn1-2-3- SxlPe SxlTG*	*Sxl TG*
$\frac{Sxl^{7BO}}{Y};\frac{TG}{+}$	68.5 (74)	73.9 (65)	69 (69)	92.3 (120)	84 (126)	56.6 (94)	93.7 (90)
$\frac{Sxl^{7BO}}{Y};\frac{TG}{TG}$	57.4 (31)	18.2 (8)	2.0 (1)	30.8 (20)	13.3 (10)	0 (0)	81.2 (39)

Crosses ♀♀ *y pn w Sxl^{7BO}*; TG/+ × ♂♂ *y pn w Sxl^{7BO}/Binsincy* /Y; TG/+
Numerical data represent percentage of male viability. Numerical data in parenthesis represent the number of viable males. The *Sxl^{7BO}*/ Y sibling males without transgenes were used as reference.

Dpn binding sites mutation induced ectopic *SxlPe* expression in males and provided evidence of transvection between transgenic alleles

To examine the effect of Dpn binding site mutations on *SxlPe* expression, *in situ* hybridization was performed on the progeny from *Sxl^{7BO}* mothers homozygous for *Dpn^{M}SxlPe-Eug-TG* and *Sxl^{7BO}* fathers homozygous for *Sxl-Persi-TG*. The *SxlPe* activity from both transgenes were detected by using probes specific for each allele.

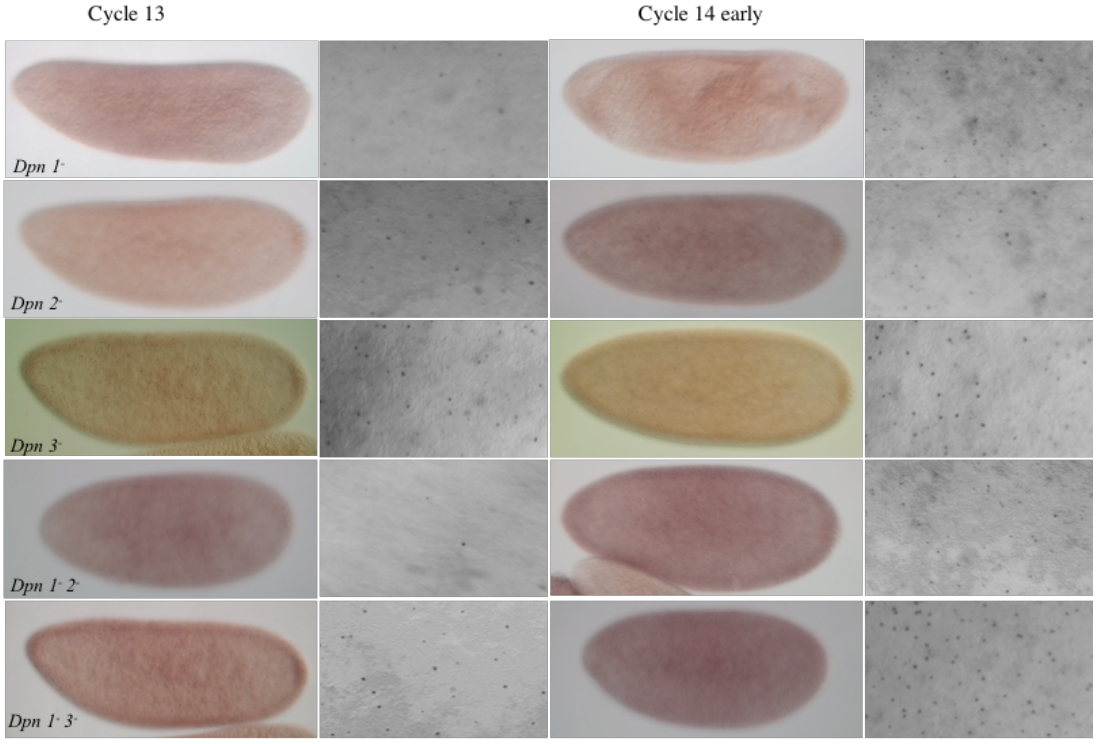

Fig. 4.6: Ectopic *SxlPe* expression in *Dpn^{M}SxlPe* transgene carrying *Sxl^{7BO}* male (XY) embryos

Nuclear dots represent nascent *SxlPe* transcripts. Surface views of embryos were shown in both 20X and 100X. 100X pictures were taken at the center of the embryos. All *Dpn^{M}SxlPe* transgenic lines showed ectopic *SxlPe* expression.

All transgenic lines carrying Dpn binding site mutations exhibited ectopic *SxlPe* expression in at least half of the male embryos during cycle 13 and early cycle 14 (Fig. 4.6). *Dpn 1^{-}* initiated a low level, *SxlPe* activity in a small fraction of nuclei in 50% of the male embryos. Typically, the ectopic expression for the *Dpn 1^{-}* mutation was characterized by the presence of a faintly stained nuclear dot in expressing nuclei. This apparent low-level expression is consistent with the minimal male lethal effects observed with the

Dpn 1^{-} mutants (Table 4.6 and Appendix B) and shows that XY embryos can establish and maintain their male identity with low-level of *SxlPe*.

The *Dpn 2*$^{-}$ mutant showed a similar ectopic expression pattern to *Dpn 1*$^{-}$. However, the percentage of male embryos with ectopic expression, the number of nuclei expressing, and the staining intensity were all slightly higher compared to *Dpn 1*$^{-}$. Since, the *Dpn 2*$^{-}$ mutations resulted in higher male lethality than *Dpn 1*$^{-}$ (Table 4.6B), this indicates that the level of ectopic *SxlPe* activity observed in *Dpn 2*$^{-}$ often exceeds the threshold level needed to stably activate *Sxl*.

Consistent with the strong male-lethal effects observed, the *Dpn 3*$^{-}$ transgene, induced ectopic *SxlPe* expression in a greater number of male embryos compared to *Dpn 1*$^{-}$ or *Dpn 2*$^{-}$. During early cycle 14, the weakest expressing one third *Dpn 3*$^{-}$ embryos showed non-uniform ectopic expression with both the percentage of nuclei expressing and staining intensity being higher than the other canonical *Dpn 1*$^{-}$ and *Dpn 2*$^{-}$ mutations (Fig. 4.6 and 4.7). The rest two thirds of the *Dpn 3*$^{-}$ embryos possessed a strongly stained nuclear dot in every nucleus. Remarkably these embryos strongly resembled XX females as they usually expressed two dots in each nucleus. This indicates that many XY embryos were able to activate *SxlPe* from both the constitutive mutant transgene and normally inactive wild-type transgene, suggesting the exciting possibility that the *SxlPe* promoter may exhibit a transvection like mechanism whereby one active promoter facilitates the activation of the other allele [91-93]. I will discuss this finding in more detail below.

Comparing the two combinatorial mutants, *Dpn 1⁻2⁻* and *Dpn 1⁻3⁻*, the latter showed a higher *SxlPe* activity in male embryos. Expression in the *Dpn 1⁻2⁻* line closely resembled that seen in the *Dpn 2⁻* single mutant consistent with *Dpn 1⁻* mediating only a weak repressive effect. Likewise, embryos bearing the *Dpn 1⁻3⁻* transgene resembled those carrying the single strong *Dpn 3⁻* transgene with the *Dpn 1⁻3⁻* appearing to express in an even greater number of nuclei than the *Dpn 3⁻* single mutant. The *Dpn 1⁻3⁻* combination also exhibited evidence of transvection, as many nuclei expressed both the *Dpn 1⁻3⁻* experimental transgene and the control (Fig. 4.6 and 4.7).

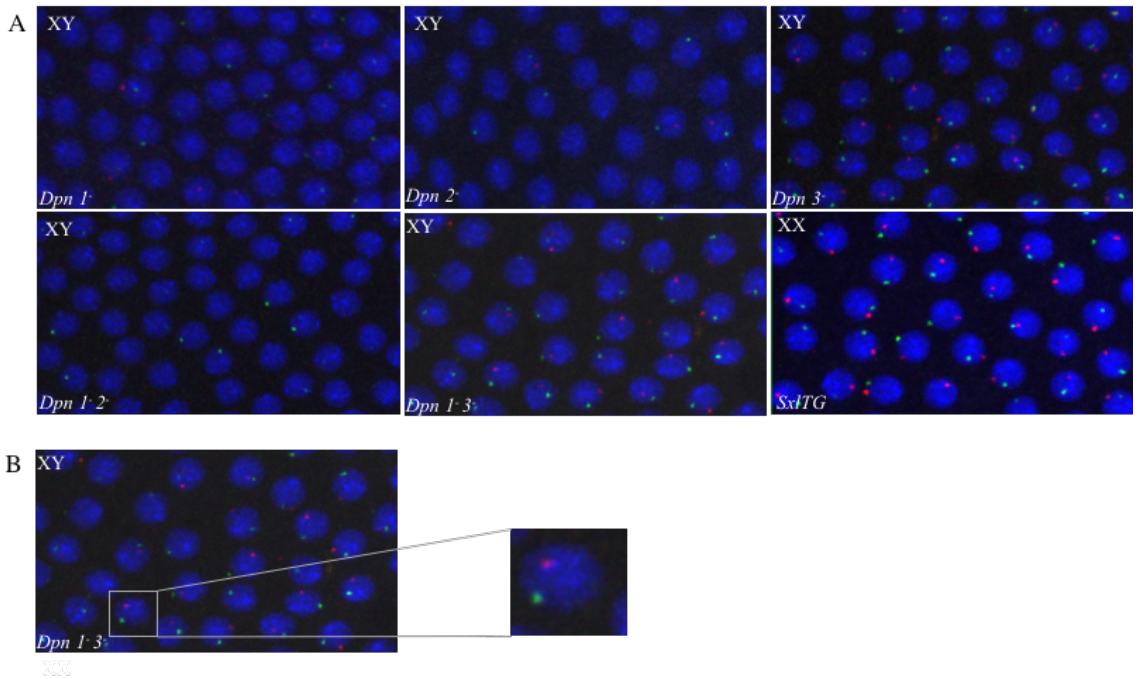

Fig 4.7: FISH image depicting the ectopic *SxlPe* expression in *Dpn^{M}SxlPe* transgene carrying *Sxl^{7BO}* male (XY) embryos

Nuclei were stained with DAPI and shown in blue. Nuclear dots (green) represent *SxlPe* transcripts from *Dpn^{M}SxlPe-Eug-TG*. Nuclear dots (red) represent *SxlPe* transcripts from *Sxl-Persi-TG*.
A) Magnified confocal images of cycle 13 embryos heterozygous for *Sxl-Persi-TG* and *Dpn^{M}SxlPe-Eug-TG* (experimental). All *Dpn^{M}SxlPe* transgenic lines showed ectopic *SxlPe* expression. B) Enlarged single nucleus from *Dpn1^{-}3^{-}* image show both constitutive *SxlPe* expression from the experimental transgene (green) and trans-activated *SxlPe* expression from the control transgene (red).

Evidence that a constitutive *SxlPe* promoter can activate a wild-type *SxlPe* promoter *in trans*

My *in situ* hybridization analysis provided the surprising finding that the Dpn site mutant lines with the strongest *SxlPe* expression appeared also to activate the control *Sxl^{+}* transgenes, which are normally completely inactive in male embryos. More direct evidence for transactivation by *SxlPe*, was obtained using fluorescent *in situ* hybridization

(FISH) to distinguish between transcripts initiated from the Dpn site mutant bearing experimental transgenes and the wild-type controls. When I examined the *Dpn 1⁻, Dpn* 2⁻ , and *Dpn 1⁻2⁻* transgenes, I found that expressing nuclei in males usually expressed *SxlPe* only the *Dpn 1⁻, Dpn* 2⁻, or *Dpn 1⁻2⁻* bearing transgene as evidenced by the presence of a single, green colored nuclear dot (Fig 4.7). Occasionally, however, a second red nuclear dot was seen indicating that the control Sxl^{+} transgene was also expressed. When I examined the more strongly expressing *Dpn 3⁻* and *Dpn 1⁻3⁻* transgenes, I found that the majority of nuclei that expressed the *Dpn* mutant transgenes (green dots) also expressed the control transgene (red dots) (Fig. 4.7).

While my data strongly suggest that some form of transactivation by *SxlPe* occurs, we have no information as to mechanism. It could be the case that the early *Sxl* protein has an unexpected transcriptional autoregulatory function. Alternatively, transactivation might involve a transient chromosomal pairing akin to seen in classical transvection [93-96], or it could reflect the production of non-coding RNAs [97] that act *in trans* to facilitate expression. Regardless of the mechanism, the possibility that one activated *SxlPe* facilitates the activation of the second copy, suggests the exciting possibility that the fly exploits this phenomenon as a means to facilitate rapid and efficient engagement of *Sxl* expression. Such a system may well be an elegant solution to the fundamental problem of ensuring that the response to XSE signal remains female-specific.

CHAPTER V

CONCLUSIONS AND METHODS

Sxl transgene system in analyzing *SxlPe* activity

The goal of my thesis research was to develop a novel transgenic system that would allow us to probe the details of *Sxl* regulation in the fly. The system was designed to allow easy introduction of genetic alterations *in vitro*, and then transform into flies so that both the tools of genetic analysis and *in situ* hybridization could be used to analyze the production of *Sxl* nascent transcripts and mature mRNAs. My focus was on the regulation of the transiently acting promoter, *SxlPe* which functions as a dose-sensitive genetic switch that measures X chromosome dose to determine the sexual fate[6, 8, 38]. Previous work on *SxlPe* employed promoter-*lacZ* fusions that provided insight into the modular structure of *SxlPe* and in the importance of several binding sites for regulators of X chromosome dose [8-10, 47, 59, 64, 71]. What *SxlPe-lacZ* fusions could not do was to allow us to fully employ the sophisticated classical genetic tools available to study sex determination, nor could they reliably identify nascent *SxlPe* transcripts, a tool that has led to considerable insight into the mechanism of primary sex determination [9, 64, 98].

The *Sxl* transgene system I developed answered how the mutations in the *Sxl* loci affected the biology of the fly and provided a true quantitative understanding of the female flies surviving, unlike just monitoring *SxlPe-lacZ* expression which were often not too conclusive. The female and male viability data obtained are very accurate and they were

similar when repeated with the same transgenic line or compared with other transgenic lines carrying the exact same mutation. This allowed reliable and uniform comparisons among transgenic lines while analyzing the different *SxlPe* mutants.

Monitoring *SxlPe* activity as nascent nuclear dots and mature transcripts in the *Sxl* transgene system made the system reliable for predicting onset of transcription, identify spatial-temporal patterns of expression and compare *SxlPe* expression between various *SxlPe* mutants. The pool of data obtained by using the *Sxl* system to study promoter deletions and binding sites mutations, deepened our understanding of *SxlPe* and gathered new insights that were either missed or unidentifiable in earlier experiments involving *SxlPe-lacZ* model.

With respect to *SxlPe* activity, the transgenes I developed appear to precisely mimic the timing, levels, and functions of the endogenous *Sxl* locus. The only noticeable difference being that the nuclear dots that mark the nascent transcripts in the embryonic nuclei were in different nuclear locations in the transgenes than for the endogenous *Sxl* gene. The nuclear dots from the transgenic copies also appear to be farther apart than with the endogenous locus [9, 10, 54, 98]. These differences almost certainly stem from the *Sxl* transgene being integrated in chromosome 2 rather than in the X chromosome.

Our initial plan was to create "marked" transgenes carrying homologous segments of DNA from different *Drosophila* species with the expectation that this would allow allele-

specific detection via *in situ* hybridization while fully preserving genetic function. What we discovered, however, was that only sequences from the most closely related species examined fully preserved all aspects of *Sxl* regulation. This created a problem for the detection of transgenic *Sxl* transcripts because of cross-hybridization between the *D. eugracilis* probe and the endogenous melanogaster gene. I solved this problem by developing higher stringency in situ hybridization conditions that ensure that the *D. eugracilis* probe only detects the *SxlPe* signal from the *Sxl-Eug-TG*. As a result, the *SxlPe* activity can now be successfully monitored in strains carrying the Sxl^{7B0} deletion or in those with wild type *Sxl*.

The sequences that I swapped between species stretched from exons E1 through L2 and thus could in theory affect *SxlPe* transcripts, which splice from E1 to L4 directly, or *SxlPm* transcripts which splice from the upstream L1 exon to L2 to L4 (or to the translation terminating L3 exon in males.) Exon E1 to L2 sequences from the closely related species, *D. erecta and D. eugracilis*, provided both early (i.e. establishment) and late (maintenance) functions. In contrast E1-L2 sequences from the more distant (~20-30 million years) *D. persimilis* and *D. pseudoobscura* provided early function but appeared to be defective in producing the maintenance *Sxl* function. Swapping in the E1-L2 segment from the even more distant *D. virilis* eliminated both the ability to provide early and late *Sxl* functions. These findings suggest that the sequences can likely affect the splicing of the early (establishment) and late (maintenance) forms of *Sxl* mRNA and thus

offer a possible experimental window into better understanding the still mysterious means by which *SxlPe* transcripts skip exons L2 and L3 [99].

It was our plan from the beginning to develop the means to quantify *SxlPe* activity using fluorescent *in situ* hybridization and automated microscopy. Such a system should recognize and be able to count the number of nuclei expressing one, two, or no nuclear dots and to measure the intensities of the fluorescent signals. Automation of this process would greatly facilitate the analysis of *cis*-acting *SxlPe* mutations. It would overcome the laborious process of counting each and every nucleus in single embryos and that it should provide quantitative or semi-quantitative information as to expression thus replacing the visual biases of the experimenter. Unfortunately, I was unable to fully develop this aspect of the transgene system. Stumbling blocks included the need to modify existing software that was designed for different imaging systems and biological measures [100-103], as well as issues of signal detection and background. The later represents a substantial obstacle. When we analyzed strong *SxlPe* mutants, for example, it proved very difficult to reliable detect and clearly identify the faint dots expressed from the mutant allele from the strong dots produced by the control allele. These dots could not be detected by the program reliably always and was a problem. With the dedicated efforts of Dr. Stan Vitha of the Texas A&M Microscopy and Imaging Lab, I anticipate that the remaining problems will be solved and that this promising aspect of the transgenic technology will be made fully available in the near future.

Structure and regulatory role of *SxlPe* enhancer in *Sxl* activation

My work on the *SxlPe* enhancers focused on defining the architecture of *SxlPe* to better understand the operation of the sex-determining switch. A central question was to determine the DNA sequences both necessary and sufficient for *SxlPe* function. Transgenic reporter fusions between *SxlPe* deletions and *lacZ* provided useful information about functional segments of *SxlPe* [47, 64, 71] but the question of whether the functional elements identified could drive sufficient expression in their native context were unanswered. We approached this larger scale definition of *SxlPe* promoter and enhancer elements by testing the exact same promoter deletions previously examined [71]. Our findings served as a strong validation of most interpretations made by Estes et al. [71] and Yang et al [47] but also offered the surprising result that a minimal 400 bp segment that drives sex-specific expression in a patchy low-level expression pattern is actually sufficient to rescue flies defective for *Sxl* early function. Summarizing the key findings, it appears that the *SxlPe* promoter/enhancer contains three structural elements. A critical promoter proximal 400 bp region that drives female-specific *SxlPe* expression, and two more distal segments that appear to augment expression of *SxlPe* allowing it to be expressed strongly in all parts of the embryo.

The augmentation functions of the *SxlPe* enhancers appear to map primarily in two segments: located approximately -1.4 to -3.0 kb upstream and from -0.8 to -1.4 kb upstream of the *SxlPe* start. The segment from -0.8 to -1.4 kb appears to play the most important augmentation function as transgenes containing it plus the minimal sex-specific

promoter express *SxlPe* nearly as strongly as wild-type transgenes and in nearly every embryonic nucleus. Such transgenes provide sufficient early *Sxl* function to fully rescue the viability of Sxl^{f9}/Sxl^{f1} females, the most defective genetic combination possible to analyze. Suggestively, the segment from -0.8 to -1.1 kb contains evolutionary conserved sequences that include two canonical binding sites for the XSE activator Sc/Da. As discussed in Chapter 3, we cannot subdivide the -1.4 to -0.8 kb segment further even though -1.1 kb transgenes do not fully rescue Sxl^{f9}/Sxl^{f1} females and contained fewer nuclei that express *SxlPe* than the longer transgenes. The differences could indeed reflect the presence of positive regulatory elements between -1.1 and -1.4 kb. However, the reduced expression could also reflect that the transgenic constructs alter the context of *SxlPe* by placing DNA normally located upstream of *SxlPm* adjacent to the regulatory elements of *SxlPe*. If this upstream DNA partially silences the activity of the -1.1 kb, but not the -1.4 kb, *SxlPe* transgene it could explain why the -1.1 kb version expresses less effectively.

Transgenes that include the full segment to -3.0 kb fully rescue Sxl^{f9}/Sxl^{f1} females and express *SxlPe* in every embryonic nucleus with the expression levels appearing indistinguishable from those of fully wild-type transgenes. It seems reasonable to conclude then that the 3kb construct be considered as containing the entire *SxlPe* regulatory region. This non-coding upstream region diverges in sequence between *Drosophila* species; however, species as distant as *D. eugracilis* all carry a cluster of 3 canonical Sc/Da binding sites suggesting that these XSE binding sites contribute to the augmentation function.

The minimal promoter region for *SxlPe* includes only the 0.4 kb immediately upstream of the promoter, as demonstrated by the ability of the 0.4kb *galK SxlPe* contruct to complement Sxl^{f9}. (We cannot exclude the possibility that sequences downstream also play a role in *SxlPe* regulation but there is no evidence suggesting this is the case.) The experiments of Estes et al [71] demonstrated the 0.4 kb region to be sufficient of sex-specific on or off regulation, but this minimal promoter element expressed weakly and in a distinctly non-uniform pattern. Our more detailed expression analysis is consistent with earlier findings in that expression is weak and patchy, with a distinct anterior and posterior bias (Fig. 3.4). My finding that the 0.4 kb construct successfully rescues most Sxl^{f9} homozygotes and many Sxl^{f9}/Sxl^{f1} females is surprising given the low-level non-uniform expression. This suggests that *Sxl* must be capable of being stably activated by locking in autoregulatory splicing in many more cells than *SxlPe* is active in. This likely reflects considerable cell non-autonomy of *Sxl* mRNA in the syncytial embryo. What is critically needed are estimates of when these cells and how many of them express *Sxl* protein. Unfortunately, our anti-SXL antibody no longer works and we have been unable to obtain a substitute that works effectively in the early embryo.

Regardless of the precise details, the ability of the imperfectly expressing 0.4 kb *SxlPe* transgenes to provide sufficient early *Sxl* protein for viability has important implications for how the sex determining mechanism might have evolved. There is a tendency when examining a complicated process like X-counting to view its present day extreme efficiency as a prerequisite for function. Analysis of the deletion transgenes, however,

reveals that a considerable degree of messiness is compatible with biological function. This suggests that there may have been considerable freedom to experiment and improve the X-counting mechanism as it evolved.

Do upstream sequences normally influence *Sxl* transcription?

My discovery that the insertion of a 1.2 kb bacterial *galK* sequence upstream of the 0.4kb *SxlPe* promoter elevated *Sxl* expression demonstrated that the upstream sequences placed next to *SxlPe* in creating the deletions had an inhibitory effect on *SxlPe* activity. The "silencing" sequences come from *CG4615* the gene immediately upstream of *Sxl*. *CG4615* is expressed maternally but does not appear to be expressed zygotically until at least the cellular blastoderm stage (Flybase, expression data). This hints that the silencing observed may result from the artificial juxtaposition of inactive chromatin next to the permissive chromatin of *SxlPe*. This raises the question of whether this "silencing" might be part of a normal mechanism that helps keep *SxlPm* inactive until it is needed in cycle 14 [11]. One could test this idea by adding spacer DNA between *SxlPm* and *CG4615*, or by replacing *CG4615* with an active gene, to see if *SxlPm* is activated earlier than normal.

The roles of Sc/Da binding sites in regulating *SxlPe*

Scute is quantitatively the strongest XSE and Sc/Da is a key regulator in *SxlPe* regulation [39, 41]. Past analysis with 0.4 kb *SxlPe-lacZ* transgenes suggested that *SxlPe* is regulated by multiple Sc/Da binding with no single site having a predominant effect or even a particularly strong effect. In striking contrast, my analysis revealed that two individual

Sc/Da binding sites had strong effects on *SxlPe* activation. Specifically, Sc/Da site 2$^-$ mutations had a significant effect on female viability and site Sc/Da site 3$^-$ mutations abolished *SxlPe* activity marking site 3 as the most critical regulatory site along *SxlPe* enhancer characterized. One possibility is its strength as a regulatory site reflects that it is the only canonical E-box in the proximal *SxlPe* enhancer, however, the *in vitro* binding affinity of Sc/Da for site 3 was no higher than that for site 2 [47] suggesting the reason for site 3 importance lies elsewhere. A reasonable possibility is that site 3 might be a nucleation site and that Sc/Da binding there may facilitate the recruitment and spreading of chromatin modifiers, which in turn increase the chromatin accessibility of the surrounding region and lead to the initiation of *SxlPe*.

Such a role could come about if Sc/Da 3 were the most accessible site or the site where the activators begin to bind first at *SxlPe.* Suggestively two overlapping copies of the TAGteam sites that are bound by the pioneering transcription factor Zelda overlap with Sc/Da site 3. TAGteam sites are bound by Zelda before and during maternal-to-zygotic transition (MZT), to help initiate transcription of early developmental genes [58, 59, 104, 105]. Although, the mechanism by which Zelda binding influences *SxlPe* activation is not established, Zelda binding could increase chromatin accessibility [61-63], rendering the Sc/Da site 3 to be one of the first accessible sites. I note that our analysis of the effects of Sc/Da site mutations are potentially complicated by the overlapping TAGteam sites. The mutation in Sc/Da site 3 was carefully designed within the three base pairs of the hexamer binding site sequence that are not shared by the TAGteam doublet. Although, the

TAGteam doublet was not mutated, it is not certain whether modifications to a neighboring base pair changes Zelda binding. If it does, then the strong effect we observed could be the cumulative effect of the loss of two positively acting factors. I do note, however, that the TAGteam doublet was characterized as a weak regulatory sequence of *SxlPe*, and indeed it was the weakest among the rest of the TAGteam sites present at *SxlPe* [59]. This suggests that the strong effects we observed are mostly likely the result of altered Sc/Da binding to site 3.

Although the exact mechanism of how Sc/Da site 3 regulates *SxlPe* activity is still not known, I successfully identified Sc/Da site 3 as a unique, key regulatory site, as mutating this single site completely eradicates *SxlPe* activity. The novel finding that Sc/Da site 3 is essential to ensure the sex-specificity of *SxlPe* enhances our understanding of how *Sxl* works as a genetic switch.

Analysis of Dpn binding site mutations: repressor function and a possible transvection mechanism for X-signal amplification

My analysis of the binding sites for Dpn, and related repressors at *SxlPe*, generally validated previous work using *SxlPe-lacZ* fusions [64] but revealed new details about the importance of individual repressor binding sites, and offered some support for the idea that some repressor binding sites may also bind activators [56].

In agreement with earlier studies [64], the non-canonical, Dpn binding site 3 proved to have a powerful regulatory role than the closely juxtaposed canonical Dpn binding sites 1 and 2. This was evidenced by the stronger male-lethal effects observed for transgenes carrying site 3 mutations compared to those with sites 1 or 2. We speculate that the importance of this site is not based on its non-canonical sequence per se but rather its location adjacent to a strong activator site Sc/Da site 2 and the nearby Sc/Da site 3 [47, 64].

The canonical, Dpn binding sites 1 and 2 have identical sequences [64, 70, 90] but their regulatory abilities appear to differ. Dpn site 2 appeared a stronger negative regulatory site in most assays than did Dpn site 1 (Table 4.6 and Appendix B) and there is no apparent reason for this. Although, Dpn site 1 is located exactly adjacent to Sc/Da site 1 [47, 64] and Dpn site 2 is adjacent to a TAGteam site [59, 104] and it is possible that the nature of activator site besides them maybe relevant to the difference in their regulatory effects. Alternatively, canonical Dpn binding sites are capable of low affinity binding in vitro to bHLH transcription factors like Myc, raising the possibility that the canonical sites have a dual nature at *SxlPe* [56]. If so, the male-lethal effects and ectopic male expression arising from the Dpn sites 1 and 2 transgenes suggest their repressive functions predominate.

What is probably the most significant result from my work on the Dpn site mutations was completely unexpected and, indeed, came about because I included what seemed at the time an unneeded control. I was analyzing the Dpn site mutant transgenes using FISH to

determine how much ectopic expression each was caused in males. The flies carried *Sxl-Eug-TG* with Dpn site mutations and also a wild type control *Sxl-Persi-TG*. Since the wild type transgene should be inactive in males there seemed no need to include the control *D. persimilis* probe but I did anyway. When I analyzed the embryos, I found the surprising result that *SxlPe* was often expressed from both *SxlTG* copies: the constitutive ones bearing the Dpn site mutations, and the wild type (Fig. 4.7). The conclusion is that, somehow, the active *SxlPe* activated the normally silent copy on the other chromosome. The obvious analogy is to transvection, the process, usually involving chromosome pairing, where one copy of an enhancer acts *in trans* to activate the other allele *in trans* [106]. Of course, other mechanisms are possible including, trans activation via expression of non-coding RNAs as well as the possibility that *Sxl* protein could be an autoregulatory transcription factor. Regardless of the actual mechanism, the notion that once activated, one *Sxl* allele promotes the activation of the second allele in trans, has considerable appeal as a female-specific mechanism to amplify the value of the XSE signal.

Given the novelty and potential importance of this "trans activation" phenomenon, it is important both to recognize that so far, we do not know if the phenomenon is limited to transgenic copies or if it applies to the native locus as well. Transactivation via paired enhancers has been observed repeatedly in analysis of transgenes [106-108] but there are reasons to think that it may well apply to the endogenous *Sxl* locus. The most suggestive evidence comes from analysis of nascent transcripts as measured by nuclear dots.

The endogenous *SxlPe* is activated to low levels in nuclear cycle 12. It has been reported that some cycle 12 embryos have nuclei expressing zero, one, or two nuclear dots, which has been interpreted as evidence of independent activation of the alleles [98]. An important caveat to that conclusion is that when embryos are examined a few minutes later, in cycle 13, every single nucleus expresses both alleles and this pattern continues through cycle 14. This suggests the possibility that the observed pattern of *SxlPe* activation could also be explained if initial activation occurs independently on each chromosome, but that once a copy of *SxlPe* is fully active, it facilitates the expression of its homologous copy. This alterative would suggest that the likelihood that transactivation will occur depends on the level of expression from the transactivating promoter. This indeed appears to be the case. With the Dpn site mutants, there was a correlation between the strength of expression of the constitutive transgene and the ability to activate *in trans* (Fig. 4.7). The weak Dpn site 1 mutation barely transactived, the slightly stronger expressing Dpn site 2 mutant did so slightly more effectively, while the strongest mutant tested Dpn site 3, transactivated in nearly every nucleus. One important limitation on the analysis of nuclear dots up till now has been the reliance on the naked eye. It will be necessary in the future to accurately quantify the number of nuclei expressing one dot versus two-dots so that inferences can be drawn with confidence. My transgenic system is ideally suited to this.

Methods

Fly stocks and genetic tests

All flies were raised on medium containing yeast, cornmeal and molasses at 25 ˚C. All genetic tests were performed at 25 ˚C in uncrowded conditions on medium topped with yeast.

Sxl^{f9}, *Sxl*^{f1} and *Sxl*^{7bO} lines were obtained from Bloomington Stock Center. *Sxl*^{f9}, *Sxl*^{f1} and *Sxl*^{7bO} alleles are homozygous female lethal. *Sxl*^{f9} affects the establishment of female identity [20, 80], *Sxl*^{f1} is a null allele that disrupts the maintenance of the sex determination pathway [109] and *Sxl*^{7bO} is a null allele that deletes the entire *Sxl* transcription unit [78]. Complementation tests were conducted by bringing *Sxl* transgenes into homozygous *Sxl*^{f9}, *Sxl*^{f1} and *Sxl*^{7bO} background to examine the viability of these flies. *+/Y; TG/+* flies were crossed with *Sxl*^{f9}*/Binsincy*, *Sxl*^{f1}*/Binsincy* and *Sxl*^{7bO}*/Binsincy* virgin females. Progeny with the genotype *Sxl*^{f9}*/Y;TG/+, Sxl*^{f1}*/ Y;TG/+* and *Sxl*^{7bO}*/ Y;TG/+* were picked and re-crossed with *Sxl*^{f9}*/Binsincy*, *Sxl*^{f1}*/Binsincy* and *Sxl*^{7bO}*/Binsincy* respectively. The progeny from this cross was counted and the viability percentage of *Sxl*^{f9}*/ Sxl*^{f9}*;TG/+, Sxl*^{f1}*/ Sxl*^{f1}*;TG/+* and *Sxl*^{7bO}*/ Sxl*^{7bO}*;TG/+* were calculated using their *Sxl*^{f9}*/Binsincy*, *Sxl*^{f1}*/Binsincy* and *Sxl*^{7bO}*/Binsincy* sister siblings as reference.

Generation of *delPe-SxlTG*

The exact regions included in *delPe-SxlTG* constructs can be found in Estes et al [71]. The regions upstream and downstream of the deleted region were PCR amplified using

AccuPrime *Pfx* DNA polymerase (Invitrogen), followed by digestion and ligation. The ligated fragment was purified and then used to replace the corresponding wildtype *SxlPe* sequence in Pacman II vector via *galK* recombineering.

Generation of binding site mutations

The binding site mutations were generated by site-directed mutagenesis PCR using primers carrying the desired mutations. After PCR, the plasmid templates were removed by DpnI treatment and the linearized PCR fragments were re-circularized by ligation using Quick Ligation Kit (New England Biolabs Inc.). *E.coli* were transformed with the ligated products. Plasmids were isolated from the transformants and sequenced to confirm that they carried the mutation of interest. The mutation of interest generated were PCR amplified using AccuPrime *Pfx* DNA polymerase (Invitrogen) and the purified fragments were ready to be used in *galK* recombineering.

***galK* recombineering**

The detailed protocol of *galK* recombinnering can be found at https://ncifrederick.cancer.gov/research/brb/protocol/protocol3_sw102_galk_v2.pdf. The following modifications were made to the original protocol. In the first step of *galK* recombineering protocol, *E.coli galK* was integrated into the *Sxl*-pacman II plasmid at the target region. The recombinant bacteria were selected on M9 agar medium with 0.2% galactose and on MacConkey indicator plate to select for *galK* positive pink colonies. In the second step, the PCR fragments carrying the specific deletions or mutations were used

to replace *galK*. The recombinant bacteria here were selected on M9 agar medium with 0.2% 2-deoxy-galactose and re-selected on MacConkey indicator plate and the white colonies were selected as the positive recombinant. Positive recombinant plasmids were purified using PureLink HiPure Plasmid Midiprep Kit (Invitrogen) and confirmed by sequencing.

Sxl transgenic flies

To obtain transformants carrying the *Sxl* transgene system, the purified and confirmed *Sxl*-pacman II plasmid constructs were injected into embryos containing *attP* docking site. All our plasmid constructs were integrated into the attP40 site on the second chromosome. The transgenic injection service was provided by BestGene Inc and Rainbow transgenic flies, Inc.

In situ hybridization

Whole mount embryo collection of 3 hour and 30 minutes were dechorionated in 50% bleach and fixed in 1XPBS, 50mM EGTA, 10% formaldehyde and heptane for 50 minutes. The detailed protocol of *in situ* is adapted from previous publication [42]. Hybridization was performed at 65 ºC.

Templates for probes were generated by PCR amplification using forward primers and reverse primers with 5' T7/T3 promoter sequence. *In vitro* transcription using MAXISCRIPT T3/T7 kit (Ambion) was performed to synthesize digoxygenin(dig)

labeled antisense RNA probes. Anti-dig antibody coupled with alkaline phosophatase (Roche) was used to detect the probe and embryos were stained with NBT/BCIP solution (Roche). DAPI staining was conducted to allow nuclei visualization by UV fluorescence. Embryos were mounted in 70% glycerol/PBS and staged based on nuclei number, shape and membrane furrows as described in previous publication [42].

Probe templates were made using the following primers:

D. persimilis SxlPe intron probe is 286bp, used at 1.5:100 dilution.

Forward primer: 5'- GAGGGGCAGATTATTTGTTAG -3'

Reverse primer: 5'- AATTAACCCTCACTAAAGGGAGAGCCAATAAATGAGAGG GAGTG -3'

D. eugracilis SxlPe intron probe is 492bp, used at 1.5:100 dilution.

Forward primer: 5'- TGAGGATAGCGACTGTATGC -3'

Reverse primer: 5'-AATTAACCCTCAAAGGGAGAGAGATGATAGAGTTGTTGTC GG -3'

FISH (fluorescence *in situ* hybridization)

Fluorescein-labeled *D. persimilis* intron probe and dig-labeled *D. eugracilis* intron probe were used at 1:100 dilution. Hybridization were performed at 65ºC overnight. Sheep anti-digoxigenin (Roche, double check) and mouse anti-fluorescein (Jackson

ImmunoResearch, Inc) were incubated with embryos at 4ºC overnight as primary antibodies. Alexa Fluor 555 donkey anti-sheep antibody (Molecular probes) and Alexa Fluor 647 chicken anti-mouse antibody (Molecular probes) were used as secondary antibodies. Embryos were stained with DAPI and mounted in VECTASHIELD mounting media (Vector Laboratories) or Prolong Diamond antifade mountant (ThermoFisher Scientific).

Confocal Imaging

Embryos were imaged using Olympus FV1000 confocal microscope from Texas A&M Microscopy and Imaging Center. Images were obtained as Z stacks of 7 to 8 sections (with 1.52micron intervals) using 20X oil objective lens. The FISH signals from the two channels were false colored as green and red. Z-stacks were projected into 2D images by combining the maximum intensity from each stack using Olympus FluoView Viewer Version 4.2.

REFERENCES

1. Driever, W., and Nusslein-Volhard, C. (1988). The bicoid protein determines position in the Drosophila embryo in a concentration-dependent manner. Cell *54*, 95-104.

2. St Johnston, D., and Nusslein-Volhard, C. (1992). The origin of pattern and polarity in the Drosophila embryo. Cell *68*, 201-219.

3. Flores-Saaib, R.D., and Courey, A.J. (2000). Regulation of dorso/ventral patterning in the Drosophila embryo by multiple dorsal-interacting proteins. Cell Biochem Biophys *33*, 1-17.

4. Grimm, O., Coppey, M., and Wieschaus, E. (2010). Modelling the Bicoid gradient. Development *137*, 2253-2264.

5. Cline, T.W., and Meyer, B.J. (1996). Vive la difference: males vs females in flies vs worms. Annual review of genetics *30*, 637-702.

6. Cline, T.W. (1993). The *Drosophila* sex determination signal: how do flies count to two?. [Review]. Trends Gen. *9*, 385-390.

7. Salz, H.K., and Erickson, J.W. (2010). Sex determination in Drosophila: The view from the top. Fly *4*, 60-70.

8. Keyes, L.N., Cline, T.W., and Schedl, P. (1992). The primary sex determination signal of Drosophila acts at the level of transcription. Cell *68*, 993-943.

9. Erickson, J.W., and Quintero, J.J. (2007). Indirect effects of ploidy suggest X chromosome dose, not the X:A ratio, signals sex in Drosophila. PLoS Biol *5*, e332.

10. Barbash, D.A., and Cline, T.W. (1995). Genetic and molecular analysis of the autosomal component of the primary sex determination signal of Drosophila melanogaster. Genetics *141*, 1451-1471.

11. Gonzalez, A.N., Lu, H., and Erickson, J.W. (2008). A shared enhancer controls a temporal switch between promoters during Drosophila primary sex determination. Proceedings of the National Academy of Sciences of the United States of America *105*, 18436-18441.

12. Bell, L.R., Horabin, J.I., Schedl, P., and Cline, T.W. (1991). Positive autoregulation of *Sex-lethal* by alternative splicing maintains the female determined state in *Drosophila*. Cell *65*, 229-239.

13. Cline, T.W. (1984). Autoregulatory functioning of a *Drosophila* gene product that establishes and maintains the sexually determined state. Genetics *107*, 231-277.

14. Horabin, J.I., and Schedl, P. (1993). Regulated splicing of the Drosophila sex-lethal male exon involves a blockage mechanism. Mol Cell Biol *13*, 1408-1414.

15. Horabin, J.I., and Schedl, P. (1993). Sex-lethal autoregulation requires multiple cis-acting elements upstream and downstream of the male exon and appears to depend largely on controlling the use of the male exon 5' splice site. Mol Cell Biol *13*, 7734-7746.

16. Nagengast, A.A., Stitzinger, S.M., Tseng, C.H., Mount, S.M., and Salz, H.K. (2003). Sex-lethal splicing autoregulation in vivo: interactions between SEX-LETHAL, the U1 snRNP and U2AF underlie male exon skipping. Development *130*, 463-471.

17. Johnson, M.L., Nagengast, A.A., and Salz, H.K. (2010). PPS, a large multidomain protein, functions with sex-lethal to regulate alternative splicing in Drosophila. PLoS genetics *6*, e1000872.

18. Bell, L.R., Maine, E.M., Schedl, P., and Cline, T.W. (1988). Sex-lethal, a Drosophila sex determination switch gene, exhibits sex-specific RNA splicing and sequence similarity to RNA binding proteins. Cell *55*, 1037-1046.

19. Penalva, L.O., and Sanchez, L. (2003). RNA binding protein sex-lethal (Sxl) and control of Drosophila sex determination and dosage compensation. Microbiol Mol Biol Rev *67*, 343-359, table of contents.

20. Siera, S.G., and Cline, T.W. (2008). Sexual back talk with evolutionary implications: stimulation of the Drosophila sex-determination gene sex-lethal by its target transformer. Genetics *180*, 1963-1981.

21. Valcarcel, J., Singh, R., Zamore, P.D., and Green, M.R. (1993). The protein Sex-lethal antagonizes the splicing factor U2AF to regulate alternative splicing of transformer pre-mRNA. Nature *362*, 171-175.

22. Heinrichs, V., Ryner, L.C., and Baker, B.S. (1998). Regulation of sex-specific selection of fruitless 5' splice sites by transformer and transformer-2. Mol Cell Biol *18*, 450-458.

23. Burtis, K.C., and Baker, B.S. (1989). Drosophila doublesex gene controls somatic sexual differentiation by producing alternatively spliced mRNAs encoding related sex-specific polypeptides. Cell *56*, 997-1010.

24. Rideout, E.J., Dornan, A.J., Neville, M.C., Eadie, S., and Goodwin, S.F. (2010). Control of sexual differentiation and behavior by the doublesex gene in Drosophila melanogaster. Nat Neurosci *13*, 458-466.

25. Camara, N., Whitworth, C., and Van Doren, M. (2008). The creation of sexual dimorphism in the Drosophila soma. Curr Top Dev Biol *83*, 65-107.

26. Rideout, E.J., Billeter, J.C., and Goodwin, S.F. (2007). The sex-determination genes fruitless and doublesex specify a neural substrate required for courtship song. Current biology : CB *17*, 1473-1478.

27. Demir, E., and Dickson, B.J. (2005). fruitless splicing specifies male courtship behavior in Drosophila. Cell *121*, 785-794.

28. Gergen, J.P. (1987). Dosage Compensation in Drosophila: Evidence That daughterless and Sex-lethal Control X Chromosome Activity at the Blastoderm Stage of Embryogenesis. Genetics *117*, 477-485.

29. Gelbart, M.E., and Kuroda, M.I. (2009). Drosophila dosage compensation: a complex voyage to the X chromosome. Development *136*, 1399-1410.

30. Birchler, J., Sun, L., Fernandez, H., Donohue, R., Xie, W., and Sanyal, A. (2011). Re-evaluation of the function of the male specific lethal complex in Drosophila. J Genet Genomics *38*, 327-332.

31. Kuroda, M.I., Kernan, M.J., Kreber, R., Ganetzky, B., and Baker, B.S. (1991). The maleless protein associates with the X chromosome to regulate dosage compensation in Drosophila. Cell *66*, 935-947.

32. Bashaw, G.J., and Baker, B.S. (1997). The regulation of the Drosophila msl-2 gene reveals a function for Sex-lethal in translational control. Cell *89*, 789-798.

33. Franke, A., and Baker, B.S. (1999). The rox1 and rox2 RNAs are essential components of the compensasome, which mediates dosage compensation in Drosophila. Mol Cell *4*, 117-122.

34. Gelbart, M.E., Larschan, E., Peng, S., Park, P.J., and Kuroda, M.I. (2009). Drosophila MSL complex globally acetylates H4K16 on the male X chromosome for dosage compensation. Nat Struct Mol Biol *16*, 825-832.

35. Smith, E.R., Pannuti, A., Gu, W., Steurnagel, A., Cook, R.G., Allis, C.D., and Lucchesi, J.C. (2000). The drosophila MSL complex acetylates histone H4 at lysine 16, a chromatin modification linked to dosage compensation. Mol Cell Biol *20*, 312-318.

36. Sass, G.L., Pannuti, A., and Lucchesi, J.C. (2003). Male-specific lethal complex of Drosophila targets activated regions of the X chromosome for chromatin remodeling. Proceedings of the National Academy of Sciences of the United States of America *100*, 8287-8291.

37. Duncan, K., Grskovic, M., Strein, C., Beckmann, K., Niggeweg, R., Abaza, I., Gebauer, F., Wilm, M., and Hentze, M.W. (2006). Sex-lethal imparts a sex-specific function to UNR by recruiting it to the msl-2 mRNA 3' UTR: translational repression for dosage compensation. Genes Dev *20*, 368-379.

38. Salz, H.K., and Erickson, J.W. (2010). Sex Determination in Drosophila: the view from the top. Fly *4*, 1-11.

39. Sanchez, L., Granadino, B., and Torres, M. (1994). Sex determination in *Drosophila melanogaster*: X-linked genes involved in the initial step of *Sex-lethal* activation. Dev. Genet. *15*, 251-264.

40. Duffy, J.B., and Gergen, J.P. (1991). The *Drosophila* segmentation gene *runt* acts as a position-specific numerator element necessary for the uniform expression of the sex-determining gene *Sex-lethal*. Genes Dev. *5*, 2176-2187.

41. Cline, T.W. (1988). Evidence that sisterless-a and sisterless-b are two of several discrete "numerator elements" of the X/A sex determination signal in Drosophila that switch Sxl between two alternative stable expression states. Genetics *119*, 829-862.

42. Erickson, J.W., and Cline, T.W. (1993). A bZIP protein, SISTERLESS-A, collaborates with bHLH transcription factors early in *Drosophila* development to determine sex. Genes Dev. *7*, 1688-1702.

43. Jinks, T.M., Polydorides, A.D., Calhoun, G., and Schedl, P. (2000). The JAK/STAT signaling pathway is required for the initial choice of sexual identity in Drosophila melanogaster. Mol Cell *5*, 581-587.

44. Sefton, L., Timmer, J.R., Zhang, Y., Beranger, F., and Cline, T.W. (2000). An extracellular activator of the Drosophila JAK/STAT pathway is a sex-determination signal element. Nature *405*, 970-973.

45. Walker, J.J., Lee, K.K., Desai, R.N., and Erickson, J.W. (2000). The Drosophila melanogaster sex determination gene sisA is required in yolk nuclei for midgut formation. Genetics *155*, 191-202.

46. Fassler, J., Landsman, D., Acharya, A., Moll, J.R., Bonovich, M., and Vinson, C. (2002). B-ZIP proteins encoded by the Drosophila genome: evaluation of potential dimerization partners. Genome research *12*, 1190-1200.

47. Yang, D., Lu, H., Hong, Y., Jinks, T.M., Estes, P.A., and Erickson, J.W. (2001). Interpretation of X Chromosome Dose at Sex-lethal Requires Non-E-Box Sites for the Basic Helix-Loop-Helix Proteins SISB and Daughterless. Molecular and Cellular Biology *21*, 1581-1592.

48. Cabrera, C.V., and Alonzo, M.C. (1991). Transcriptional activation by heterodimers of the *achaete-scute* and *daughterless* gene products of *Drosophila*. EMBO J. *10*, 2965-2973.

49. Jan, Y.N., and Jan, L.Y. (1993). HLH proteins, fly neurogenesis, and vertebrate myogenesis. Cell *75*, 827-830.

50. Caudy, M., Grell, E.H., Dambly-Chaudiere, C., Ghysen, A., Jan, L.Y., and Jan, Y.N. (1988). The maternal sex determination gene daughterless has zygotic activity necessary for the formation of peripheral neurons in Drosophila. Genes Dev *2*, 843-852.

51. Gergen, J.P., and Butler, B.A. (1988). Isolation of the Drosophila segmentation gene runt and analysis of its expression during embryogenesis. Genes Dev *2*, 1179-1193.

52. Torres, M., and Sanchez, L. (1992). The segmentation gene runt is needed to activate Sex-lethal, a gene that controls sex determination and dosage compensation in Drosophila. Genet Res *59*, 189-198.

53. Kramer, S.G., Jinks, T.M., Schedl, P., and Gergen, J.P. (1999). Direct activation of *Sex-lethal* transcription by the *Drosophila runt* protein. Development *126*, 191-200.

54. Avila, F.W., and Erickson, J.W. (2007). Drosophila JAK/STAT pathway reveals distinct initiation and reinforcement steps in early transcription of Sxl. Current biology : CB *17*, 643-648.

55. Harrison, D.A., McCoon, P.E., Binari, R., Gilman, M., and Perrimon, N. (1998). Drosophila unpaired encodes a secreted protein that activates the JAK signaling pathway. Genes Dev *12*, 3252-3263.

56. Kappes, G., Deshpande, G., Mulvey, B.B., Horabin, J.I., and Schedl, P. (2011). The Drosophila Myc gene, diminutive, is a positive regulator of the Sex-lethal establishment promoter, Sxl-Pe. Proceedings of the National Academy of Sciences of the United States of America *108*, 1543-1548.

57. Lott, S.E., Villalta, J.E., Schroth, G.P., Luo, S., Tonkin, L.A., and Eisen, M.B. (2011). Noncanonical compensation of zygotic X transcription in early Drosophila melanogaster development revealed through single-embryo RNA-seq. PLoS Biol *9*, e1000590.

58. Liang, H.L., Nien, C.Y., Liu, H.Y., Metzstein, M.M., Kirov, N., and Rushlow, C. (2008). The zinc-finger protein Zelda is a key activator of the early zygotic genome in Drosophila. Nature *456*, 400-403.

59. ten Bosch, J.R., Benavides, J.A., and Cline, T.W. (2006). The TAGteam DNA motif controls the timing of Drosophila pre-blastoderm transcription. Development *133*, 1967-1977.

60. Nien, C.Y., Liang, H.L., Butcher, S., Sun, Y., Fu, S., Gocha, T., Kirov, N., Manak, J.R., and Rushlow, C. (2011). Temporal coordination of gene networks by Zelda in the early Drosophila embryo. PLoS genetics *7*, e1002339.

61. Foo, S.M., Sun, Y., Lim, B., Ziukaite, R., O'Brien, K., Nien, C.Y., Kirov, N., Shvartsman, S.Y., and Rushlow, C.A. (2014). Zelda potentiates morphogen

activity by increasing chromatin accessibility. Current biology : CB *24*, 1341-1346.

62. Sun, Y., Nien, C.Y., Chen, K., Liu, H.Y., Johnston, J., Zeitlinger, J., and Rushlow, C. (2015). Zelda overcomes the high intrinsic nucleosome barrier at enhancers during Drosophila zygotic genome activation. Genome research *25*, 1703-1714.

63. Schulz, K.N., Bondra, E.R., Moshe, A., Villalta, J.E., Lieb, J.D., Kaplan, T., McKay, D.J., and Harrison, M.M. (2015). Zelda is differentially required for chromatin accessibility, transcription factor binding, and gene expression in the early Drosophila embryo. Genome research *25*, 1715-1726.

64. Lu, H., Kozhina, E., Mahadevaraju, S., Yang, D., Avila, F.W., and Erickson, J.W. (2008). Maternal Groucho and bHLH repressors amplify the dose-sensitive X chromosome signal in Drosophila sex determination. Dev Biol *323*, 248-260.

65. Chen, G., and Courey, A.J. (2000). Groucho/TLE family proteins and transcriptional repression. Gene *249*, 1-16.

66. Payankaulam, S., and Arnosti, D.N. (2009). Groucho corepressor functions as a cofactor for the Knirps short-range transcriptional repressor. Proceedings of the National Academy of Sciences of the United States of America *106*, 17314-17319.

67. Sekiya, T., and Zaret, K.S. (2007). Repression by Groucho/TLE/Grg proteins: genomic site recruitment generates compacted chromatin in vitro and impairs activator binding in vivo. Mol Cell *28*, 291-303.

68. Jennings, B.H., Pickles, L.M., Wainwright, S.M., Roe, S.M., Pearl, L.H., and Ish-Horowicz, D. (2006). Molecular recognition of transcriptional repressor motifs by the WD domain of the Groucho/TLE corepressor. Mol Cell *22*, 645-655.

69. Younger-Shepherd, S., Vaessin, H., Bier, E., Jan, L.Y., and Jan., Y.N. (1992). *deadpan* an essential pan-neural gene encoding an HLH protein, acts as a denominator element in *Drosophila* sex determination. Cell *70*, 911-921.

70. Winston, R.L., Millar, D.P., Gottesfeld, J.M., and Kent, S.B. (1999). Characterization of the DNA binding properties of the bHLH domain of Deadpan to single and tandem sites. Biochemistry *38*, 5138-5146.

71. Estes, P.A., Keyes, L.N., and Schedl, P. (1995). Multiple response elements in the *Sex-lethal* early promoter ensure its female-specific expression pattern. Mol. Cell Biol. *15*, 904-917.

72. Louis, M., Holm, L., Sanchez, L., and Kaufman, M. (2003). A theoretical model for the regulation of Sex-lethal, a gene that controls sex determination and dosage compensation in Drosophila melanogaster. Genetics *165*, 1355-1384.

73. Deshpande, G., Stukey, J., and Schedl, P. (1995). *scute (sis-b*) function in *Drosophila* sex determination. Mol. Cell Biol. *15*, 4430-4440.

74. Erickson, J.W., and Cline, T.W. (1991). Molecular nature of the Drosophila sex determination signal and its link to neurogenesis. Science *251*, 1071-1074.

75. Venken, K.J., He, Y., Hoskins, R.A., and Bellen, H.J. (2006). P[acman]: a BAC transgenic platform for targeted insertion of large DNA fragments in D. melanogaster. Science *314*, 1747-1751.

76. Warming, S., Costantino, N., Court, D.L., Jenkins, N.A., and Copeland, N.G. (2005). Simple and highly efficient BAC recombineering using galK selection. Nucleic Acids Res *33*, e36.

77. Groth, A.C., Fish, M., Nusse, R., and Calos, M.P. (2004). Construction of transgenic Drosophila by using the site-specific integrase from phage phiC31. Genetics *166*, 1775-1782.

78. Salz, H.K., Cline, T.W., and Schedl, P. (1987). Functional changes associated with structural alterations induced by mobilization of a P element inserted in the Sex-lethal gene of Drosophila. Genetics *117*, 221-231.

79. Bopp, D., Calhoun, G., Horabin, J.I., Samuels, M., and Schedl, P. (1996). Sex-specific control of Sex-lethal is a conserved mechanism for sex determination in the genus Drosophila. Development *122*, 971-982.

80. Maine, E.M., Salz, H.K., Schedl, P., and Cline, T.W. (1985). Sex-lethal, a link between sex determination and sexual differentiation in Drosophila melanogaster. Cold Spring Harbor symposia on quantitative biology *50*, 595-604.

81. Bernstein, M., and Cline, T.W. (1994). Differential effects of Sex-lethal mutations on dosage compensation early in Drosophila development. Genetics *136*, 1051-1061.

82. Jinks, T.M., Calhoun, G., and Schedl, P. (2003). Functional conservation of the sex-lethal sex determining promoter, Sxl-Pe, in Drosophila virilis. Development genes and evolution *213*, 155-165.

83. Paroush, Z., Finley, R.L., Jr., Kidd, T., Wainwright, S.M., Ingham, P.W., Brent, R., and Ish-Horowicz, D. (1994). Groucho is required for Drosophila neurogenesis, segmentation, and sex determination and interacts directly with hairy-related bHLH proteins. Cell *79*, 805-815.

84. Carter, P. (1986). Site-directed mutagenesis. Biochem J *237*, 1-7.

85. Chen, X., Liu, W., Quinto, I., and Scala, G. (2002). Site-directed mutagenesis mediated by a single polymerase chain reaction product. Methods Mol Biol *182*, 67-70.

86. Fisher, A.L., and Caudy, M. (1998). Groucho proteins: transcriptional corepressors for specific subsets of DNA-binding transcription factors in vertebrates and invertebrates. Genes Dev *12*, 1931-1940.

87. Bier, E., Vaessin, H., Younger-Shepherd, S., Jan, L.Y., and Jan, Y.N. (1992). deadpan, an essential pan-neural gene in Drosophila, encodes a helix-loop-helix protein similar to the hairy gene product. Genes Dev *6*, 2137-2151.

88. Ohsako, S., Hyer, J., Panganiban, G., Oliver, I., and Caudy, M. (1994). Hairy function as a DNA-binding helix-loop-helix repressor of *Drosophila* sensory organ formation. Genes Dev *8*, 2743-2755.

89. Van Doren, M., Bailey, A., Esnayra, J., Ede, K., and Posakony, J.W. (1994). Negative regulation of proneural gene activity: hairy is a direct transcriptional repressor of *achaete*. Genes Dev *8*, 2729-2742.

90. Hoshijima, K., Kohyama, A., Watakabe, I., Inoue, K., Sakamoto, H., and Shimura, Y. (1995). Transcriptional regulation of the Sex-lethal gene by helix-loop-helix proteins. Nucleic Acids Res *23*, 3441-3448.

91. Geyer, P.K., Green, M.M., and Corces, V.G. (1990). Tissue-specific transcriptional enhancers may act in trans on the gene located in the homologous chromosome: the molecular basis of transvection in Drosophila. The EMBO journal *9*, 2247-2256.

92. Morris, J.R., Chen, J.L., Geyer, P.K., and Wu, C.T. (1998). Two modes of transvection: enhancer action in trans and bypass of a chromatin insulator in cis. Proceedings of the National Academy of Sciences of the United States of America *95*, 10740-10745.

93. Morris, J.R., Geyer, P.K., and Wu, C.-t. (1999). Core promoter elements can regulate transcription on a separate chromosome in trans. Genes & Development *13*, 253-258.

94. Duncan, I.W. (2002). Transvection effects in Drosophila. Annual review of genetics *36*, 521-556.

95. Kennison, J.A., and Southworth, J.W. (2002). Transvection in Drosophila. Adv Genet *46*, 399-420.

96. Lewis, E.B. (1954). The Theory and Application of a New Method of Detecting Chromosomal Rearrangements in Drosophila melanogaster. The American Naturalist *88*, 225-239.

97. Mulvey, B.B., Olcese, U., Cabrera, J.R., and Horabin, J.I. (2014). An interactive network of long non-coding RNAs facilitates the Drosophila sex determination decision. Biochim Biophys Acta *1839*, 773-784.

98. Erickson, J.W., and Cline, T.W. (1998). Key aspects of the primary sex determination mechanism are conserved across the genus Drosophila. Development *125*, 3259-3268.

99. Zhu, C., Urano, J., and Bell, L.R. (1997). The Sex-lethal early splicing pattern uses a default mechanism dependent on the alternative 5' splice sites. Mol Cell Biol *17*, 1674-1681.

100. Boettiger, A.N., and Levine, M. (2013). Rapid transcription fosters coordinate snail expression in the Drosophila embryo. Cell reports *3*, 8-15.

101. Bothma, J.P., Magliocco, J., and Levine, M. (2011). The snail repressor inhibits release, not elongation, of paused Pol II in the Drosophila embryo. Current biology : CB *21*, 1571-1577.

102. Lagha, M., Bothma, J.P., Esposito, E., Ng, S., Stefanik, L., Tsui, C., Johnston, J., Chen, K., Gilmour, D.S., Zeitlinger, J., et al. (2013). Paused Pol II coordinates tissue morphogenesis in the Drosophila embryo. Cell *153*, 976-987.

103. Ferraro, T., Esposito, E., Mancini, L., Ng, S., Lucas, T., Coppey, M., Dostatni, N., Walczak, A.M., Levine, M., and Lagha, M. (2016). Transcriptional Memory in the Drosophila Embryo. Current biology : CB *26*, 212-218.

104. Harrison, M.M., Botchan, M.R., and Cline, T.W. (2010). Grainyhead and Zelda compete for binding to the promoters of the earliest-expressed Drosophila genes. Dev Biol *345*, 248-255.

105. Harrison, M.M., Li, X.Y., Kaplan, T., Botchan, M.R., and Eisen, M.B. (2011). Zelda binding in the early Drosophila melanogaster embryo marks regions subsequently activated at the maternal-to-zygotic transition. PLoS genetics *7*, e1002266.

106. Bateman, J.R., Johnson, J.E., and Locke, M.N. (2012). Comparing enhancer action in cis and in trans. Genetics *191*, 1143-1155.

107. Keefe, M.D., and Bonkowsky, J.L. (2017). Transvection Arising from Transgene Interactions in Zebrafish. Zebrafish *14*, 8-9.

108. Blick, A.J., Mayer-Hirshfeld, I., Malibiran, B.R., Cooper, M.A., Martino, P.A., Johnson, J.E., and Bateman, J.R. (2016). The Capacity to Act in Trans Varies Among Drosophila Enhancers. Genetics *203*, 203-218.

109. Cline, T.W. (1986). A female-specific lethal lesion in an X-linked positive regulator of the Drosophila sex determination gene, Sex-lethal. Genetics *113*, 641-663.

APPENDIX A

This appendix contains all the supplement tables and figures for Chapter III.

Data tables of all the genetic tests performed on *delPe-SxlTG*
In the following tables, numerical data represent percentage of female viability. Numerical data in parenthesis represent the number of viable females.

Complete table (viability data) for Table 3.1 (Complementation of *Sxl^{f9}* mutants by *delPe-SxlTG*)

Genotype	*SxlPe$_{0.2kb}$ SxlTG*	*SxlPe$_{0.4kb}$ SxlTG*	*SxlPe$_{0.8kb}$ SxlTG*	*SxlPe$_{1.1kb}$ SxlTG*	*SxlPe$_{1.4kb}$ SxlTG*	*SxlPe$_{3.0kb}$ SxlTG*	*SxlPe$_{3.7kb}$ SxlTG*	*SxlTG*	*ΔPe SxlTG*
$\frac{Sxl^{f9}}{Sxl^{f9}}; \frac{+}{+}$	0 (0)	0 (0)	0 (0)	0 (0)	0 (0)	0 (0)	0 (0)	0 (0)	0 (0)
$\frac{Sxl^{f9}}{Sxl^{f9}}; \frac{TG}{+}$	0 (0)	0 (0)	92.4 (171)	111.2 (99)	98 (147)	92.3 (168)	140.3 (94)	110.9 (112)	0 (0)
$\frac{Sxl^{f9}}{Bincy}; \frac{+}{+}$	100 (110)	100 (82)	100 (185)	100 (89)	100 (150)	100 (182)	100 (67)	100 (101)	100 (125)
$\frac{Sxl^{f9}}{Bincy}; \frac{TG}{+}$	108.2 (119)	108.5 (89)	119.5 (221)	104.5 (93)	106.7 (160)	119.2 (217)	123.9 (83)	107.9 (109)	123.2 (154)
$\frac{Sxl^{f9}}{Y}; \frac{+}{+}$	100 (107)	100 (87)	100 (175)	100 (105)	100 (154)	100 (181)	100 (78)	100 (132)	100 (140)
$\frac{Sxl^{f9}}{Y}; \frac{TG}{+}$	95.3 (102)	104.6 (91)	126.3 (221)	161.4 (124)	107.8 (166)	91.7 (166)	115.4 (90)	96.2 (127)	98.6 (138)
$\frac{Bincy}{Y}; \frac{+}{+}$	92.5 (99)	44.8 (39)	45.7 (80)	32.4 (34)	41.6 (64)	32.6 (59)	34.6 (27)	36.4 (48)	40.7 (57)
$\frac{Bincy}{Y}; \frac{TG}{+}$	77.6 (83)	35.6 (31)	61.1 (107)	36.2 (38)	39 (60)	2.8 (5)	9 (7)	3.8 (5)	6.4 (9)

Crosses ♀♀ *w Sxl^{f9}ct*/*Binsincy*; +/+ × ♂♂ *w Sxl^{f9} ct* /Y; TG/+

Complete table (viability data) for Table 3.2 (Complementation of *Sxl^{f9}/Sxl^{f1}* mutants by *delPe-Sxl-Eug-TG*)

Genotype	*SxlPe$_{0.8kb}$ SxlTG*	*SxlPe$_{1.1kb}$ SxlTG*	*SxlPe$_{1.4kb}$ SxlTG*	*SxlPe$_{3.0kb}$ SxlTG*	*SxlPe$_{3.7kb}$ SxlTG*	*SxlTG*	*ΔPe SxlTG*
$\frac{Sxl^{f9}}{Sxl^{f1}}$; $\frac{+}{+}$	0 (0)	0 (0)	0 (0)	0 (0)	0 (0)	0 (0)	0 (0)
$\frac{Sxl^{f9}}{Sxl^{f1}}$; $\frac{TG}{+}$	38.6 (39)	74.1 (83)	99.1 (106)	104.2 (99)	99.0 (99)	114.6 (55)	0 (0)
$\frac{Sxl^{f9}}{Bincy}$; $\frac{+}{+}$	100 (101)	100 (112)	100 (107)	100 (95)	100 (100)	100 (48)	100 (84)
$\frac{Sxl^{f9}}{Bincy}$; $\frac{TG}{+}$	106.9 (108)	88.4 (99)	90.6 (97)	113.7 (108)	100 (100)	93.8 (45)	66.7 (56)
$\frac{Sxl^{f1}}{Y}$; $\frac{+}{+}$	100 (112)	100 (98)	100 (99)	100 (92)	100 (93)	100 (40)	100 (61)
$\frac{Sxl^{f1}}{Y}$; $\frac{TG}{+}$	99.4 (99)	87.8 (86)	86.9 (86)	94.6 (87)	122.6 (114)	110.0 (44)	116.4 (71)
$\frac{Bincy}{Y}$; $\frac{+}{+}$	58.0 (65)	48.0 (47)	43.4 (43)	71.7 (66)	65.6 (61)	117.5 (47)	108.2 (66)
$\frac{Bincy}{Y}$; $\frac{TG}{+}$	48.2 (54)	36.7 (36)	34.3 (34)	48.9 (45)	34.4 (32)	12.5 (5)	108.2 (66)

Crosses ♀♀ *y w cm Sxl^{f1} ct*/*Binsincy*; +/+ × ♂♂ *w Sxl^{f9} ct* /Y; TG/+

Complete table (viability data) for Fig.3.4A (Complementation of *Sxl^{f9}* mutants by one or two copies of *0.2kbSxlPe-SxlTG* and *0.4kbSxlPe-SxlTG*)

Genotype	*SxlPe$_{0.2kb}$ SxlTG*	*SxlPe$_{0.4kb}$ SxlTG*	*SxlTG*
$\frac{Sxl^{f9}}{Sxl^{f9}}$; $\frac{+}{+}$	0 (0)	0 (0)	0 (0)
$\frac{Sxl^{f9}}{Sxl^{f9}}$; $\frac{TG}{+}$	0 (0)	0 (0)	102.3 (88)
$\frac{Sxl^{f9}}{Sxl^{f9}}$; $\frac{TG}{TG}$	0 (0)	0 (0)	104.6 (47)
$\frac{Sxl^{f9}}{Bincy}$; $\frac{+}{+}$	100 (67)	100 (69)	100 (43)
$\frac{Sxl^{f9}}{Bincy}$; $\frac{TG}{+}$	78.3 (105)	113.8 (157)	105.8 (91)
$\frac{Sxl^{f9}}{Bincy}$; $\frac{TG}{TG}$	59.7 (40)	89.8 (62)	111.6 (48)
$\frac{Sxl^{f9}}{Y}$; $\frac{+}{+}$	100 (42)	100 (83)	100 (51)
$\frac{Sxl^{f9}}{Y}$; $\frac{TG}{+}$	129.8 (109)	104.8 (174)	96.1 (98)
$\frac{Sxl^{f9}}{Y}$; $\frac{TG}{TG}$	83.3 (35)	72.3 (60)	86.3 (44)
$\frac{Bincy}{Y}$; $\frac{+}{+}$	100 (24)	100 (32)	100 (210
$\frac{Bincy}{Y}$; $\frac{TG}{+}$	122.9 (59)	100 (64)	116.7 (49)
$\frac{Bincy}{Y}$; $\frac{TG}{TG}$	62.5 (15)	43.8 (17)	42.8 (9)

Crosses ♀♀ *w Sxl^{f9}ct*/*Binsincy*; TG/+ × ♂♂ *w Sxl^{f9} ct* /Y; TG/+

Complete table (viability data) for Fig. 3.5B (Complementation of *Sxl^{f9}* mutants by *0.4kbSxlPe-SxlTG* and *0.4kbgalKSxlPe-SxlTG*)

Genotype	*SxlPe$_{0.4kb}$ SxlTG*	*SxlPe$_{0.4kbgalK}$ SxlTG*	*SxlPe$_{0.8kb}$ SxlTG*	*SxlTG*
$\frac{Sxl^{f9}}{Sxl^{f9}}; \frac{+}{+}$	0 (0)	0 (0)	0 (0)	0 (0)
$\frac{Sxl^{f9}}{Sxl^{f9}}; \frac{TG}{+}$	0 (0)	92.6 (100)	102.9 (142)	89.7 (96)
$\frac{Sxl^{f9}}{Bincy}; \frac{+}{+}$	100 (85)	100 (108)	100 (138)	100 (107)
$\frac{Sxl^{f9}}{Bincy}; \frac{TG}{+}$	116.5 (99)	97.2 (105)	110.1 (152)	90.6 (97)
$\frac{Sxl^{f9}}{Y}; \frac{+}{+}$	100 (92)	100 (109)	100 (127)	100 (98)
$\frac{Sxl^{f9}}{Y}; \frac{TG}{+}$	104.3 (96)	106.4 (116)	115 (146)	112.2 (110)
$\frac{Bincy}{Y}; \frac{+}{+}$	26.1 (24)	23.8 (26)	26.8 (34)	31.6 (31)
$\frac{Bincy}{Y}; \frac{TG}{+}$	20.6 (19)	45.9 (50)	51.2 (65)	3.1 (3)

Crosses ♀♀ *w Sxl^{f9}ct/Binsincy*; +/+ ×♂♂ *w Sxl^{f9} ct* /Y; TG/+

Complete table (viability data) for Fig. 3.5C (Complementation of *Sxl^{f9}/Sxl^{f1}* mutants by *0.4kbSxlPe-SxlTG* and *0.4kbgalKSxlPe-SxlTG*)

Genotype	*SxlPe$_{0.4kb}$ SxlTG*	*SxlPe$_{0.4kbgalK}$ SxlTG*	*SxlPe$_{0.8kb}$ SxlTG*	*SxlTG*
$\frac{Sxl^{f9}}{Sxl^{f1}}; \frac{+}{+}$	0 (0)	0 (0)	0 (0)	0 (0)
$\frac{Sxl^{f9}}{Sxl^{f1}}; \frac{TG}{+}$	0 (0)	28.9 (28)	38.6 (39)	114.6 (55)
$\frac{Sxl^{f9}}{Bincy}; \frac{+}{+}$	100 (96)	100 (97)	100 (101)	100 (48)
$\frac{Sxl^{f9}}{Bincy}; \frac{TG}{+}$	109.4 (105)	90.7 (88)	106.9 (108)	93.8 (45)
$\frac{Sxl^{f1}}{Y}; \frac{+}{+}$	100 (102)	100 (103)	100 (112)	100 (40)
$\frac{Sxl^{f1}}{Y}; \frac{TG}{+}$	86.3 (88)	108.7 (112)	99.4 (99)	110.0 (44)
$\frac{Bincy}{Y}; \frac{+}{+}$	61.8 (63)	66.0 (68)	58.0 (65)	117.5 (47)
$\frac{Bincy}{Y}; \frac{TG}{+}$	48.0 (49)	52.4 (54)	48.2 (54)	12.5 (5)

Crosses ♀♀ *y w cm Sxl^{f1} ct/Binsincy*; +/+ ×♂♂ *w Sxl^{f9} ct* /Y; TG/+

Complementation of *Sxl*^{7BO} mutants by *delPe-SxlTG*

Genotype	*SxlPe*$_{0.2kb}$ *SxlTG*	*SxlPe*$_{0.4kb}$ *SxlTG*	*SxlPe*$_{0.8kb}$ *SxlTG*	*SxlPe*$_{1.1kb}$ *SxlTG*	*SxlPe*$_{1.4kb}$ *SxlTG*	*SxlPe*$_{3.0kb}$ *SxlTG*	*SxlPe*$_{3.7kb}$ *SxlTG*	*SxlTG*	*ΔPe SxlTG*
$\frac{Sxl^{7BO}}{Sxl^{7BO}}; \frac{+}{+}$	0 (0)	0 (0)	0 (0)	0 (0)	0 (0)	0 (0)	0 (0)	0 (0)	0 (0)
$\frac{Sxl^{7BO}}{Sxl^{7BO}}; \frac{TG}{+}$	0 (0)	0 (0)	0 (0)	0 (0)	0 (0)	0 (0)	0 (0)	110.7 (93)	0 (0)
$\frac{Sxl^{7BO}}{Bincy}; \frac{+}{+}$	100 (105)	100 (102)	100 (80)	100 (84)	100 (94)	100 (96)	100 (93)	100 (84)	100 (88)
$\frac{Sxl^{7BO}}{Bincy}; \frac{TG}{+}$	108.6 (114)	107.8 (110)	92.5 (74)	110.7 (93)	84 (79)	75 (72)	110.7 (103)	103.6 (87)	109.1 (96)
$\frac{Sxl^{7BO}}{Y}; \frac{+}{+}$	100 (103)	100 (134)	100 (57)	100 (102)	100 (78)	100 (112)	100 (108)	100 (60)	100 (105)
$\frac{Sxl^{7BO}}{Y}; \frac{TG}{+}$	107.8 (111)	90.3 (121)	115.8 (66)	110.8 (113)	83.3 (65)	100 (112)	90.7 (98)	105 (63)	109.5 (115)
$\frac{Bincy}{Y}; \frac{+}{+}$	84.5 (87)	86.6 (116)	115.8 (66)	61.8 (63)	98.7 (77)	57.1 (64)	56.5 (61)	70 (42)	48.6 (51)
$\frac{Bincy}{Y}; \frac{TG}{+}$	68.9 (71)	68.7 (92)	103.5 (59)	61.8 (63)	75.6 (59)	42 (47)	23.1 (25)	85 (51)	61.9 (65)

Crosses ♀♀ *y pn w Sxl*^{7BO}*/Binsincy*; +/+ × ♂♂ *y pn w Sxl*^{7BO}/Y; TG/+

Complementation of *Sxl*^{f1} mutants by *delPe-SxlTG*

Genotype	*SxlPe*$_{0.2kb}$ *SxlTG*	*SxlPe*$_{0.4kb}$ *SxlTG*	*SxlPe*$_{0.8kb}$ *SxlTG*	*SxlPe*$_{1.1kb}$ *SxlTG*	*SxlPe*$_{1.4kb}$ *SxlTG*	*SxlPe*$_{3.0kb}$ *SxlTG*	*SxlPe*$_{3.7kb}$ *SxlTG*	*SxlTG*	*ΔPe SxlTG*
$\frac{Sxl^{f1}}{Sxl^{f1}}; \frac{+}{+}$	0 (0)	0 (0)	0 (0)	0 (0)	0 (0)	0 (0)	0 (0)	0 (0)	0 (0)
$\frac{Sxl^{f1}}{Sxl^{f1}}; \frac{TG}{+}$	0 (0)	0 (0)	0 (0)	0 (0)	0 (0)	0 (0)	0 (0)	109.9 (111)	0 (0)
$\frac{Sxl^{f1}}{Bincy}; \frac{+}{+}$	100 (67)	100 (50)	100 (108)	100 (126)	100 (148)	100 (89)	100 (60)	100 (101)	100 (105)
$\frac{Sxl^{f1}}{Bincy}; \frac{TG}{+}$	103.0 (69)	128.0 (64)	137 (148)	130.9 (165)	110.8 (164)	167.4 (149)	168.3 (101)	130.7 (132)	106.7 (112)
$\frac{Sxl^{f1}}{Y}; \frac{+}{+}$	100 (69)	100 (61)	100 (141)	100 (126)	100 (136)	100 (112)	100 (67)	100 (119)	98 (100)
$\frac{Sxl^{f1}}{Y}; \frac{TG}{+}$	102.9 (71)	78.7 (48)	133.3 (188)	126.2 (159)	151.5 (206)	113.4 (127)	213.4 (143)	127.7 (152)	90.8 (89)
$\frac{Bincy}{Y}; \frac{+}{+}$	75.4 (52)	80.3 (49)	53.2 (75)	36.5 (46)	83.8 (114)	89.3 (100)	28.4 (19)	44.5 (53)	66.3 (65)
$\frac{Bincy}{Y}; \frac{TG}{+}$	69.6 (48)	65.6 (40)	97.9 (138)	88.1 (111)	87.5 (119)	84.8 (95)	140.3 (94)	52.9 (65)	74.5 (73)

Crosses ♀♀ *y w cm Sxl*^{f1} *ct/Binsincy*; +/+ × ♂♂ *y w cm Sxl*^{f1} *ct* /Y; TG/+

Complementation of *Sxl^{f1}* mutants by *delPe-Sxl-Eug-TG*

Genotype	*SxlPe$_{0.4kb}$ SxlTG*	*SxlPe$_{0.8kb}$ SxlTG*	*SxlPe$_{1.1kb}$ SxlTG*	*SxlPe$_{1.4kb}$ SxlTG*	*SxlPe$_{3.0kb}$ SxlTG*	*SxlPe$_{3.7kb}$ SxlTG*	*SxlTG*	*ΔPe SxlTG*
$\frac{Sxl^{f1}}{Sxl^{f1}}; \frac{+}{+}$	0 (0)	0 (0)	0 (0)	0 (0)	0 (0)	0 (0)	0 (0)	0 (0)
$\frac{Sxl^{f1}}{Sxl^{f1}}; \frac{TG}{+}$	0 (0)	0 (0)	0 (0)	0 (0)	0 (0)	0 (0)	109.9 (111)	0 (0)
$\frac{Sxl^{f1}}{Bincy}; \frac{+}{+}$	100 (72)	100 (38)	100 (43)	100 (34)	100 (115)	100 (101)	100 (101)	100 (105)
$\frac{Sxl^{f1}}{Bincy}; \frac{TG}{+}$	127.8 (92)	142.1 (54)	148.8 (64)	100 (34)	80.4 (143)	115.8 (117)	130.7 (132)	106.7 (112)
$\frac{Sxl^{f1}}{Y}; \frac{+}{+}$	100 (89)	100 (65)	100 (67)	100 (28)	100 (121)	100 (85)	100 (119)	98 (100)
$\frac{Sxl^{f1}}{Y}; \frac{TG}{+}$	96.6 (86)	123.1 (80)	94 (63)	139.3 (39)	129.8 (157)	156.5 (133)	127.7 (152)	90.8 (89)
$\frac{Bincy}{Y}; \frac{+}{+}$	60.7 (54)	65.6 (42)	74.6 (50)	114 (11)	54.5 (66)	85.9 (73)	44.5 (53)	66.3 (65)
$\frac{Bincy}{Y}; \frac{TG}{+}$	93.2 (83)	83.1 (54)	80.6 (54)	75 (21)	77.7 (94)	83.5 (71)	52.9 (65)	74.5 (73)

Crosses ♀♀ *y w cm Sxl^{f1} ct*/*Binsincy*; +/+ × ♂♂ *y w cm Sxl^{f1} ct* /Y; TG/+

Complementation of *Sxl^{f9}* mutants by *delPe-Sxl-Eug-TG*

Genotype	*SxlPe$_{0.4kb}$ SxlTG*	*SxlPe$_{0.8kb}$ SxlTG*	*SxlPe$_{1.1kb}$ SxlTG*	*SxlPe$_{1.4kb}$ SxlTG*	*SxlPe$_{3.0kb}$ SxlTG*	*SxlPe$_{3.7kb}$ SxlTG*	*SxlTG*	*ΔPe SxlTG*
$\frac{Sxl^{f9}}{Sxl^{f9}}; \frac{+}{+}$	0 (0)	0 (0)	0 (0)	0 (0)	0 (0)	0 (0)	0 (0)	0 (0)
$\frac{Sxl^{f9}}{Sxl^{f9}}; \frac{TG}{+}$	0 (0)	102.9 (142)	104.8 (109)	77.1 (118)	118.9 (132)	88.3 (129)	110.9 (112)	0 (0)
$\frac{Sxl^{f9}}{Bincy}; \frac{+}{+}$	100 (85)	100 (138)	100 (104)	100 (153)	100 (111)	100 (146)	100 (101)	100 (125)
$\frac{Sxl^{f9}}{Bincy}; \frac{TG}{+}$	116.5 (99)	110.1 (152)	90.4 (94)	103.4 (122)	82.6 (109)	102 (149)	107.9 (109)	123.2 (154)
$\frac{Sxl^{f9}}{Y}; \frac{+}{+}$	100 (92)	100 (127)	100 (121)	100 (123)	100 (123)	100 (128)	100 (132)	100 (140)
$\frac{Sxl^{f9}}{Y}; \frac{TG}{+}$	104.3 (96)	115 (146)	88.4 (107)	88.6 (109)	98.4 (121)	121.9 (156)	96.2 (127)	98.5 (138)
$\frac{Bincy}{Y}; \frac{+}{+}$	26.1 (24)	26.8 (34)	36.4 (44)	42.3 (52)	36.6 (45)	25 (32)	36.4 (48)	40.7 (57)
$\frac{Bincy}{Y}; \frac{TG}{+}$	20.6 (19)	51.2 (65)	53.7 (65)	37.4 (46)	9.7 (12)	13.3 (17)	3.8 (5)	6.4 (9)

Crosses ♀♀ *w Sxl^{f9}ct*/*Binsincy*; +/+ × ♂♂ *w Sxl^{f9} ct* /Y; TG/+

Complementation of Sxl^{f9}/Sxl^{f1} mutants by *delPe-Sxl-TG*

Genotype	$SxlPe_{0.8kb}$ *SxlTG*	$SxlPe_{1.1kb}$ *SxlTG*	$SxlPe_{1.4kb}$ *SxlTG*	$SxlPe_{3.0kb}$ *SxlTG*	$SxlPe_{3.7kb}$ *SxlTG*	*SxlTG*	*ΔPe SxlTG*
$\frac{Sxl^{f9}}{Sxl^{f1}}; \frac{+}{+}$	0 (0)	0 (0)	0 (0)	0 (0)	0 (0)	0 (0)	0 (0)
$\frac{Sxl^{f9}}{Sxl^{f1}}; \frac{TG}{+}$	42.2 (46)	87.3 (89)	94.7 (142)	85.6 (119)	100 (128)	114.6 (55)	0 (0)
$\frac{Sxl^{f9}}{Bincy}; \frac{+}{+}$	100 (109)	100 (102)	100 (150)	100 (139)	100 (128)	100 (48)	100 (84)
$\frac{Sxl^{f9}}{Bincy}; \frac{TG}{+}$	108.3 (118)	104.9 (107)	79.3 (119)	76.9 (107)	91.3 (104)	93.8 (45)	66.7 (56)
$\frac{Sxl^{f1}}{Y}; \frac{+}{+}$	100 (102)	100 (83)	100 (121)	100 (120)	100 (133)	100 (40)	100 (61)
$\frac{Sxl^{f1}}{Y}; \frac{TG}{+}$	96.1 (98)	114.5 (95)	98.3 (119)	94.2 (113)	91.7 (122)	110.0 (44)	116.4 (71)
$\frac{Bincy}{Y}; \frac{+}{+}$	74.5 (76)	100 (83)	73.6 (89)	84.2 (101)	76.7 (102)	117.5 (47)	108.2 (66)
$\frac{Bincy}{Y}; \frac{TG}{+}$	86.3 (88)	96.4 (80)	78.5 (95)	69.2 (83)	55.6 (74)	12.5 (5)	108.2 (66)

Crosses ♀♀ *y w cm* Sxl^{f1} *ct*/*Binsincy*; +/+ × ♂♂ *w* Sxl^{f9} *ct* /Y; TG/+

In situ hybridization of $SxlPe_{0.2kb}$ and $SxlPe_{0.4kb}$ transgenic lines

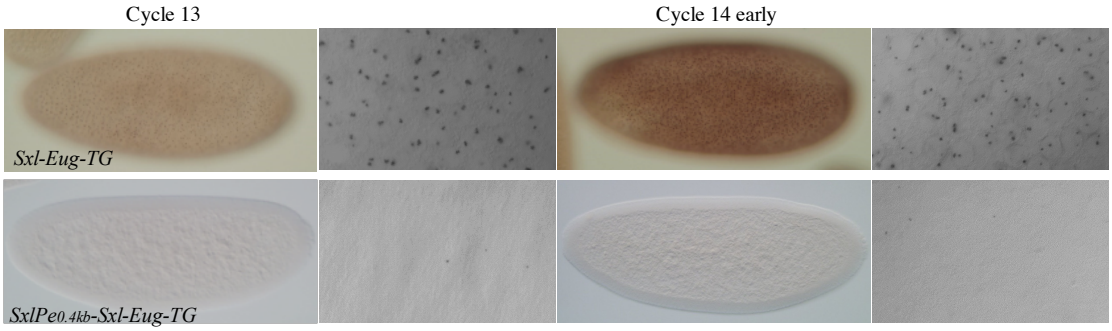

Surface views of embryos were shown in both 20X and 100X.

All categories of *SxlPe* activity observed in cycle 13 females carrying *delPe-Sxl-Eug-TG*

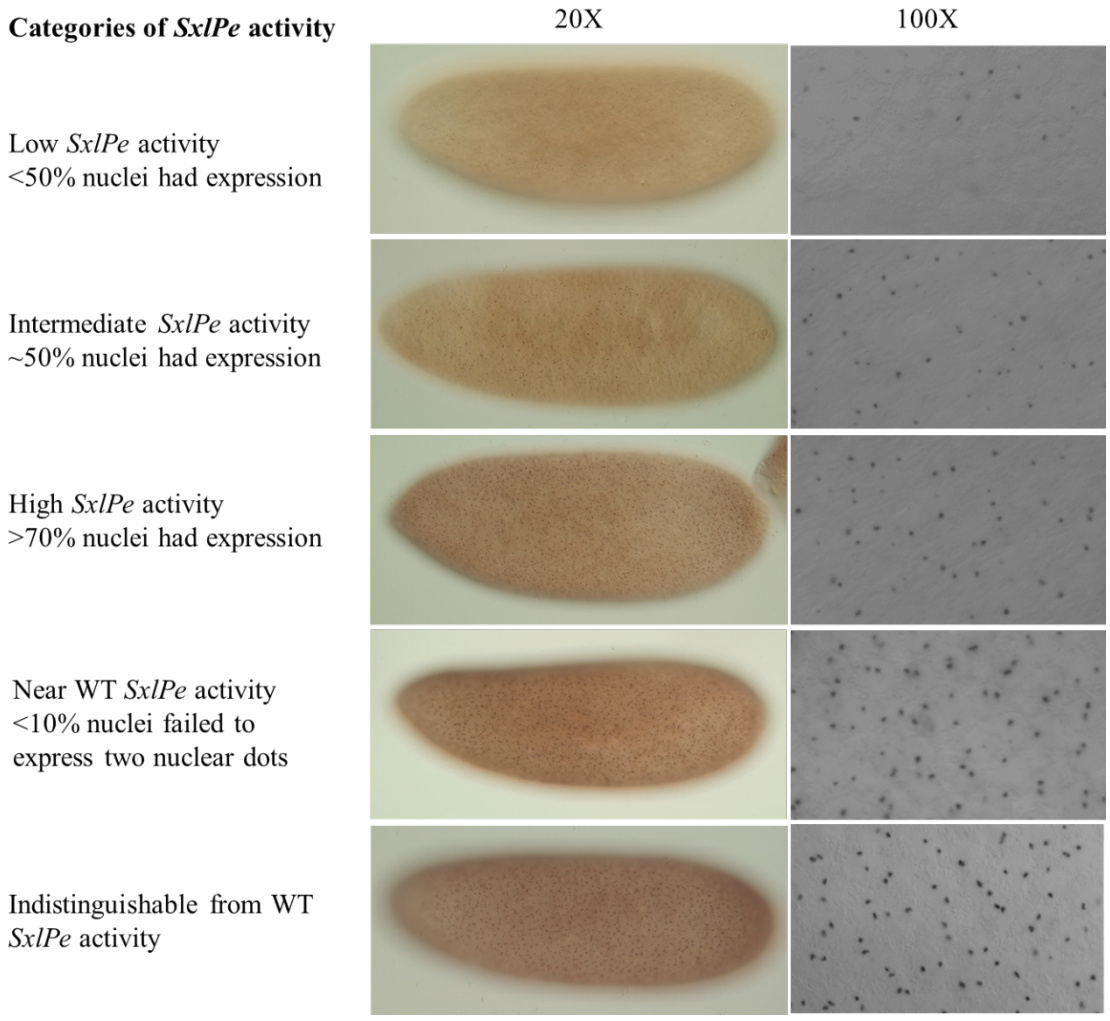

Nuclear dots represent nascent *SxlPe* transcripts. Surface views of embryos were shown in both 20X and 100X. 100X pictures were taken at the center of the embryos.

All categories of *SxlPe* activity observed in early cycle 14 females carrying *delPe-Sxl-Eug-TG*

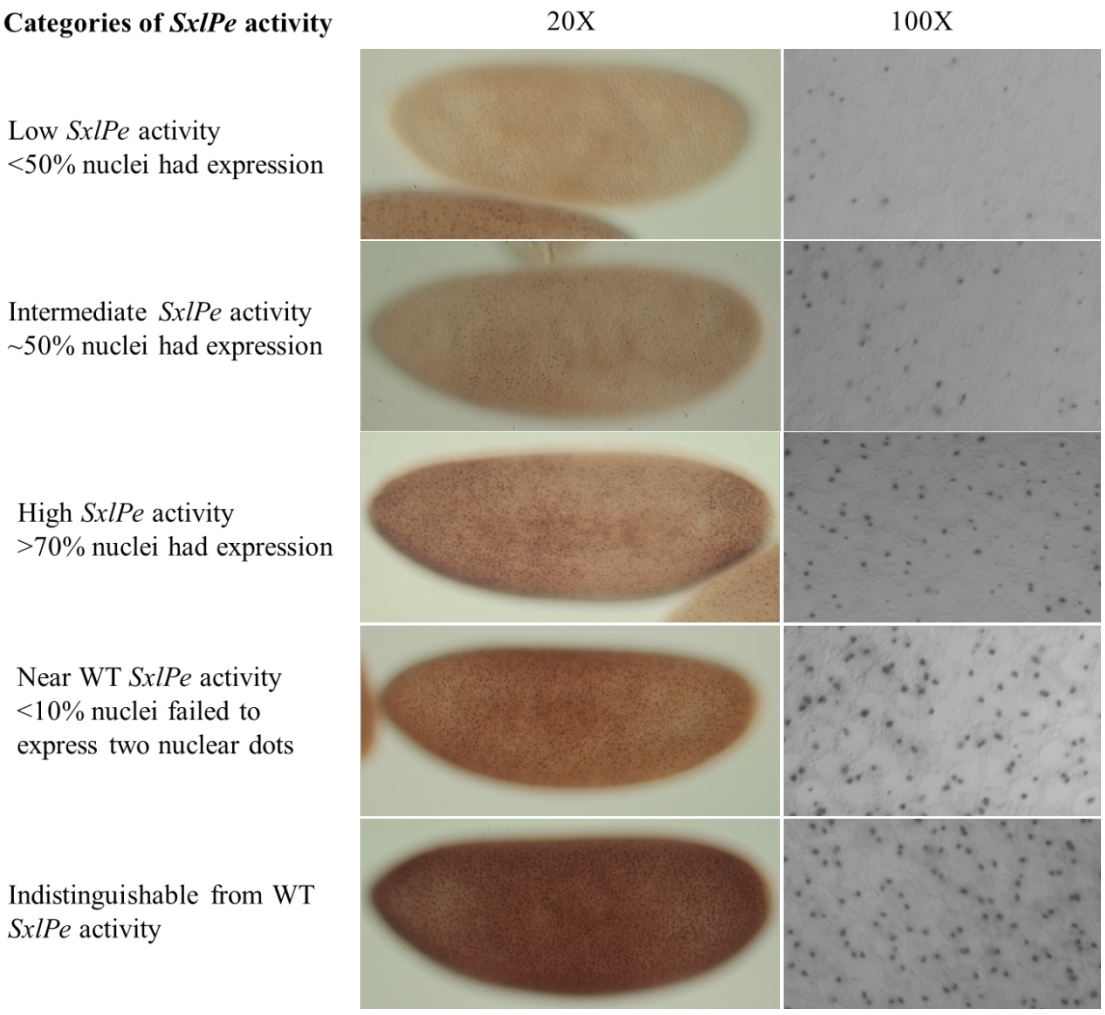

Nuclear dots represent nascent *SxlPe* transcripts. Surface views of embryos were shown in both 20X and 100X. 100X pictures were taken at the center of the embryos.

APPENDIX B

This appendix contains all the supplement tables and figures for Chapter IV.

Data tables of all the genetic tests performed on *Sc/Da^{M}SxlPe-SxlTG*
In the following tables, numerical data represent percentage of female viability. Numerical data in parenthesis represent the number of viable females.

Complete table (viability data) for Table 4.2A (Complementation of *Sxl^{f1}* mutants by *Sc/Da^{M}SxlPe-SxlTG*)

Genotype	*Sc/Da1^{-} SxlPe SxlTG*	*Sc/Da2^{-} SxlPe SxlTG*	*Sc/Da3^{-} SxlPe SxlTG*	*Sxl TG*
$\frac{Sxl^{f1}}{Sxl^{f1}}; \frac{+}{+}$	0 (0)	0 (0)	0 (0)	0 (0)
$\frac{Sxl^{f1}}{Sxl^{f1}}; \frac{TG}{+}$	77.9 (74)	32.2 (29)	1.3 (1)	109.9 (111)
$\frac{Sxl^{f1}}{Bincy}; \frac{+}{+}$	100 (95)	100 (90)	100 (76)	100 (101)
$\frac{Sxl^{f1}}{Bincy}; \frac{TG}{+}$	106.3 (101)	120 (120)	102.6 (78)	130.7 (132)
$\frac{Sxl^{f1}}{Y}; \frac{+}{+}$	100 (95)	100 (96)	100 (81)	100 (119)
$\frac{Sxl^{f1}}{Y}; \frac{TG}{+}$	114.7 (109)	86.5 (83)	109.9 (89)	127.7 (152)
$\frac{Bincy}{Y}; \frac{+}{+}$	51.6 (49)	66.7 (64)	70.4 (57)	44.5 (53)
$\frac{Bincy}{Y}; \frac{TG}{+}$	45.3 (43)	76.0 (73)	67.9 (55)	54.6 (65)

Crosses ♀♀ *y w cm Sxl^{f1} ct*/*Binsincy*; +/+ × ♂♂ *y w cm Sxl^{f1} ct* /Y; TG/+

Complete table (viability data) for Table 4.2B (Complementation of *Sxl^{7BO}* mutants by *Sc/Da^{M}SxlPe-SxlTG*)

Genotype	*Sc/Da1^{-} SxlPe SxlTG*	*Sc/Da2^{-} SxlPe SxlTG*	*Sc/Da3^{-} SxlPe SxlTG*	*Sxl TG*
$\frac{Sxl^{7BO}}{Sxl^{7BO}}; \frac{+}{+}$	0 (0)	0 (0)	0 (0)	0 (0)
$\frac{Sxl^{7BO}}{Sxl^{7BO}}; \frac{TG}{+}$	73.1 (68)	39.0 (39)	7.7 (6)	110.7 (93)
$\frac{Sxl^{7BO}}{Bincy}; \frac{+}{+}$	100 (93)	100 (100)	100 (78)	100 (84)
$\frac{Sxl^{7BO}}{Bincy}; \frac{TG}{+}$	105.4 (98)	78.0 (78)	157.7 (123)	103.6 (87)
$\frac{Sxl^{7BO}}{Y}; \frac{+}{+}$	100 (103)	100 (83)	100 (102)	100 (60)
$\frac{Sxl^{7BO}}{Y}; \frac{TG}{+}$	98.1 (101)	127.7 (106)	130.4 (133)	105.0 (63)
$\frac{Bincy}{Y}; \frac{+}{+}$	56.3 (58)	63.8 (53)	66.7 (68)	70.0 (42)
$\frac{Bincy}{Y}; \frac{TG}{+}$	49.5 (51)	65.1 (54)	62.7 (64)	85.0 (51)

Crosses ♀♀ *y pn w Sxl^{7BO}*/*Binsincy*; +/+ × ♂♂ *y pn w Sxl^{7BO}*/Y; TG/+

Complementation of *Sxl*^{f9} mutants by *Sc/Da*^{M}*SxlPe-SxlTG*

Genotype	*Sc/Da1-SxlPe SxlTG*	*Sc/Da2-SxlPe SxlTG*	*Sc/Da3-SxlPe SxlTG*	*Sc/Da1-2 SxlPe SxlTG*	*Sc/Da1-4-SxlPe SxlTG*	*Sxl TG*
$\frac{Sxl^{f9}}{Sxl^{f9}}; \frac{+}{+}$	0 (0)	0 (0)	0 (0)	0 (0)	0 (0)	0 (0)
$\frac{Sxl^{f9}}{Sxl^{f9}}; \frac{TG}{+}$	97.0 (96)	121.6 (152)	78.7 (74)	98.9 (93)	120 (102)	110 (112)
$\frac{Sxl^{f9}}{Bincy}; \frac{+}{+}$	100 (99)	100 (125)	100 (94)	100 (94)	100 (85)	100 (101)
$\frac{Sxl^{f9}}{Bincy}; \frac{TG}{+}$	110.1 (109)	93.6 (117)	93.6 (88)	87.2 (82)	111.8 (95)	107.9 (109)
$\frac{Sxl^{f9}}{Y}; \frac{+}{+}$	100 (83)	100 (138)	100 (105)	100 (101)	100 (97)	100 (132)
$\frac{Sxl^{f9}}{Y}; \frac{TG}{+}$	132.5 (110)	109.4 (151)	111.4 (117)	129.7 (131)	113.4 (110)	96.2 (127)
$\frac{Bincy}{Y}; \frac{+}{+}$	30.1 (25)	21.0 (29)	37.1 (39)	37.6 (38)	59.8 (58)	36.4 (48)
$\frac{Bincy}{Y}; \frac{TG}{+}$	25.3 (21)	34.1 (47)	48.6 (51)	47.5 (48)	29.9 (29)	3.8 (5)

Crosses ♀♀ *y w cm Sxl*^{fl} *ct*/*Binsincy*; +/+ × ♂♂ *y w cm Sxl*^{fl} *ct* /Y; TG/+

Complete table (viability data) for Table 4.3A (Complementation of *Sxl^{f1}* mutants by *Sc/Da^{M}SxlPe-SxlTG*)

Genotype	*Sc/Da1-2 SxlPe SxlTG*	*Sc/Da1-4- SxlPe SxlTG*	*Sxl TG*
$\frac{Sxl^{f1}}{Sxl^{f1}}; \frac{+}{+}$	0 (0)	0 (0)	0 (0)
$\frac{Sxl^{f1}}{Sxl^{f1}}; \frac{TG}{+}$	8.6 (9)	34.2 (40)	109.9 (111)
$\frac{Sxl^{f1}}{Bincy}; \frac{+}{+}$	100 (105)	100 (117)	100 (101)
$\frac{Sxl^{f1}}{Bincy}; \frac{TG}{+}$	110.5 (116)	109.4 (128)	130.7 (132)
$\frac{Sxl^{f1}}{Y}; \frac{+}{+}$	100 (94)	100 (123)	100 (119)
$\frac{Sxl^{f1}}{Y}; \frac{TG}{+}$	108.5 (102)	99.2 (122)	127.7 (152)
$\frac{Bincy}{Y}; \frac{+}{+}$	67.0 (63)	23.6 (29)	44.5 (53)
$\frac{Bincy}{Y}; \frac{TG}{+}$	97.9 (92)	34.1 (42)	54.6 (65)

Crosses ♀♀ *y w cm Sxl^{f1} ct*/*Binsincy*; +/+ × ♂♂ *y w cm Sxl^{f1} ct* /Y; TG/+

Complete table (viability data) for Table 4.3B (Complementation of *Sxl^{7BO}* mutants by *Sc/Da^{M}SxlPe-SxlTG*)

Genotype	*Sc/Da1-2 SxlPe SxlTG*	*Sc/Da1-4 SxlPe SxlTG*	*Sxl TG*
$\frac{Sxl^{7BO}}{Sxl^{7BO}}; \frac{+}{+}$	0 (0)	0 (0)	0 (0)
$\frac{Sxl^{7BO}}{Sxl^{7BO}}; \frac{TG}{+}$	25.0 (29)	62.1 (59)	110.7 (93)
$\frac{Sxl^{7BO}}{Bincy}; \frac{+}{+}$	100 (116)	100 (95)	100 (84)
$\frac{Sxl^{7BO}}{Bincy}; \frac{TG}{+}$	144.0 (167)	112.6 (107)	103.6 (87)
$\frac{Sxl^{7BO}}{Y}; \frac{+}{+}$	100 (128)	100 (95)	100 (60)
$\frac{Sxl^{7BO}}{Y}; \frac{TG}{+}$	135.9 (174)	118.9 (113)	105.0 (63)
$\frac{Bincy}{Y}; \frac{+}{+}$	72.6 (93)	17.9 (17)	70.0 (42)
$\frac{Bincy}{Y}; \frac{TG}{+}$	93.0 (119)	43.1 (41)	85.0 (51)

Crosses ♀♀ *y pn w Sxl^{7BO}*/*Binsincy*; +/+ × ♂♂ *y pn w Sxl^{7BO}*/Y; TG/+

Sc/Da binding site mutant embryos categorized based on their level of *SxlPe* activity

Binding sites mutation		*SxlPe* activity					Total number of embryos counted
		Wild-type activity (%)	Slightly affected activity and moderately affected activity (%)	Strongly affected activity (%)	Severely affected activity (%)	No activity (%)	
Sc/Da 1-	Cycle 12			48		52	15
	Cycle 13	36	15	3		46	33
	Cycle 14 early	54				46	26
Sc/Da 2-	Cycle 12			44		56	18
	Cycle 13	20	10	22		48	40
	Cycle 14 early	11	33	2		54	46
Sc/Da 3-	Cycle 12				10	90	10
	Cycle 13		2		42	56	36
	Cycle 14 early		25	25		50	28
Sc/Da 1- 2-	Cycle 12			50		50	12
	Cycle 13		30	20		50	44
	Cycle 14 early		38	10		52	21
Sc/Da 1- 4-	Cycle 12			56		44	9
	Cycle 13	22	22			56	27
	Cycle 14 early	47	7			44	45

***SxlPe* activity observed in cycle 13 female embryos carrying Sc/Da binding site mutations**

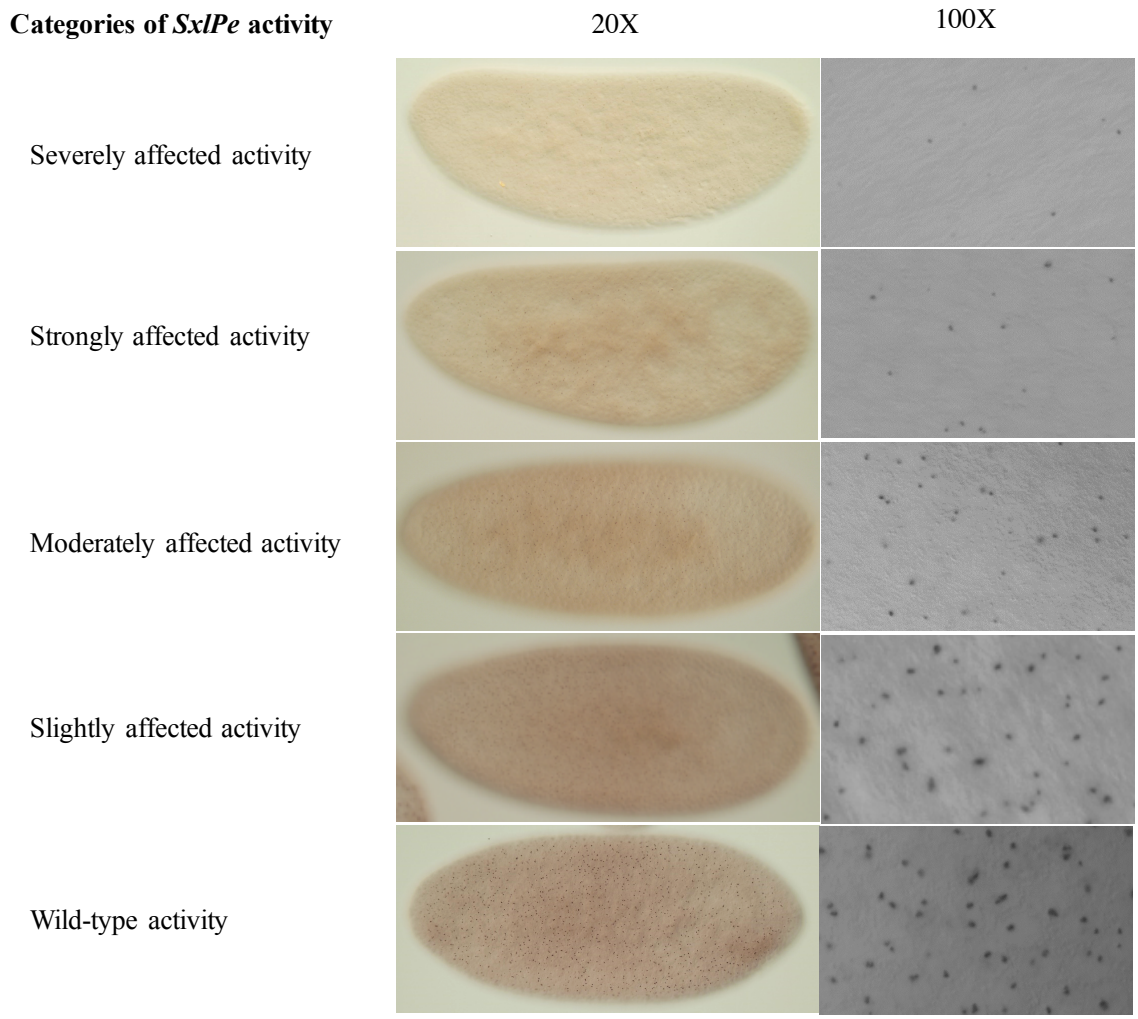

Nuclear dots represent nascent *SxlPe* transcripts. Surface views of embryos were shown in both 20X and 100X. 100X pictures were taken at the center of the embryos.

***SxlPe* activity observed in early cycle 14 female embryos carrying Sc/Da binding site mutations**

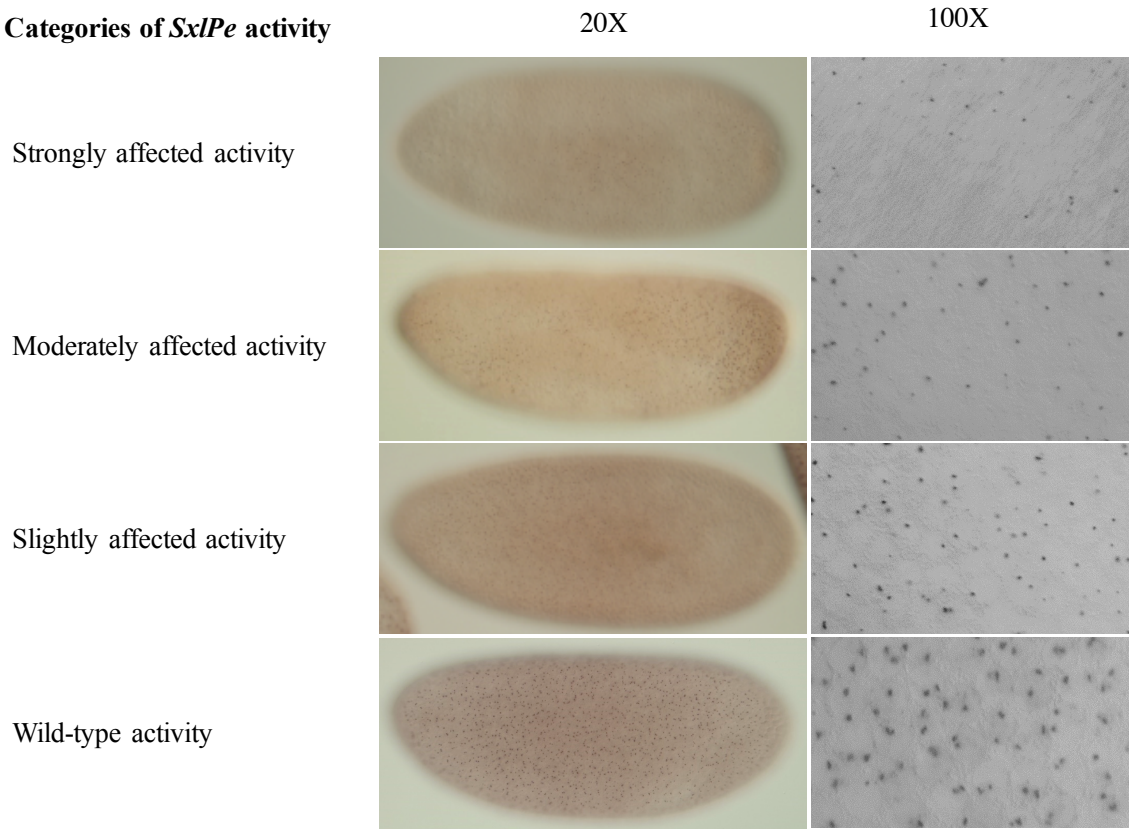

Nuclear dots represent nascent *SxlPe* transcripts. Surface views of embryos were shown in both 20X and 100X. 100X pictures were taken at the center of the embryos.

Data tables of all the genetic tests performed on *Dpn^{M}SxlPe-SxlTG*

In the following tables, numerical data represent percentage of female viability. Numerical data in parenthesis represent the number of viable females.

Complementation of *Sxl^{f1}* mutants by *Dpn^{M}SxlPe-SxlTG*

Genotype	*Dpn1^{-} SxlPe SxlTG*	*Dpn2^{-} SxlPe SxlTG*	*Dpn3^{-} SxlPe SxlTG*	*Dpn1-2^{-} SxlPe SxlTG*	*Dpn1-3^{-} SxlPe SxlTG*	*Dpn1-2-3^{-} SxlPe SxlTG*	*Sxl TG*
$\frac{Sxl^{f1}}{Sxl^{f1}}$; $\frac{+}{+}$	0 (0)	0 (0)	0 (0)	0 (0)	0 (0)	0 (0)	0 (0)
$\frac{Sxl^{f1}}{Sxl^{f1}}$; $\frac{TG}{+}$	109.5 (92)	103.4 (91)	97 (97)	94.8 (92)	111.8 (57)	105.1 (144)	109.9 (111)
$\frac{Sxl^{f1}}{Bincy}$; $\frac{+}{+}$	100 (84)	100 (88)	100 (100)	100 (97)	100 (51)	100 (137)	100 (101)
$\frac{Sxl^{f1}}{Bincy}$; $\frac{TG}{+}$	102.4 (86)	123.9 (109)	90 (90)	96.9 (94)	105.9 (54)	110.9 (152)	130.7 (132)
$\frac{Sxl^{f1}}{Y}$; $\frac{+}{+}$	100 (89)	100 (97)	100 (81)	100 (104)	100 (50)	100 (130)	100 (119)
$\frac{Sxl^{f1}}{Y}$; $\frac{TG}{+}$	97.8 (87)	122.7 (119)	112.3 (91)	103.8 (108)	132 (66)	57.7 (75)	127.7 (152)
$\frac{Bincy}{Y}$; $\frac{+}{+}$	38.2 (34)	16.5 (16)	72.8 (59)	54.8 (57)	74 (37)	36.9 (48)	44.5 (53)
$\frac{Bincy}{Y}$; $\frac{TG}{+}$	0 (0)	2.1 (2)	0 (0)	0 (0)	0 (0)	0 (0)	52.9 (65)

Crosses ♀♀ *y w cm Sxl^{f1} ct*/*Binsincy*; +/+ × ♂♂ *y w cm Sxl^{f1} ct* /Y; TG/+
For *Dpn 1^{-}2^{-}3^{-}SxlPe-SxlTG*, the crosses were set up as ♀♀ *y w cm Sxl^{f1} ct* /*Binsincy*; TG/+ × ♂♂ *y w cm Sxl^{f1} ct* /*Y*; +/+.

Complementation of Sxl^{7BO} mutants by Dpn^{M}SxlPe-SxlTG

Genotype	*Dpn1⁻ SxlPe SxlTG*	*Dpn2⁻ SxlPe SxlTG*	*Dpn3⁻ SxlPe SxlTG*	*Dpn1⁻2⁻ SxlPe SxlTG*	*Dpn1⁻3⁻ SxlPe SxlTG*	*Dpn1⁻2⁻3⁻ SxlPe SxlTG*	*Sxl TG*
$\frac{Sxl^{7BO}}{Sxl^{7BO}}; \frac{+}{+}$	0 (0)	0 (0)	0 (0)	0 (0)	0 (0)	0 (0)	0 (0)
$\frac{Sxl^{7BO}}{Sxl^{7BO}}; \frac{TG}{+}$	106.4 (99)	108.5 (89)	81.7 (134)	116.1 (115)	107.6 (128)	88.2 (82)	110.7 (93)
$\frac{Sxl^{7BO}}{Bincy}; \frac{+}{+}$	100 (93)	100 (82)	100 (164)	100 (99)	100 (119)	100 (93)	100 (84)
$\frac{Sxl^{7BO}}{Bincy}; \frac{TG}{+}$	95.7 (89)	115.8 (95)	101.2 (166)	121.2 (120)	79.8 (95)	114.0 (106)	103.6 (87)
$\frac{Sxl^{7BO}}{Y}; \frac{+}{+}$	100 (85)	100 (85)	100 (168)	100 (114)	100 (122)	100 (80)	100 (60)
$\frac{Sxl^{7BO}}{Y}; \frac{TG}{+}$	97.6 (83)	104.7 (89)	96.4 (162)	101.8 (116)	96.7 (118)	47.5 (38)	105 (63)
$\frac{Bincy}{Y}; \frac{+}{+}$	52.9 (45)	41.2 (35)	53.6 (90)	44.7 (51)	59 (72)	57.5 (46)	70 (42)
$\frac{Bincy}{Y}; \frac{TG}{+}$	2.4 (2)	1.2 (1)	0 (0)	0 (0)	0.8 (1)	0 (0)	85 (51)

Crosses ♀♀ *y pn w* Sxl^{7BO}*/Binsincy*; +/+ × ♂♂ *y pn w* Sxl^{7BO}/Y; TG/+
For *Dpn 1⁻2⁻3⁻SxlPe-SxlTG*, the crosses were set up as ♀♀ *y pn w* Sxl^{7BO} */Binsincy*; TG/+ × ♂♂ *y pn w* Sxl^{7BO} */Y*; +/+.

Complementation of Sxl^{f9} mutants by Dpn^{M}SxlPe-SxlTG

Genotype	*Dpn1⁻ SxlPe SxlTG*	*Dpn2⁻ SxlPe SxlTG*	*Dpn3⁻ SxlPe SxlTG*	*Dpn1⁻2⁻ SxlPe SxlTG*	*Dpn1⁻3⁻ SxlPe SxlTG*	*Dpn1⁻2⁻3⁻ SxlPe SxlTG*	*Sxl TG*
$\frac{Sxl^{f9}}{Sxl^{f9}}; \frac{+}{+}$	0 (0)	0 (0)	0 (0)	0 (0)	0 (0)	0 (0)	0 (0)
$\frac{Sxl^{f9}}{Sxl^{f9}}; \frac{TG}{+}$	91.1 (82)	104.6 (114)	91.7 (89)	121 (121)	113.4 (92)	80.4 (86)	110.9 (112)
$\frac{Sxl^{f9}}{Bincy}; \frac{+}{+}$	100 (90)	100 (109)	100 (97)	100 (100)	100 (81)	100 (107)	100 (101)
$\frac{Sxl^{f9}}{Bincy}; \frac{TG}{+}$	105.6 (95)	92.7 (101)	93.8 (91)	108 (108)	108.6 (88)	88.8 (95)	97.3 (109)
$\frac{Sxl^{f9}}{Y}; \frac{+}{+}$	100 (90)	100 (137)	100 (101)	100 (128)	100 (92)	100 (105)	100 (132)
$\frac{Sxl^{f9}}{Y}; \frac{TG}{+}$	98.9 (89)	92.7 (127)	0 (0)	104.7 (134)	0 (0)	0 (0)	96.2 (127)
$\frac{Bincy}{Y}; \frac{+}{+}$	37.8 (34)	16.0 (22)	26.7 (27)	63.3 (81)	22.8 (22)	47.6 (50)	36.4 (48)
$\frac{Bincy}{Y}; \frac{TG}{+}$	0 (0)	0 (0)	0 (0)	0 (0)	0 (0)	0 (0)	3.8 (5)

Crosses ♀♀ *w* Sxl^{f9}*ct/Binsincy*; +/+ × ♂♂ *w* Sxl^{f9} *ct* /Y; TG/+
For *Dpn 1⁻2⁻3⁻SxlPe-SxlTG*, the crosses were set up as ♀♀ *w* Sxl^{f9}*ct / Binsincy*; TG/+ × ♂♂ *w* Sxl^{f9}*ct /Y*; +/+.

Lethality test in wildtype flies carrying one copy of *Dpn^{M}SxlPe-SxlTG*

Genotype	*Dpn1⁻ SxlPe SxlTG*	*Dpn2⁻ SxlPe SxlTG*	*Dpn3⁻ SxlPe SxlTG*	*Dpn1⁻2⁻ SxlPe SxlTG*	*Dpn1⁻3⁻ SxlPe SxlTG*	*Dpn1⁻2⁻3⁻ SxlPe SxlTG*	*Sxl TG*
$\frac{+}{+};\frac{+}{+}$	100 (102)	100 (112)	100 (133)	100 (114)	100 (116)	100 (130)	100 (98)
$\frac{+}{+};\frac{TG}{+}$	97.0 (99)	97.3 (109)	112.0 (149)	95.6 (109)	100.9 (117)	112.3 (146)	99.0 (97)
$\frac{+}{Y};\frac{+}{+}$	100 (100)	100 (104)	100 (149)	100 (120)	100 (141)	100 (161)	100 (105)
$\frac{+}{Y};\frac{TG}{+}$	86 (86)	67.3 (70)	59.7 (89)	73.3 (88)	13.5 (19)	0 (0)	88.6 (93)

Crosses ♀♀+/+; TG/+ × ♂♂+/Y; +/+

Complete table (viability data) for Table 4.4A (Lethality test in wildtype flies carrying one and two copies of *Dpn^{M}SxlPe-SxlTG*)

Genotype	*Dpn1⁻ SxlPe SxlTG*	*Dpn2⁻ SxlPe SxlTG*	*Dpn3⁻ SxlPe SxlTG*	*Dpn1⁻2⁻ SxlPe SxlTG*	*Dpn1⁻3⁻ SxlPe SxlTG*	*Sxl TG*
$\frac{+}{+};\frac{+}{+}$	100 (40)	100 (46)	100 (60)	100 (69)	100 (44)	100 (51)
$\frac{+}{+};\frac{TG}{+}$	92.5 (74)	92.4 (85)	97.5 (117)	76.8 (106)	122.7 (108)	104.9 (107)
$\frac{+}{+};\frac{TG}{TG}$	97.5 (39)	91.3 (42)	35 (21)	84.0 (58)	88.6 (39)	94.1 (48)
$\frac{+}{Y};\frac{+}{+}$	100 (56)	100 (52)	100 (76)	100 (80)	100 (43)	100 (55)
$\frac{+}{Y};\frac{TG}{+}$	75.0 (84)	62.5 (65)	55.3 (84)	72.5 (116)	46.5 (40)	102.7 (113)
$\frac{+}{Y};\frac{TG}{TG}$	21.4 (12)	11.5 (6)	0 (0)	12.5 (10)	0 (0)	74.5 (41)

Crosses ♀♀+/+; TG/+ × ♂♂+/Y; TG/+

Complete table (viability data) for Table 4.4B (Lethality test of *Sxl^{7BO}* mutants carrying one/two copies of *Dpn^{M}SxlPe-SxlTG*)

Genotype	*Dpn1⁻ SxlPe SxlTG*	*Dpn2⁻ SxlPe SxlTG*	*Dpn3⁻ SxlPe SxlTG*	*Dpn1⁻2⁻ SxlPe SxlTG*	*Dpn1⁻3⁻ SxlPe SxlTG*	*Dpn1⁻2⁻3⁻ SxlPe SxlTG*	*Sxl TG*
$\frac{Sxl^{7BO}}{Sxl^{7BO}}; \frac{+}{+}$	0 (0)	0 (0)	0 (0)	0 (0)	0 (0)	0 (0)	0 (0)
$\frac{Sxl^{7BO}}{Sxl^{7BO}}; \frac{TG}{+}$	80.6 (87)	95.4 (84)	91 (91)	96.2 (125)	70 (105)	79.5 (132)	97.9 (94)
$\frac{Sxl^{7BO}}{Sxl^{7BO}}; \frac{TG}{TG}$	85.2 (46)	97.7 (43)	78 (39)	78.5 (51)	37.3 (28)	59 (49)	89.6 (43)
$\frac{Sxl^{7BO}}{Y}; \frac{+}{+}$	100 (54)	100 (44)	100 (50)	100 (65)	100 (75)	100 (83)	100 (48)
$\frac{Sxl^{7BO}}{Y}; \frac{TG}{+}$	68.5 (74)	73.9 (65)	69 (69)	92.3 (120)	84 (126)	56.6 (94)	93.7 (90)
$\frac{Sxl^{7BO}}{Y}; \frac{TG}{TG}$	57.4 (31)	18.2 (8)	2.0 (1)	30.8 (20)	13.3 (10)	0 (0)	81.2 (39)

Crosses ♀♀ *y pn w Sxl^{7BO}*; TG/+ × ♂♂ *y pn w Sxl^{7BO}/Binsincy* /Y; TG/+

Data tables of the genetic tests performed on other binding site mutations
In the following tables, numerical data represent percentage of female viability. Numerical data in parenthesis represent the number of viable females.

Complementation of *Sxl^{f1}* mutants by other binding site mutations

Genotype	*Sc/Da3⁻&Dpn1⁻2⁻3⁻ SxlPe SxlTG*	*Sc/Da1⁻& Dpn1⁻ SxlPe SxlTG*	*STAT1⁻ SxlPe SxlTG*	*TAGteam doublet SxlPe SxlTG*	*Sxl TG*
$\frac{Sxl^{f1}}{Sxl^{f1}}$; $\frac{+}{+}$	0 (0)	0 (0)	0 (0)	0 (0)	0 (0)
$\frac{Sxl^{f1}}{Sxl^{f1}}$; $\frac{TG}{+}$	89.9 (80)	79.6 (74)	40.5 (47)	23.6 (26)	109.9 (111)
$\frac{Sxl^{f1}}{Bincy}$; $\frac{+}{+}$	100 (89)	100 (93)	100 (116)	100 (110)	100 (101)
$\frac{Sxl^{f1}}{Bincy}$; $\frac{TG}{+}$	100.0 (89)	88.2 (82)	110.3 (128)	115.4 (127)	130.7 (132)
$\frac{Sxl^{f1}}{Y}$; $\frac{+}{+}$	100 (79)	100 (71)	100 (121)	100 (121)	100 (119)
$\frac{Sxl^{f1}}{Y}$; $\frac{TG}{+}$	112.6 (89)	107.0 (76)	97.5 (118)	115.7 (135)	127.7 (152)
$\frac{Bincy}{Y}$; $\frac{+}{+}$	59.5 (47)	42.2 (30)	32.2 (39)	45.4 (55)	44.5 (53)
$\frac{Bincy}{Y}$; $\frac{TG}{+}$	6.3 (5)	7.0 (5)	43.8 (53)	69.4 (84)	54.6 (65)

Crosses ♀♀ *y w cm Sxl^{f1} ct*/*Binsincy*; +/+ × ♂♂ *y w cm Sxl^{f1} ct* /Y; TG/+

Complementation of *Sxl^{7BO}* mutants by other binding site mutations

Genotype	*Sc/Da3$^-$&Dpn1$^-$2$^-$3$^-$ SxlPe SxlTG*	*Sc/Da1$^-$& Dpn1$^-$ SxlPe SxlTG*	*STAT1$^-$ SxlPe SxlTG*	*TAGteam doublet SxlPe SxlTG*	*Sxl TG*
$\frac{Sxl^{7BO}}{Sxl^{7BO}}; \frac{+}{+}$	0 (0)	0 (0)	0 (0)	0 (0)	0 (0)
$\frac{Sxl^{7BO}}{Sxl^{7BO}}; \frac{TG}{+}$	72.4 (84)	118.9 (132)	62.6 (57)	31.6 (37)	110.7 (93)
$\frac{Sxl^{7BO}}{Bincy}; \frac{+}{+}$	100 (116)	100 (111)	100 (91)	100 (117)	100 (84)
$\frac{Sxl^{7BO}}{Bincy}; \frac{TG}{+}$	89.6 (104)	105.4 (117)	120.9 (110)	106.8 (125)	103.6 (87)
$\frac{Sxl^{7BO}}{Y}; \frac{+}{+}$	100 (109)	100 (119)	100 (99)	100 (107)	100 (60)
$\frac{Sxl^{7BO}}{Y}; \frac{TG}{+}$	106.4 (116)	108.4 (129)	111.1 (110)	115.9 (124)	105.0 (63)
$\frac{Bincy}{Y}; \frac{+}{+}$	55.0 (60)	32.8 (39)	42.4 (42)	26.2 (28)	70.0 (42)
$\frac{Bincy}{Y}; \frac{TG}{+}$	0.9 (1)	1.7 (2)	45.4 (45)	37.4 (40)	85.0 (51)

Crosses ♀♀ *y pn w Sxl^{7BO}*/*Binsincy*; +/+ × ♂♂ *y pn w Sxl^{7BO}*/Y; TG/+

Complementation of *Sxl^{f9}* mutants by other binding site mutations

Genotype	*Sc/Da3⁻&Dpn1⁻2⁻3⁻ SxlPe SxlTG*	*Sc/Da1⁻& Dpn1⁻ SxlPe SxlTG*	*STAT1⁻ SxlPe SxlTG*	*TAGteam doublet SxlPe SxlTG*	*Sxl TG*
$\frac{Sxl^{f9}}{Sxl^{f9}}; \frac{+}{+}$	0 (0)	0 (0)	0 (0)	0 (0)	0 (0)
$\frac{Sxl^{f9}}{Sxl^{f9}}; \frac{TG}{+}$	107.3 (102)	95.4 (103)	85.2 (92)	103.4 (91)	110 (112)
$\frac{Sxl^{f9}}{Bincy}; \frac{+}{+}$	100 (95)	100 (108)	100 (108)	100 (88)	100 (101)
$\frac{Sxl^{f9}}{Bincy}; \frac{TG}{+}$	92.6 (88)	113.9 (123)	96.3 (104)	108.0 (95)	107.9 (109)
$\frac{Sxl^{f9}}{Y}; \frac{+}{+}$	100 (105)	100 (118)	100 (117)	100 (108)	100 (132)
$\frac{Sxl^{f9}}{Y}; \frac{TG}{+}$	96.2 (101)	114.4 (135)	103.4 (121)	100.9 (109)	96.2 (127)
$\frac{Bincy}{Y}; \frac{+}{+}$	20.0 (21)	55.1 (65)	41.0 (48)	14.8 (16)	36.4 (48)
$\frac{Bincy}{Y}; \frac{TG}{+}$	0 (0)	0 (0)	15.4 (18)	18.5 (20)	3.8 (5)

Crosses ♀♀ *w Sxl^{f9}ct/Binsincy*; +/+ × ♂♂ *w Sxl^{f9} ct* /Y; TG/+